Simulation and Experimental Study on Energy Management of Circulating Centrifugal Pumping Plants with Variable Speed Drives

LEVON GEVORKOV

TALLINN UNIVERSITY OF TECHNOLOGY
School of Engineering
Department of Electrical Power Engineering and Mechatronics

Dissertation was accepted for the defence of the degree of Doctor of Philosophy in Engineering on April 24, 2017

Supervisor: Professor, Ph.D. Valery Vodovozov, Department of Electrical Power Engineering and Mechatronics, Tallinn University of Technology

Opponents: Professor, Dr. Istvan Vajda, Institute of Automation, Obuda University, Hungary

Professor Alecksey Anuchin, Moscow Power Engineering Institute, Russia

Defence of the thesis: June 15, 2017, 14:00, room NRG-422, Tallinn University of Technology, Ehitajate tee 5, Tallinn, Estonia.

Declaration:
Hereby I declare that this doctoral thesis, my original investigation and achievement, submitted for the doctoral degree at Tallinn University of Technology, has not been submitted for any academic degree.

Levon Gevorkov..........................

Muudetava kiirusega ajamitega tsentrifugaalpumpadega varustatud tsirkulatsioonpumbajaamade energiahaldussüsteemide simuleerimine ja eksperimentaalne uurimine

LEVON GEVORKOV

CONTENTS

ACKNOWLEDGEMENTS

First, I would like to express my appreciation and gratitude to my supervisor Professor Valery Vodovozov for his continuous support, encouragement and valuable help during the years of my research.

In addition, I would like to thank my fellow colleagues Dr. Sc. Dmitri Vinnikov, Ph.D. Anton Rassõlkin, Ph.D. Ilja Bakman, Prof. Tõnu Lehtla, Ph.D. Elmo Pettai, Mr. Kristjan Peterson, Ms. Ilda Timmerman, Ph.D. Andrii Chub, Ph.D. Liisa Liivik, Ph.D. Zoja Raud, Ph.D. Oleksandr Husev, Ph.D. Janis Zakis, Ph.D. Tanel Jalakas, Ph.D. Indrek Roasto, PhD student Roman Kosenko, PhD student Elena Makovenko for their kind attitude and help.

My special thanks are due to Mare-Anne Laane for language revision of my thesis.

Levon Gevorkov

ABBREVIATIONS

ac   alternating current

AOR   Acceptable Operating Region

BEA   Best Efficiency Area

BEP   Best Efficiency Point

CoDeSys   Controller Development System

CPP   Centrifugal Pumping Plant

dc   direct current

DTC   Direct Torque Control

EHA   Electro Hydraulic Actuator

EMM   Energy Management Module

HIL   Hardware-in-the-Loop

IML   Inline Monitoring of Losses

MEC   Minimal Energy Consumption

NOP   Nominal Operating Point

NPSH   Net Positive Suction Head

PEC   Power Electronic Converter

PID   Proportional-Integral-Derivative

PLC   Programmable Logic Controller

PWM   Pulse Width Modulation

STL   Standard Template Library

VSD   Variable Speed Drive

SYMBOLS

A	cross-sectional area of the pipeline
C	friction factor
I	current
J	moment of inertia
L	natural coordinate
P	power
R	resistance
T	torque
U	voltage
f	frequency
g	gravity acceleration
h	head
i	initial value
j	new value
k	coefficient
n	speed
p	pressure
q	flowrate
s	differential operator
t	time
v	liquid velocity in a pipeline
ρ	density
φ	angle
ψ	flux linkage
η	efficiency
τ	time constant
*	demanded value

LIST OF AUTHOR'S MAIN PUBLICATIONS

The present doctoral thesis is based on the following publications that are referred to in the text by Roman numbers.

[PAPER-I] Gevorkov, L.; Vodovozov, V.; Raud, Z.; Lehtla, T. PLC-Based Hardware-in-the-Loop Simulator of a Centrifugal Pump. *5th International Conference on Power Engineering, Energy and Electrical Drives (POWERENG 2015), Latvia, Riga, May 11th to May 13th, 2015*. IEEE, pp. 1 – 6.

[PAPER-II] Gevorkov, L.; Bakman, I.; Vodovozov, V. Hardware-in-the-Loop Simulation of Motor Drives for Pumping Applications. *Electric Power Quality and Supply Reliability Conference (PQ 2014)*, Rakvere, Estonia, June 11th to 13th, 2014. pp. 1 – 6.

[PAPER-III] Bakman, I.; Gevorkov, L.; Vodovozov, V. Optimization of Method of Adjustment of Productivity of Multi-Pump System Containing Directly Connected Motors. *Electric Power Quality and Supply Reliability Conference (PQ 2014)*, Rakvere, Estonia, June 11th to 13th, 2014. IEEE, pp. 1 – 6.

[PAPER-IV] Bakman, I.; Gevorkov, L.; Vodovozov, V. Predictive Control of a Variable-Speed Multi-Pump Motor Drive. *IEEE 23rd International Symposium on Industrial Electronics (ISIE 2014)*, Istanbul, Turkey, June 1st to 4th, 2014. IEEE, pp. 1409 – 1414.

[PAPER-V] Bakman, I.; Gevorkov, L.; Vodovozov, V. Efficiency Control for adjustment of Number of Working Pumps in Multi-pump System. *9th International Conference on Compatibility and Power Electronics (CPE 2015)*, Lisbon, Portugal, June 24-26, 2015, pp. 396 – 402.

[PAPER-VI] Vodovozov, V.; Raud, Z.; Bakman, I.; Lehtla, T.; Gevorkov, L. Hardware-in-the-Loop Simulator of Vessel Propulsion Drive. *9th International Conference on Compatibility and Power Electronics (CPE 2015)*, Lisbon, Portugal, June 24-26, 2015, pp. 396 – 402.

[PAPER-VII] Vodovozov, V.; Raud, Z.; Gevorkov, L. PLC-Based Pressure Control in Multi-Pump Applications. *The Scientific Journal of Riga Technical University: Electrical, Control and Communication Engineering*. Vol. 9, 2015, pp.23-29.

[PAPER-VIII] Gevorkov, L.; Vodovozov, V.; Lehtla, T.; Bakman, I. (2015). PLC-Based Flow Rate Control System for Centrifugal Pumps. 56th International Scientific Conference on Power and Electrical Engineering of Riga Technical University (RTUCON 2015), Riga, Latvia, October 14th, 2015. IEEE, 239−243.

[PAPER-IX] Bakman, I.; Gevorkov, L. (2015). Speed Control Strategy Selection for Multi-Pump Systems. 56th International Scientific

Conference on Power and Electrical Engineering of Riga Technical University (RTUCON 2015), Riga, Latvia, October 14th, 2015. IEEE, 353−356.

[PAPER-X]   Vodovozov, V.; Gevorkov, L.; Raud, Z (2014). Modeling and Analysis of Pumping Motor Drives in Hardware-in-the-Loop Environment. Journal of Power and Energy Engineering, 2 (10), 19−27.

[PAPER-XI]   Gevorkov, L.; Vodovozov, V.; Lehtla, T.; Raud, Z. (2016). Hardware-in-the-Loop Simulator of a Flow Control System for Centrifugal Pumps. *10th International Conference on Compatibility, Power Electronics and Power Engineering (CPE-POWERENG 2016)*. IEEE, 472−477.

[PAPER-XII] Gevorkov, L.; Vodovozov, V. (2016). Study of the Centrifugal Pump Efficiency at Throttling and Speed Control. *15th biennial Baltic Electronics Conference (BEC 2016)*, Tallinn, Estonia, October 3rd to October 5th . IEEE, 199−202.

[PAPER-XIII] Gevorkov, L.; Vodovozov, V.; Raud, Z. (2016). Simulation Study of the Pressure Control System for a Centrifugal Pump. *57th International Scientific Conference on Power and Electrical Engineering of Riga Technical University (RTUCON 2016)*, Riga, Latvia, October 13th-14th, 2016. IEEE, 1−5.

[PAPER-XIV] Gevorkov, L.; Vodovozov, V. Mixed Pressure Control System for a Centrifugal Pump, *11th International Conference on Compatibility, Power Electronics and Power Engineering (CPE-POWERENG 2017)*, Cadiz, Spain, 2017. IEEE, 364−369.

[PAPER-XV]   Vodovozov, V.; Gevorkov, L.; Raud, Z. Circulation Centrifugal Pump with Variable Speed Drives and Minimal Electricity Consumption, *11th International Conference on Compatibility, Power Electronics and Power Engineering (CPE-POWERENG 2017)*, Cadiz, Spain, 2017. IEEE, 334−339.

INTRODUCTION

I.1. Background

Rapid advancement in energy awareness has a significant impact on the community. Therefore, it becomes imperative that energy consumers are looking for ways of how to achieve *minimal energy consumption* (MEC). The primary reason for reduction of energy usage is targeted to the increasing costs of electricity. Another reason is the commitment of the European Union to reduce greenhouse emissions in accordance with the Kyoto Protocol [1].

The bulk of substantial energy consumption is due to systems that convert electricity into mechanical motion. It was reported that electrically driven systems consume about 70 % of generated electrical energy that is more than 20000 terawatt-hours annually. Currently 75 % of that equipment operates at pump, fan, and compressor applications. Pumping systems account for nearly 20 % of the world energy and up to 50 % of the total electricity consumption in industrialized countries. These systems produce above 80 million tonnes of emissions [2].

Among them, *centrifugal pumping plants* (CPPs) represent the highest price constituent and often dominate in the industry lifecycle cost [3]. Today, it is required to reduce energy consumption in pumping systems, the energy costs of which may account up to 50 % and more of pump ownership costs (Fig. I.1) [4], [5]. According to [6], the amount of global water withdrawal is approximately 4500 cubic kilometers per year. At rational liquid flow control, the loss of water for urban, industrial and agricultural purposes can be reduced significantly. A similar forecast concerns wastewater treatment.

- Initial costs 15%
- Energy costs 50%
- Other costs 7%
- Maintenance costs 28%
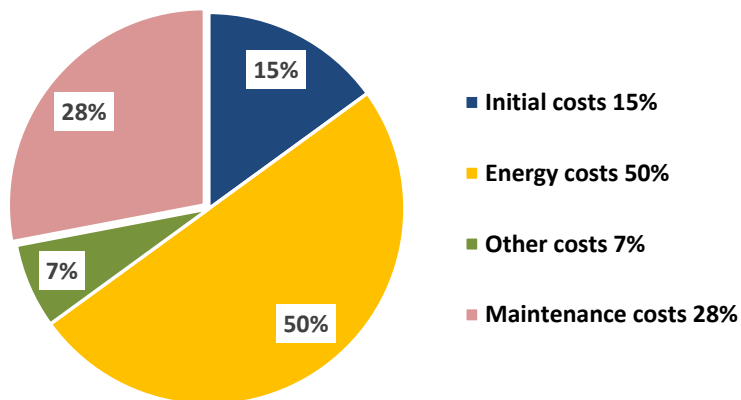
Figure I.1 Pumping cost distribution [5]

Because of rather low efficiency, often ranging from 35 to 65 % [7], it is required to address cost saving, more efficient and power dense equipment, which has stimulated rapid development of CPP technologies. Need for efficient pumping has brought many issues into the spotlight. However, despite multiple improvements introduced over the last decades, the CPPs still lose a considerable amount of liquid and energy.

To meet energy saving demands, all the interacting system resources – pumps, drives, control equipment, and network infrastructure – are to be involved in the optimization process. As the quality of pressure and flow maintenance strictly depends on the pumping speed whereas energy consumption is proportional to speed cube, MEC may be reached using appropriate *variable-speed drives* (VSDs). At the same time, as the VSD and pump constraints restrict the pumping speed, additional energy losses may be eliminated using adjustable throttling along with the speed variation.

Thus, potentially, MEC could be achieved by finding the best CPP design and literate management solutions. These feasible solutions are in the focus of the thesis research. Major results of this thesis research contribute to both the international and Estonian economy.

I.2. Objective and Tasks

The objective of this research is to reduce energy consumption of centrifugal pumping plants by means of an enlargement of the pumping operating region and specifying the best efficiency area of pumping at the expense of zones that have not been earlier employed.

The primary task is to account the specific power losses in the motor drives to decrease pump oversize and waste energy within the operating region.

The second task is to enhance the high-pressure, high-flow, and high-speed pumping ability to exclude expensive multi-pump equipment.

I.3. Scientific Results

1. **Energy management methodology** that provides best energy utilization at fluctuating demands and loads associated with pumping.

2. **Hybrid management system** for centrifugal pumping plants, that carries out pressure and flowrate maintenance with mutual throttling and speed control.

3. **Method for inline monitoring of energy losses** that maintains a working point in low-loss pumping areas.

4. **Procedures of high-pressure, high-flow, and high-speed pumping** that enlarge the operating region for pumping without increasing the number of pumps.

I.4. Practical Outcomes

1. PLC-based **experimental setup** the hardware and software tools of which provide exploring, validation, and demonstration of new algorithms and procedures in various pumping modes.
2. **Simulation model** of pumping plants intended for design, estimation, and assessment of system resources and their interaction.
3. **Hardware-in-the-loop imitator** for high-quality study of competitive management methodologies and comparison of different pumping layouts.
4. **Sensorless model-based software** for accurate intelligent control of liquid pressure and network flowrate.
5. **Collection of educational modules** including laboratory equipment and appropriate methodology for enhanced learning and teaching in the field of pumping automation.

I.5. Confirmation and dissemination of results

The profitability of the work has been confirmed by analytical exploration and computer simulation along with verification in the real experimental environment.

The results of the thesis research were disseminated at 10 international conferences and 2 scientific journals. 15 of the author's papers are published in collections indexed by IEEE Explore, WoS, and Scopus.

I.6. Thesis Outline

Chapter 1 presents the motivation of the thesis based on the examination of the key features of CPPs, the energy model of pumping processes, and challenges in management methods. A detailed description of a CPP, pipeline and pump properties, system and performance characteristics are given. The power analysis has revealed the main efficiency and torque issues. By comparing the two regulation methods – throttling and speed adjustment – major constraints of efficient pumping are identified.

Chapter 2 introduces the hybrid management system, that is for both pressure and flowrate maintenance. To conduct mutual throttling and speed control within an expanded operating region, a method for inline monitoring of energy losses and the procedures of high-pressure, high-flow, and high-speed pumping are proposed and grounded. Using this basis, a new pressure maintenance and flowrate maintenance modules are developed. To justify the methodology, a layout of a hybrid management system, its implementation, and performance are depicted.

An experimental setup composed of VSDs, DriveStudio toolkit, and AC500 controller and two simulation systems – Matlab modelling environment and a hardware-in-the-loop pumping imitator – was developed to observe, compare,

and improve pumping properties and characteristics. The exploratory set was used to determine process quality and energy consumption of VSD-driven equipment and help in the assessment of the novelties proposed. Chapter 3 demonstrates energy saving examples supported by successful simulating solutions.

Chapter 4 is devoted to the enhancement of adjacent processes and future research perspectives. The first step, addresses the flow metering problems and their resolving in the scope of the sensorless approach. In addition, some problems of pressure measurement are solved using similar sensorless tools. Major improvements are introduced in the field of pumping education based on the new laboratory stand and appropriate experimentation methodology. Future research directions rely on the use of the HIL imitation approach for exploring vessel electric propulsion and on the application of the hybrid system for reforming aircraft pumping equipment.

The list of 78 references and Web links consummates the thesis.

CHAPTER 1. THESIS MOTIVATION IN LIGHT OF PUMPING MANAGEMENT

1.1 Key Features of Centrifugal Pumping Plants

1.1.1 Centrifugal pumping plants

Centrifugal pumps are widely used in everyday life in water supply networks, sewerage systems, oil production, and many other industries where they are used to transport liquids by the conversion of rotational kinetic energy of an electrical motor to the hydrodynamic energy of the liquid flow. One of the most attractive features of a centrifugal pump is its ability to perform under a broad range of operating conditions. They operate satisfactorily with different liquid types, densities, varying properties, at multiple loads and velocities.

CPPs dominate in a variety of infrastructure systems, such as artificial waterways, shipping, and oil supply to consumers, the drainage of low-lying lands, and the sewage removal from processing sites. The CPPs represent facilities that involve both the pumps and accompanying equipment for pumping liquids from one place to another, such as piping, pipeline networks, tanks, and appropriate inline components: fittings, valves, and devices that typically sense and control the flowrate, pressure, and temperature of the transmitted liquids.

A simplified diagram of a typical centrifugal pump in Fig. 1.1 shows relative locations of the pump parts [8]. It consists of a stationary casing and an impeller mounted on a rotating shaft. Liquid enters via the suction (inlet) axially through eye of the casing being caught up in the impeller blades that impart a radial and rotary motion to liquid. It is whirled tangentially and radially outward until it comes to the outer periphery called a volute. The fluid gains both velocity and pressure and finally leaves the pump through the discharge (outlet).

The impeller is fixed on the shaft, usually driven by an electric motor. Absolute velocity of the fluid and its pressure gradually increase as the fluid moves along the impeller towards the periphery. The shape of the housing of a centrifugal pump is designed to allow a uniform velocity distribution during the fluid movement towards the discharge side.

To rotate the pumps, electrical drives are used. Mostly, non-adjustable drives prevail built on the induction and synchronous machine basis. In such CPPs, the liquid regulation is conducted with the help of discharge valves. The VSDs bring substantial benefits to the pumping management. The speed control can be brought by the induction motor VSDs, synchronous machine VSDs, switch-reluctance motor drives, or some other drive systems. To increase control possibilities, *programmable logical controllers* (PLCs) are introduced to the contemporary CPPs.

To illustrate the studied pumping processes, a VSD-driven experimental CPP setup described in 3.1.1 was used in this research.
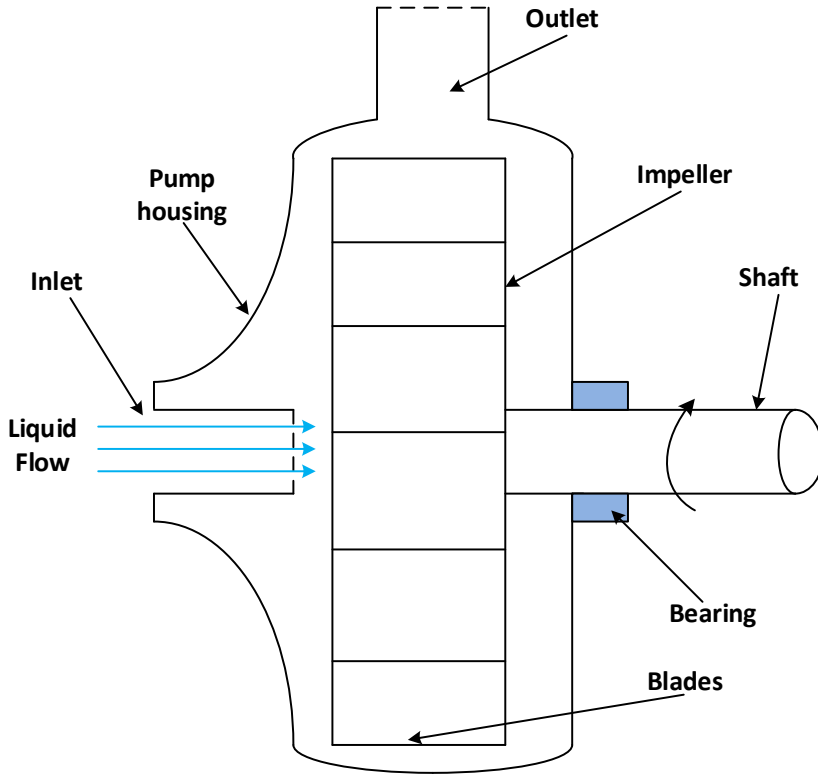
Figure 1.1 Main parts of a centrifugal pump

1.1.2 Pipeline properties and system characteristics

Total energy the pump must supply involves two components: a flowrate and a total head.

The amount of liquid displaced per unit time is called *a flowrate* [9] and designated as q in this work. It is measured by cubic meters per second m^3/s but in the thesis it is given in m^3/h, which is more convenient for small-scale applications. The flowrate determines the CPP capacity of overcoming the losses caused by liquid flow in the pipes, valves, bends, and other piping plant devices. These losses are completely flow-dependent and nonlinear. Hence, the flowrate represents the *kinetic energy* component of the pump output.

In general, losses are represented by the liquid *head* designated as h, which may be of two types: the static head and the friction head. The first one is simply the difference in the height of the supply and destination tanks. It

provides *elevation energy* of the liquid lifted on a certain height. The static head is independent of a flow.

The friction head, called also a dynamic head loss, is the loss to the environment due to the movement of the liquid through pipes and fittings in the system. It provides *velocity energy* that the moving objects have. This loss is proportional to the square of the flowrate.

The sum of the static and friction heads, called a *total head*, shows the amount of energy per unit weight of the liquid the pump creates between its inlet and outlet. The total head is expressed as a height of liquid surface above or below some reference plane (usually the centreline of the pump).

A *system characteristic*, $h_s(q)$, demonstrates how the total head varies with the flowrate. It may be expressed as a set of points $\{[h_{si}\ q_{si}],..[\ h_{sj}\ q_{sj}]\}$ or as a polynomial:

$$h_s(q) = h_{s0} + C_s q^2 , \qquad\qquad (1.1)$$

where h_{S0} is a system static head, C_S is a system friction (dynamic) factor, and s designates a system state. Its graphic representation in Fig. 1.2 is called a *resistance curve* or a *system curve*.
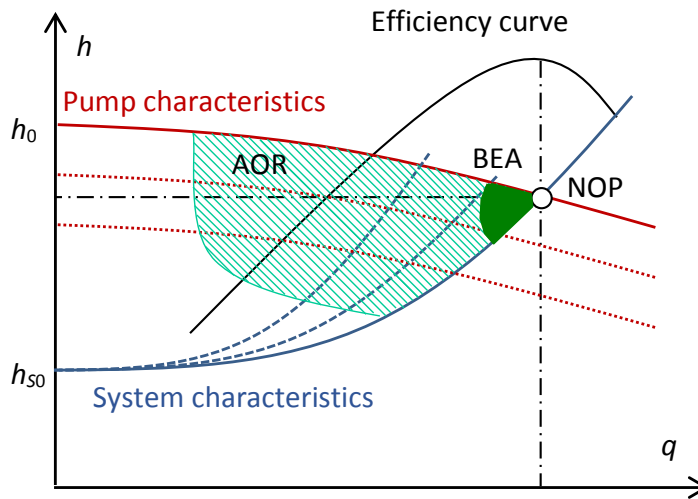
Figure 1.2 System and pump characteristics: h_{S0} – static head; h_0 – shutoff head; NOP – normal operating point; AOR – acceptable operating region; BEA – best efficiency area

A collection of such curves shown in Fig. 1.2 by the stroke lines representing the family of the system characteristics for various piping conditions. The system characteristics may change all the time during pumping influenced by a number of variables including variations in fluid viscosity and pumping rate. A designer may have an overloaded pump, the piping may corrode, filters and heat exchangers may clog, reservoir levels often alternate, and CPP demand may change.

Based on the system characteristics, all the CPPs may be tentatively categorized into three basic types – low static head, medium static head, and high static head systems.

Particularly, the CPPs for liquid transportation primarily overcome pipeline friction. As these systems have no head without a flow, their system characteristic goes close to the zero point in Fig. 1.2. A hot-water baseboard fin-tube system may serve as an example. Such close loop circulating systems without a surface open to the atmospheric pressure would exhibit only friction losses. They are the primary focus of this study.

In the CPPs for liquid elevation where liquid is moved from one level to another, there is a head difference between the two reservoirs. The static head dominates there and the system curve goes through a non-zero h_{S0} point in Fig. 1.2. Most systems have a combination of friction, elevation, and velocity heads and apply them as an energy measure of the CPP.

1.1.3 Pump properties and characteristics

By analogy with piping systems, performance of pumps is characterized in terms of their flowrate and discharge head.

Every pump has its *performance characteristic*, often called a pump characteristic. It describes the pump head as a function of the flowrate, $h(q)$, while the pump speed, designated as n, is assumed constant:

$$h(q) = h_0 - C_{h1}q - C_{h2}q^2 . \qquad (1.2)$$

Here, h_0 is a pump shutoff head and $C_{h1,2}$ are the head friction factors of the pump. Its graphic representation is called a *performance curve* or *a pump curve*.

Pump manufacturers provide the nominal characteristics of their pumps as a basis for relevant studies. These characteristics are usually given among other passport data in either the polynomial or the graphical form accompanied with a set of characteristic points. They are generated while testing the pump using cold water as liquid. Every passport pump characteristic is fixed for a nominal speed and impeller diameter. This continuously drooping trajectory from the shutoff (no-flow) condition to the maximal flowrate called a *nominal operating point* (NOP) is shown in Fig. 1.2 above the system curves.

The pump manufacturer guarantees the nominal flowrate, q_{NOP}, and the corresponding head, h_{NOP}, in NOP. That usually, is in excess by 5 to 10% of the

conditions at which the pump will be employed most of the times or as specified by process demands.

In reality, the pump operates in some accidental pumping *working point*, [h_N q_N], in which the system curve intersects the nominal pump curve. Moreover, pump performance throughout its life often has to take place at some other speeds or impeller diameters and services. To this aim, the CPPs usually require a variation of the flowrate or the head and a pump has to adapt to the temporary and permanent changes in the process demand. This variation is called *regulation*. At regulation, either the system curve or the pump curve has to be changed to reach another working point, [h q], in which the pump flowrate and the head generated will differ.

To determine approximate pump characteristics at any speed other than the nominal, *affinity laws* are conventionally used. These laws are based on Bernoulli's equation, which is, basically, a conservation of energy equation for fluids. The affinity laws are mathematical expressions that best define changes in the pump flowrate and head when the pump speed is changed, with all the rest remaining constant.

The first affinity law determines the relationship between the flowrate from the pump and the pumping speed:

$$\frac{q_i}{q_j} = \frac{n_i}{n_j}. \tag{1.3}$$

Here, an index *i* denotes initial states and an index *j* – new states of the variables.

The second affinity law defines the relationship between the head of the pump and the pumping speed.

$$\frac{h_i}{h_j} = \left(\frac{n_i}{n_j}\right)^2. \tag{1.4}$$

The affinity laws for the description of the centrifugal pump operation must be applied with caution. The general guideline is to use the affinity laws when the system has a friction head dominated upon the static head. In this case, the flowrate varies directly with the speed and the head varies as the square of the speed.

Fig. 1.3 exemplifies a family of pump characteristics obtained from the experimental setup. This collection of trajectories acquired at various *n* is crossed by the system curves represented as tiny, thin, average, and thick pipes. A family of pump performance curves was obtained for five rotational speeds: 2760 rpm, 2500 rpm, 2200 rpm, 1800 rpm and 1000 rpm. Intersections of performance and system curves denote the working points of the pump.
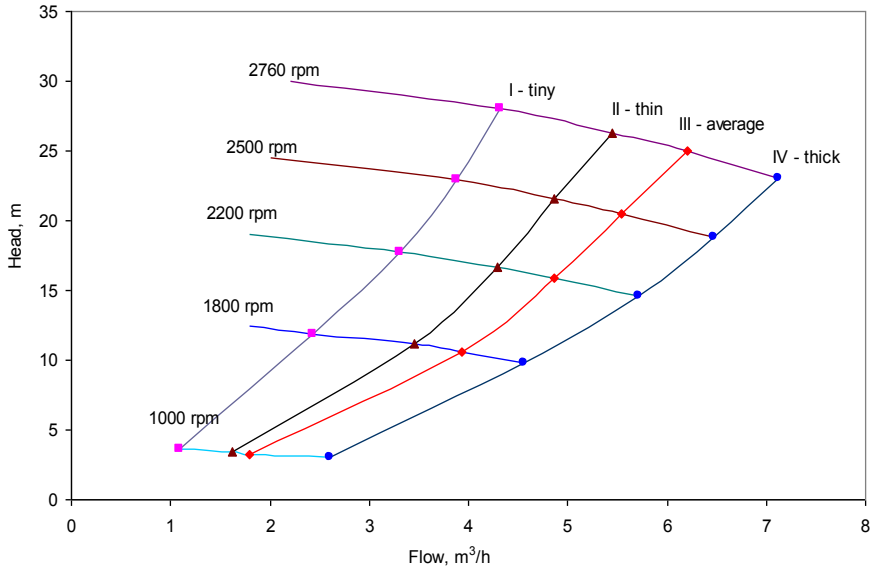
Figure 1.3 Family of performance and system curves for Ebara CDX120/12

For every particular liquid, the head was recalculated to outlet *pressure*, designated as *p* in this research. Pressure is the mass of liquid processing in the pump by its centrifugal force [10]. Pressure is measured in Pa. In industry, it is more common to use another unit for pressure definition, which is *bar*. Further, mainly *bar* units will be used. By analogy with the head, pressure is split into static pressure and dynamic pressure. The former component is constant whereas the latter one represents a function of the fluid velocity. *Total pressure* involves both components [11], though in the circulation systems, the dynamic part is usually much less compared with the static one:

$$p = g\rho\left(h - h_d - \frac{v^2}{2g}\right) \approx g\rho(h - h_d),\qquad(1.5)$$

where

ρ – liquid density (1000 kg/m^3 for water),
g – acceleration due to gravity (9.81 m/s^2),
$g\rho h$ – pressure at the suction,
$g\rho h_d$ – pressure at the discharge,
$g\rho(h - h_d)$ – static pressure,

$\rho\dfrac{v^2}{2}$ – dynamic pressure,

$v = \dfrac{q}{A}$ – liquid velocity in a pipeline,

A – cross-sectional area of the pipe.

Appropriate system characteristics of CPPs take the form of pressure across the pump as a function of the liquid flowrate [12]:

$$p(q) = p_0 + C_p q^2 . \tag{1.6}$$

Respectively, pump characteristics can be rescaled to the pressure:

$$p(q) = p_0 + C_{p1} q + C_{p2} q^2 . \tag{1.7}$$

In this case, the second affinity law describes the relationship between the outlet pressure and the speed of the pump:

$$\frac{p_i}{p_j} = \left(\frac{n_i}{n_j} \right)^2 . \tag{1.8}$$

The pump datasheet, contains all the pressure data, including start-up, shutdown, and upset conditions. In addition, the shutoff level restricts the maximal pressure a pump will develop under the no-flow condition reflecting a fully blocked outlet [9].

1.1.4 Resume

1. As industrial equipment, CPPs are most popular in systems of highest energy consumption. Multiple interacting system components – pumps, drives, control equipment, and network infrastructure – are involved in the CPP environment.

2. A piping system carries two kinds of energy: a flowrate and a total head. To describe how the total head varies with the flowrate, the system characteristic is used.

3. By analogy with a piping system, every pump has its performance characteristic describing the pump head as a function of the flowrate obtained at some pump speed. To determine pump characteristics at any speed other than the nominal one, affinity laws are used.

4. Instead of the head, energy-producing capability of a centrifugal pump and its characteristics are often defined by the outlet pressure, which depends on both the speed and the liquid density.

1.2 Energy Model of Pumping [I, III, IV, V]

1.2.1 Power analysis of a pumping plant

Pumping *power*, designated as *P* in this study, as an amount of energy consumed per unit time, is an important property to be addressed in energy management problems. Three forms of power participate in the energy conversion within the CPP [13].

Hydraulic power is developed by the pump to deliver the demanded liquid flowrate at the desired head range:

$$P_{out} = \rho g h q. \tag{1.9}$$

Brake power, called also a *shaft power*, is a mechanical power on the pump shaft required to develop the hydraulic power and to compensate pump losses.

Consumed power is an electrical power required to deliver the brake power and to cover all VSD losses.

A *system power characteristic*, $P_s(q)$, demonstrates how system power losses vary with the flowrate:

$$P_s(q) = P_{s0} + C_{ps}q^3, \tag{1.10}$$

where P_{S0} is the system static power and C_{PS} is the system friction (dynamic) loss factor. Its graphical representation is called a *power loss curve.* Unlike the head, the power has a cubical dependence on the flowrate.

The *power characteristic* of a pump, $P(q)$, and an appropriate *power curve* describe the pump brake power as a function of the flowrate taking place at a constant pump speed:

$$P(q) = P_0 + C_{p1}q + C_{p2}q^2, \tag{1.11}$$

where P_0 is the pump shutoff power and $C_{P1,2}$ are the pump loss factors. The shapes of power curves are dependent on the pump specific speed. Centrifugal pumps of low and medium specific speeds have power curves that rise upward. At higher specific speeds, these curves may be approximately flat and horizontal.

The break powers at different speeds are usually estimated with the help of an appropriate affinity law for power:

$$\frac{P_i}{P_j} = \left(\frac{n_i}{n_j}\right)^3, \tag{1.12}$$

Again, this affinity law must be applied with caution, i.e., only when the CPP has no power losses in the steady state and hydraulic power requirements

vary as the cube of the pump speed. Due to the cubical relation, any small decrease in the speed or the flowrate can significantly reduce the power.

This relationship is based on the assumption that system losses remain fixed while transferring from a demanded point on one pump curve to a homologous point on another curve. In real practice, the affinity law for power is not as accurate, especially when the speed change is more than 25 %. If the affinity law for power is used, the computed power requires justification taking into account instability of losses. For that reason, pump manufacturers recommend modifying power equations based on consumer experience.

1.2.2 Pumping efficiency

Differences between the hydraulic, the brake, and the consumed power are explained by volumetric, mechanical, hydraulic, and electrical energy losses. *Volumetric losses* are those of leakage through small clearances between wearing rings in the pump casing and the rotating element. *Mechanical losses* are caused by mechanical friction in the stuffing boxes and bearings, by internal disc friction, and by fluid shear. Friction within flow passages accounts for the *hydraulic losses*. *Electrical losses* take place in the electrical parts of the pump VSD. In view of these losses, it is useful to observe pump and VSD operation separately.

CPP *efficiency* is the ratio of the hydraulic power P_{out} developed by the pump and the electrical power, P_{in}, consumed by the plant:

$$\eta_{CPP} = \frac{P_{out}}{P_{in}} = \eta\eta_{VSD}\,,\qquad\qquad(1.13)$$

where

$\eta = \dfrac{P_{out}}{P}$ is the pump efficiency,

$\eta_{VSD} = \dfrac{P}{P_{in}}$ is the efficiency of the VSD,

P is the brake power on the pump shaft.

This ratio is valid for all serviced liquids.

The *pump efficiency characteristic* as a function of the flowrate, $\eta(q)$, is similar to an inverted U-shaped curve in Fig. 1.2. At no flow, the efficiency is zero and then rises to a maximal value in a NOP, which simultaneously serves as the *best efficiency point* (BEP). Beyond the BEP flowrate, the curve again drops. Pumps may operate in a broad range of flows but it has to be kept in mind that they are designed primarily for the BEP mode.

Operation ahead and behind the BEP flowrate results in higher hydraulic, volumetric, and mechanical losses and hence, a lower pump efficiency. A zone of the head-flow diagram, where the highest efficiency is supported may be called a *best efficiency area* (BEA). It is filled in green colour in Fig. 1.2.

According to the affinity laws, the efficiency of pumps with loads that have pure dynamic resistance keeps its value while the working point moves along a system curve. Constant efficiency characteristics superimposed above the pump characteristics are called *iso-efficiency curves*. They could be either represented in the three-dimensional space or flattened into a two-dimensional figure.
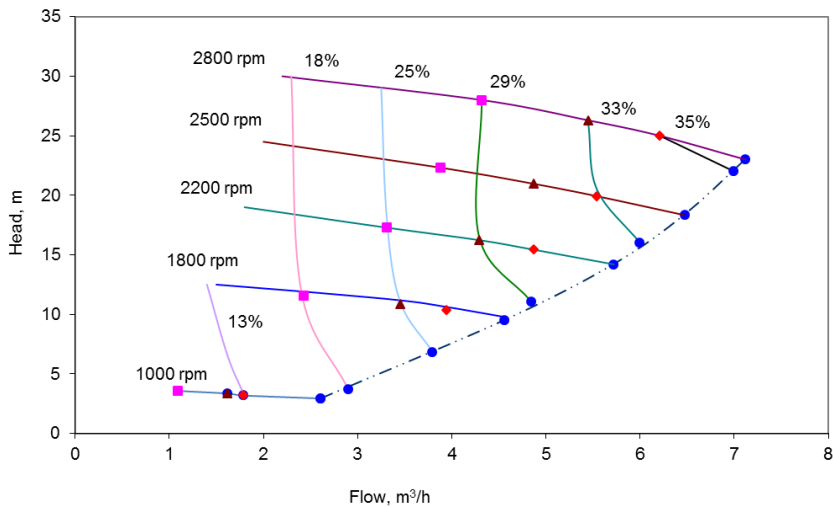
Figure 1.4 Iso-efficiency curves of the experimental setup

An example obtained from the experimental setup operated at different speeds is demonstrated in Fig. 1.4. Here, iso-efficiency traces go above the characteristics of the pump like a set of truncated U-shaped curves around the system characteristic drawn by the stroke line. One of the iso-efficiency curves, for example 33 %, bounds the BEA of this pump.

In contrast to the pump efficiency that keep a stable value while the working point moves along the system curve, the same cannot be concluded regarding the VSD efficiency. The VSD efficiency depends on two major factors: design (materials, construction, power, etc.) and operating conditions (loading, speed, power quality, ambient temperature, etc.). In practice, VSDs reach the maximal efficiency at close to 70 – 80 % loading. As the load decreases or increases, the efficiency is reduced dramatically.

Both the pump and the VSD have the highest efficiency when operating near their individual NOP, at nominal speeds and loads. Their efficiencies start decreasing substantially with speeds and loads dropping below or raising above the nominal conditions [10].

Insofar as the pump and the VSD have different NOPs and, different BEPs in the common CPP, respectively, the integrated BEA of the CPP does not correspond to the passport pump BEA. These areas move and change in size depending on the VSD loading and speed. This is an actual problem of energy-efficient management that remains open in the current situation and affects many national and company standards [14].

1.2.3 Study of torque requirements

To insure proper CPP employment, it is essential to rate the pump to its VSD. To match these two machines, it is required to develop an appropriate torque of the VSD. Using the known relation between the power P, speed n, and torque [15] designated as T in this study:

$$T = \frac{30P}{\pi n},$$ (1.14)

the torque versus the flowrate characteristic $T(q)$ may be derived from the brake power data as follows:

$$T(q) = T_0 + C_{T1}q + C_{T2}q^2,$$ (1.15)

where T_0 is pump shutoff torque and $C_{T1,2}$ are the pump torque factors. Similarly, by expanding the set of affinity laws with an additional affinity law for torque:

$$\frac{T_i}{T_j} = \left(\frac{n_i}{n_j}\right)^2,$$ (1.16)

a family of the torque versus flowrate curves may be obtained within the full speed range.

Torque may be readily calculated for any given power and speed with the help of these formulae. In simple terms, torque is proportional to the square of the speed. Again, this is true for systems with zero static head, and even in that case such an assumption must be made with caution, presuming that the CPP has no static torque. Unlike the centrifugal pump, the VSD develops very high driving torque.

1.2.4 Resume

1. Three forms of power participate in the energy conversion within the CPP: hydraulic power, brake power, and consumed power.

2. A system power characteristic connects power losses with the flowrate. A power characteristic of a pump describes the pump brake power as a function of the flowrate taking place at a constant pump speed. The break powers at different speeds are estimated with the help of an affinity law for power.

3. Differences between hydraulic and brake powers are explained by volumetric, mechanical, hydraulic losses in the pump. A difference between the brake and the consumed power exists due to electrical energy losses in the VSD. The ratio of the hydraulic and the electrical power shows the CPP efficiency, which is a nonlinear function of the speed and torque.

4. To produce the required hydraulic power, the VSD has to develop proper rotational torque. Therefore, the pump is additionally described by a torque characteristic and an affinity law for torque.

1.3 Challenges in Management Methods as the Motivation of the Thesis [IX, XII]

1.3.1 Challenges of pump regulation by throttling

The most common adjusting device for a constant-speed CPP is a control valve in the discharge line, which changes the amount of liquid delivered to the process. The valve takes a pressure drop equal to the difference between the pressure supplied by the pump and the pressure required by the process. This method is called regulation by *throttling* [16]. By throttling, the flow control, the level control, or a temperature control (for example, coolant flowrate) may be performed.
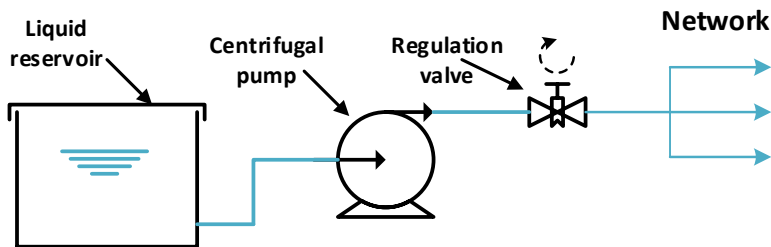
Figure 1.5 Throttling-operated CPP

The throttling-operated CPP in Fig. 1.5 comprises a constant-speed pump and a regulation valve. Because throttling is a mechanical method of the flowrate reduction, various valve angles affect different flowrates and corresponding heads [9]. Throttling changes the system curve by an increase of friction losses. This steepens the system resistance curve with a resultant decrease in the flowrate, but the pump curve is not altered and the pump continues to operate at full speed.

The drawbacks of throttling relate to the mechanical stresses, such as excessive pressure and temperature distortions in the CPP that can cause premature seal or bearing failures. More importantly, this also consumes an additional amount of energy. As the head or pressure losses across the throttling valve are obviously energy losses, throttling is an energy wasteful flow control method.

Thus, this method is recommended mainly when the demanded regulation changes temporarily, when the flowrate deviates from the nominal value for short periods of operation [17]. It is encountered, mainly on radial pumps that have flatter pump characteristics and suit better for such kind of control.

1.3.2 Challenges in pumping speed regulation

In most variable-speed applications, the idea is to use the VSD for slowing the running speed down from the nominal speed. Today, the VSDs are among the front-ranking solutions proposed by Schneider Electric, ABB, Danfoss, and other manufacturers.
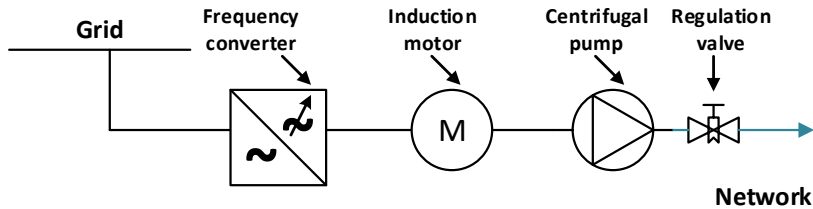
Figure 1.6 Pressure and/or flow speed regulation system

The CPP includes a variable-speed centrifugal pump and a VSD (Fig. 1.6). Multiple studies have demonstrated the benefits of VSDs in feeding pumps. In view of MEC, the method of discharge regulation by varying the pump speed is one of the most economical approaches. This method enables reduction of the energy to the pump with the decrease in speed as compared to throttling where full energy is supplied even for a lower operating point. Introducing a VSD to the CPP allows controlling the pump speed using only electrical energy needed to produce a demanded flowrate.

In addition to speed regulation, VSDs improve the controllability of the process and enhance their reliability by minimizing the number of pump switching operations, which improves the pump lifecycle and reduces its maintenance costs. Though the speed control is often more expensive than throttling [17], wear on the pump and valves is lower, hence the lifespan of both is generally increased at dropping energy consumption. At this, the pressure level may be reduced, which helps to decrease the mechanical stresses generated by throttling devices. Unlike throttling, speed control leaves the piping system characteristic unchanged, while the pump characteristic moves in accordance with the speed change.

Another benefit of VFDs is their soft-starting capability [18]. During start-up, most motors experience inrush currents that are 5 – 6 times higher than normal operating currents. This high current fades when the motor spins up to normal speed. VDFs allow the motor to be started with a lower start-up current thus reducing the wear on the motor and its controller.

However, pump speed adjustment is not appropriate for all systems. VSD-driven pumps meet several problems that need solutions and improvement, especially in term of energy management perspective [18].

- One of problems concerns high-pressure, high-flow, and high-speed operation. Whenever the demanded pressure, flow, or speed levels overcome the pump NOP level, the traditional solution is to run two pumps presuming that a spare pump has been installed. In turn, multi-pump equipment raises the CPP cost and lowers its reliability. In other cases, the shaft can hit a critical speed on its way to the normal operating speed. Though it is routinely possible to increase the pump speed above the passport rating, this procedure has not been yet discussed in the literature on pumping because several mechanical problems appear in operation above the nominal speed. However, high-speed operation without an increase of the number of pumps seems a very good prospect in view of MEC.

- In applications with a high static head, slowing a pump may induce vibrations and create performance problems that are similar to those found when a pump operates against its shutoff head. For systems in which the static head represents a large portion of the total head, manufacturers apply many restrictions. For the non-Newtonian fluids at those viscosity changes with speed, careful selection should be taken in deciding whether to use adjustable pumps or throttling.

- As NOPs of pumps, their drives, and gears have usually different locations, operating out of the BEP for one of them can cause mechanical deflections, hydraulic instability, or additional electrical losses for other parts.

1.3.3 Constraints of an operating region

As shown in Fig. 1.2, pump characteristics along with system characteristics describe the CPP performance region in respect to the low flowrate, head, and speed as well as the high flowrate, head, and speed operations.

An area around the NOP is termed as an *acceptable operating region* (AOR) in the standard ANSI/HI 9.6.3-1997 [19], which states that operation outside the AOR is at the risk of increased vibration, damaging hydraulic forces, cavitation effects, and reduced service life. Although its borders are adequate, some manufacturers consider a pump as generally oversized even if it acts below 20% of the NOP flowrate, head, or speed.

In order to justify topicality of the current study, it is reasonable categorize all the AOR constraints into physically reasonable and advisable. Such restrictions as low/high head, low/high flow, and low/high speed may belong to both the first, and the second group.

Physically reasonable boarders are defined by the CPP topology, pumping liquids, piping material, etc. Pumping outside these boarders is prohibited by the manufacturers.

Low-head operation. As liquid flows from the pump inlet into the impeller, it undergoes a drop in the head due to acceleration. If the liquid entering contains dissolved air, tiny bubbles of this air come out as the head drops. This phenomenon is called *cavitation*. When cavitation occurs in a pump, it has the potential to cause performance degradation, namely, losses of the head and capacity, permanent damage due to erosion, and mechanical failure of pump components and structures. To assign the minimum flow referred to the minimum capacity of a pump, that prevents its thermal and mechanical damage, a property called a *net positive suction head* (NPSH) is indicated by a manufacturer. Its supplementary characteristic shows the measured head obtained while throttling the suction flow until a 3 % drop in the head is observed at any particular flowrate.

Low-flow operation. The lowest pump delivery that can be maintained for extended periods of operation without excessive wear or even damage is called a *minimum flowrate* [17]. All the centrifugal pumps encounter difficulty at low flow. In general, the low-flow problems are worse for the following pumps: large high-energy, handling hot or abrasives-laden liquids, specially designed for high efficiency operation, and those operated at the low suction head. When the CPP operates very far left of the NOP, the inefficient part of the energy is expended for heating up a liquid, which may lead to potential problems, such as vapour formation, expansion of internals, overcoming the operating temperature limits, or for other purposes.

High-flow operation. There could be a case when the demanded flowrate has risen substantially above the maximal design flowrate of the pump. The traditional immediate solution in this case is to run two pumps in parallel, presuming that a spare pump has been installed [16]. Their combined curve is formed by adding their flowrates for each point on the individual pump characteristic, while keeping the same value of the head. In the single-pump CPPs, such demand is unacceptable.

Pump overloading to the right of the NOP causes problems that ultimately lead to the pump tripping. Some other important problems happen at overload resulting from clogged pipes, viscous fluids, and clotty particles in suspension that either bind up the pump or increase the density of the fluid.

Low-speed operation. System hydraulics, rather than mechanical considerations, often dictate the minimum running speed. If there is a significant static head in the system, the danger is that as speeds reduce, the pump head will drop below the system static head and the pump will be running at zero flow or will experience reverse flow if there are no check valves. Therefore, the pump speed must always be high enough to ensure that the

developed head exceeds the system static head sufficiently to maintain the minimal pump flowrate.

In addition, at low speeds such factor is often queried as less effective motor cooling due to the lower cooling fan speed. Because the power required by a centrifugal pump reduces with the cube of the speed change, the motor and other VSD applications may need auxiliary cooling. When the pump itself has a shaft-driven cooling fan in a hot service application, the reduced cooling capacity on the pump may need to be addressed.

1.3.4 Rationale of thesis topicality

An advisable area adjoins the physically reasonable boarders being the reason of the AOR constriction. The operation in this area is not recommended by the manufacturers but these recommendations are relevant. They may enlarge or decrease the AOR depending on the control methodology and tools. These restrictions may be relieved by appropriate management.

As a rule, the VSDs and pumps are designed and integrated to satisfy maximal load conditions of the CPP. In practice, most of the time, the CPPs are employed at low or medium loads due to unoccupied buildings and/or favourable atmospheric conditions. Bearing in mind the restrictions above, it was estimated in [20] that 75 % of the CPPs are oversized, many of which by more than 20 %. In the first step, it means that pumps mostly operate outside their passport BEA. Secondly, it shows that the real AOR of CPPs is narrow in terms of MEC achievement.

Although efficiencies of 50 % or lower are quite common in many pumping stations [21], it does not display, however, that all oversized CPPs always operate with high energy consumption outside the pump AOR [22]. On the other hand, even when the CPP operates within the passport BEA, it does not display the optimal operation in view of all energy optimization criteria. These two factors clearly point out that there still is a great energy saving potential in industrial and municipal CPPs equipped with more and more sophisticated controlling and monitoring applications.

One of the primary reasons of BEA constrains originates from ignorance of specific power losses in the VSDs. Most VSDs are normally running at 50 to 100 % of rated load and speed. Neglect of this factor leads to pump oversize and increased power consumption.

The second important reason is that it is impossible for the VSD to adjust pressure above the NOP pressure level and to adjust the flow above the NOP flowrate.

The third source of the narrow AOR concerns high-speed pumping abilities. Because of unreasonable constrains, for operation above the nominal speed additional pumps are often requested instead of applying high control possibilities of the contemporary VSDs [23].

This thesis relies on the optimization of pumping energy. Taking into account perspective needs in MEC, their dependence on the application areas, and alternation in CPP demands and loads, an urgency of the offered study is becoming essential. The objective of the thesis is to enlarge the AOR and to specify the BEA at the expense of areas that have not been recommended for pumping. In order to overcome the three obstacles above, an algorithm of affinity laws correction, a method of inline energy losses monitoring, and the procedures of high-pressure, high-flow, and high-speed pumping were developed in the frame of common energy management methodology and a new energy management system. The proposed approach combines benefits of throttling and the speed control and brings together both the pressure and the flowrate adjustment possibilities. Consequently, the outcome of the thesis is composed of energy consumption minimization and energy cost reduction.

1.4 Summary of Chapter 1

VSDs are among the front-ranking resources of Schneider Electric, ABB, Danfoss, and other pump manufacturers today. However, the following considerations should be taken into account.

1. CPP operating region is narrow and, even when servicing in the NOP area, the CPP efficiency appears lower than that of nominal because of ignorance of nonlinear VSD losses.

2. VSDs are commonly applied for slowing the pump speed down from its nominal value. When the demanded speed is higher, bulk multi-pump solutions are applied.

3. Although throttling is an energy wasteful flow control method, it may be effectively used for the CPP AOR enlargement.

Rationale of the thesis topicality results from its focus on the solution of the three above problems.

CHAPTER 2. HYBRID ENERGY MANAGEMENT OF CENTRIFUGAL PUMPING PLANTS

2.1 Enlargement of an Operating Region

2.1.1 Method for the inline monitoring of VSD losses

As it follows from (1.13), estimation of total power consumption of the CPP, P_{in}, is not possible without VSD losses, ΔP_{VSD}, taken into account:

$$P_{in} = P + \Delta P_{VSD}, \qquad (2.1)$$

In most cases, VSD losses for part-load operation at different speeds can be found from the manufacturers' documentation. In this study, these losses were additionally approximated accurately enough by a polynomial:

$$\Delta P_{VSD}(T,n) = \Delta P_0(n) - C_{\Delta 1}(n)T - C_{\Delta 2}(n)T^2, \qquad (2.2)$$

where, $\Delta P_0(n)$ are VSD speed-dependent losses, and $C_{\Delta 1,\Delta 2}(n)$ are the VSD speed-dependent loss factors. Normally, losses are growing in the process of loading and speeding as exemplified in Table 2.1 for the experimental setup [24].

Table 2.1 Losses (W) dependence on torque and speed for ACQ810 VSD

Speed, rpm	Torque, Nm				
	0.14	0.58	1.30	2.30	3.60
560	121	124	135	163	221
1120	131	134	145	174	236
1680	143	146	157	188	251
2240	156	158	171	203	270
2800	170	174	189	227	307

While the torque and speed values increase, the VSD efficiency grows. At the same time, it is noticeable that VSD losses grow simultaneously. One method to use this contradictory tendency in consumed power estimation and correction procedures is to furnish the control system with a lookup table, which may be applied for pumping performance optimization, correction, and prediction of the most economical mode.

The layout of the CPP capable off the *inline monitoring of VSD losses* (IML) is shown in Fig. 2.1. It includes a variable-speed centrifugal pump, pressure and flow sensors, a VSD, and a PLC-based control system. The VSD involves a pump motor M feeding by the power electronic converter, which, in turn, is managed by the *direct-torque control* (DTC) system of the traditional topology [25]. The PLC incorporates both the pump characteristic (1.2) and the

power characteristic (1.11) for the nominal speed n_N. In addition, the PLC keeps a lookup table [ΔP T n] needed for the VSD losses prediction.
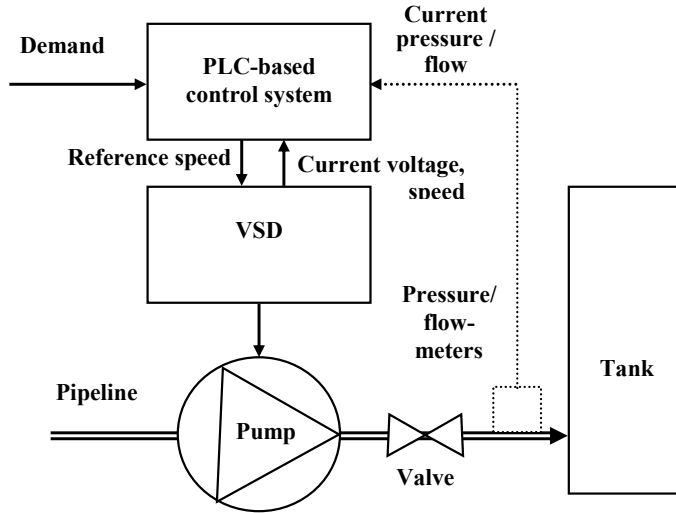
Figure 2.1 CPP with IML of VSD

The IML of the VSD method is illustrated as follows (Fig. 2.2):
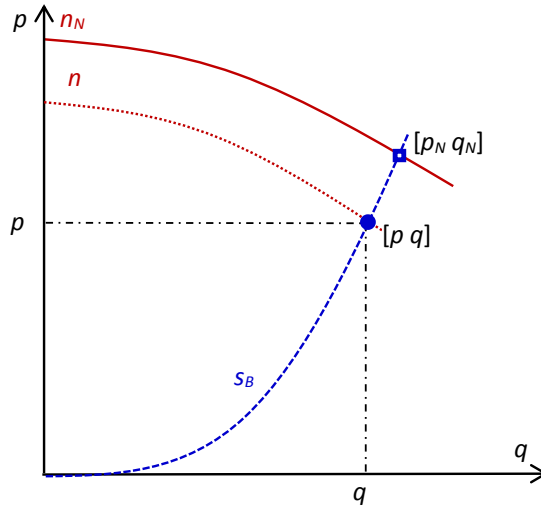
Figure 2.2 Explanation of power estimation

1. Once the pump is running, the PLC conducts periodic real-time readings on the current pressure p, flowrate q and speed n.

2. In the intersection of the nominal pump characteristic and the system curve, the nominal point coordinates [p_N q_N] are derived using the affinity laws (1.3), (1.8). Additionally, the nominal shaft power P_N is retrieved in this point from the power characteristic applied (1.11).

3. After that, the shaft power on the current speed can be found with the help of the affinity law for power (1.12):

$$P = P_N \left(\frac{n}{n_N} \right)^3 , \qquad (2.3)$$

whereas current torque is yielded from (1.14).

4. Obtained torque and speed data address the required cell of the VSD losses lookup table (Table 2.1). The losses, ΔP_{VSD}, retrieved in this way are used in (2.1) to identify the consumed power.

5. In turn, the consumed power data may be applied for moving the working point to the low-loss regions.

2.1.2 Procedure of high-speed pumping

The areas above the rated speed need the designers' attention in many applications. There could be a case when a single pump cannot meet the total head requirement within its nominal speed restrictions. At this, the operation might be shared with additional pumps. This group performance prevents pumps from being overloaded. However, the benefits of doing this – increased production, for example – often outweigh many concomitant disadvantages. Some conventional issues of multi-pump stations may be listed as follows:

• The total pump output is usually requested only in a limited period of the CPP lifespan.

• Pump selection for multi-pump installations is a key for minimizing energy costs. If the pumps are improperly chosen, the CPP reliability and overall system energy efficiency can be compromised and energy per unit volume will increase.

• Multi-pump operations are sensitive to individual pump characteristics. The total flowrate or the total head developed may not be a simple addition of the individual flowrates and heads. In cases when pumps have dissimilar pump curves, a likely serious operating problem is highlighted. In this scenario, the pump with the lower head may be stalled, and assuming that a non-return valve has been fitted, it will be running at closed valve with all the attendant risks and damage.

On the other hand, a sufficiently high head might be also obtained by running the single pump at the speed above the nominal value. This is a case, of high-speed pumping (HSP).

According to [15], in the case of induction motors the applied voltage is approximately proportional to a product of the designed value of the core flux (at which the motor will perform best) and the source frequency. Therefore, in all cases when the voltage and frequency are scaled in a manner that their ratio

remains the same as the nameplate values, it should be normal because no excessive core losses occur.

At the same time, the voltage may not overcome the motor rating due to insulation stresses. Once the maximal voltage is achieved, it is normal practice to keep it constant. If higher speeds are requested, operation in the field-weakening mode is to be taken into account. Contemporary VSDs provide successful operation in this so-called "constant power region" at the speeds above the rated value within the limited motor torque. Therefore, pumping in this region under the accurate torque control would bring many benefits without increasing the number of pumps.

Maximal speed and power restrictions at different speeds are as follows:

$$n \le n_{max}$$
$$P \le P_{NOP} \qquad , \qquad (2.4)$$
$$P_{VSD} \le P_{VSD\_NOP}$$

where $P = f(n)$ comes from (1.11) and (1.12); $P_{VSD} = f(T, n)$ results from (2.2); $T = f(n)$ follows from (1.15) and (1.16); n_{max}, P_{NOP} and P_{VSD_NOP} are nameplate speed and power data from manufacturer's documentation. Consequently, speed and power restrictions depend on both the pump and the pipeline states together and may change during the pumping process.

In Fig. 2.3, the constant power borderline is exemplified for the experimental setup. This diagram clearly demonstrates that to meet the constant power requirement, the maximal head level might approach almost 50 m at higher speeds while the nominal head of the tested pump does not overcome 30 m at the nominal speed of 2800 rpm.
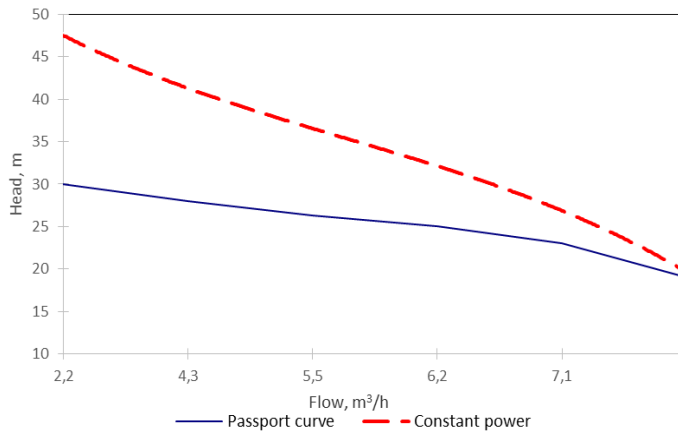
Figure 2.3 The constant power region borderline

Taking into account mechanical restrictions of the pump and the motor, the real maximal speed borderline is usually below the obtained 3500 rpm.

Nevertheless, this methodology offers important enlargement of the demanded head levels by overcoming an impossibility to increase the head due to the speed restriction.

The system layout shown in Fig. 2.1 fully meets the HSP conditions. Every time the shaft power is estimated, both the speed and the power have to be validated by appropriate software. If their values fit the permissible speed range, the remaining PLC procedures aim to predict the consumed power, which is validated as well. If its level fits the permissible power range, the PLC will send the demanded speed signal n* to the VSD and continue the CPP performance in the traditional way.

2.1.3 Resume

1. The IML of the VSD method is based on the current information about the system state and the speed and on the tabulated VSD loss lookup table.

2. The IML of the VSD method contributes to waste energy minimization by moving the working point to the low-loss regions.

3. The new HSP procedure opens a way for providing the best overall efficiency by running the minimal number of pumps for specific system demand conditions.

2.2 Pressure and Flow Maintenance with IML and HSP [VIII]

2.2.1 Related studies of pressure management and problem statement

A lack or excess of pump pressure can degrade the CPP performance.

For example, in aerospace applications where flight surfaces are moved by hydraulic actuators, pump pressure fluctuation may result in disastrous consequences. In other applications, pressure alternations cause unintentional leakages and the liquid volume instability due to temperature changes. Some common cases where pressure stabilization is requested are the district heating networks and hot water circulation systems [26]. Pressure maintenance in such systems is aimed to prevent cavitation.

Recent publications in the field of pumping management have brought accurate pressure adjustment to the spotlight. In [27], model-based pressure monitoring was proposed to detect and partially isolate some faulty working conditions. The feed-forward fuzzy immune algorithm reported in [28] is intended for tuning controllers in time-varying nonlinear pressure loops. The proportional pressure control of the multi-valve heating system with a single VSD-fed pump is discussed in [29]. A constant-pressure supply water station, which adopts an embedded PLC-based controller, is described in [30]. Using a new PLC built-in fuzzy PID controller suggested in [31], pressure regulation was improved. Under invariant control presented in [32], steam pressure

overshoots were decreased in comparison with the traditional feedback control methods. Regretfully, all these studies mitigated energy-saving problems.

Only several studies were focused on pressure maintenance assuming energy-efficiency issues. In [13], a method for centrifugal pump process identification was established based on the flowrate and head readings obtained from the manufacturers' characteristics. Later, in [33] and [34], the efficiency was introduced as a major quality index for the pressure control.

Below, a pressure maintenance problem is formulated for the case when the demanded pressure $p*$ is fixed at a variable system state of the VSD-fed single pump.

Let us assume initially that the CPP was in a working point $[p*q_i]$ shown in Fig. 2.4. It means that a pump rotating with a current speed n_i maintained demanded pressure $p*$ at some flowrate q_i of the system state s_i.

Assume that, under an impact of disturbances, the system has been turned into a new state s. This is called a transition of the working point to the position $[p\ q]$ of the pressure p and flowrate q at the same speed n_i. Using the speed control, the working point of the pump can be moved in order to match the prescribed pressure $p*$ in the new system state. The control task is to shift this working point to a new position $[p*q*]$ of the system characteristic s in order to maintain the prescribed pressure $p*$ at some new speed $n*$, which has to be searched by the control system.
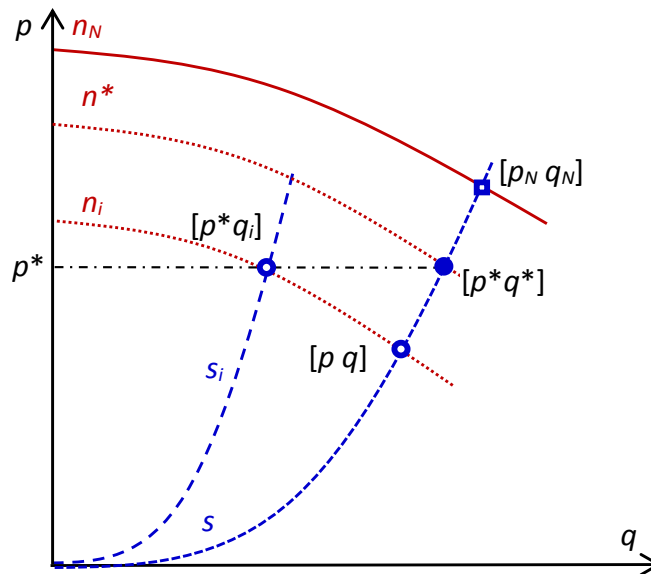
Figure 2.4 The pressure maintenance problem

2.2.2 Energy-efficient pressure maintenance

The new CPP providing pressure maintenance fits to Fig. 2.1. The PLC incorporates the pump characteristic (1.2) for the nominal speed n_N and power characteristic (1.11) for the same speed. In addition, the PLC keeps a lookup table $[\Delta P\ T\ n]$ for VSD losses prediction.

Once the pump is running, the PLC conducts periodic real-time readings on the demanded pressure p^*, current pressure p, and current flowrate q in the pipe network. Any difference between p^* and p shows that the system allocated an invalid state $[p\ q]$ where $p \neq p^*$. In reply, the PLC performs the following actions.

1. First, the PLC estimates the friction factor C_S of the new system characteristic s by applying p and q readings in (1.1) where p replaces h:

$$C_S = \frac{p}{q^2},\qquad(2.5)$$

2. The working point is to be shifted to a new location $[p^*q^*]$ on this system curve.

3. The flowrate at the demanded pressure level may be found from (1.1) where h is replaced by p:

$$q^* = \sqrt{\frac{p^*}{C_S}},\qquad(2.6)$$

4. In the intersection of the nominal pump characteristic and the system curve, the nominal point $[p_N\ q_N]$ coordinates are derived using the affinity laws. Additionally, the nominal shaft power P_N is retrieved in this point from the power characteristic (1.11).

5. Now, the searched speed and appropriate shaft power can be found with the help of affinity laws (1.8) and (1.12):

$$n^* = n_N \sqrt{\frac{p^*}{p_N}},\qquad(2.7)$$

$$P^* = P_N \left(\frac{n^*}{n_N}\right)^3\qquad(2.8)$$

6. Both the speed and the shaft power have to be validated. If their values fit the permissible range, the remaining PLC procedures aim to predict the consumed power. It is especially important if the new working point $[p^*q^*]$ is located in high-speed or high-load areas.

7. To jump from the shaft power to the consumed power, VSD losses (2.2) have to be taken into account as given in (2.1). They are acquired from the lookup table (Table 2.1) based on the speed n^* and torque T data (1.14).

8. Consumed power is validated as well. If its level fits the permissible range, the PLC sends the demanded speed signal n^* to the VSD.

2.2.3 Energy-efficient flowrate maintenance

Flow maintenance is an actual problem of pumping management. According to [35], even the flowrate instability of 20 % can increase the input power requirements up to 50 %. Accuracy of the flowrate maintenance is an important criterion used to compare one pumping system with another or to select a proper pump for a station [36]. In particular, it concerns the centrifugal pumps the flowrate adjustment of which is more complicated than that of positive displacement pumps that can provide the required flow independent of the system it is installed in.

To begin with, a flowrate maintenance problem is formulated for the case when the demanded flowrate q^* is fixed at the variable system state of the VSD-fed single pump.
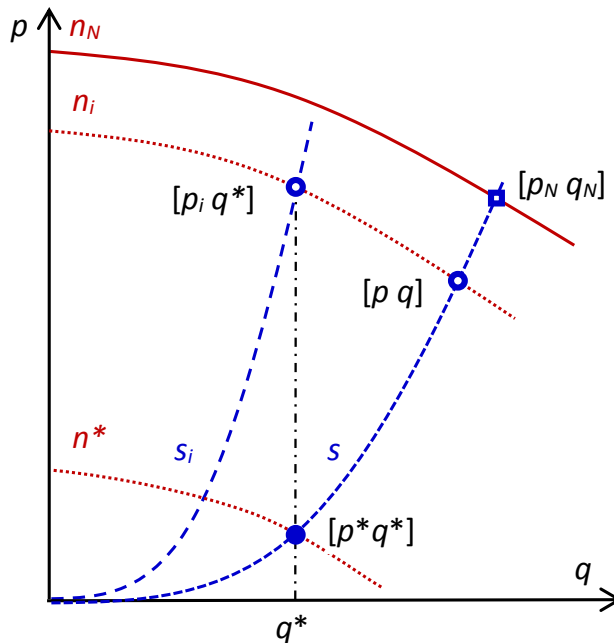
Figure 2.5 Flowrate maintenance problem

Let us assume initially that the CPP was in a working point $[p_i\, q^*]$ shown in Fig. 2.5. It means that a pump rotating with a current speed n_i maintained the demanded flowrate q^* at some pressure p_i of the system state s_i.

Assume that, under an impact of disturbances, the system has been turned into a state s. This is called a transition of the working point to a position $[p \; q]$ at the same speed n_i. The control task is to shift this working point to a new position $[p^*q^*]$ of the system characteristic s to maintain the prescribed flowrate q^* at some new speed n^*, which has to be found.

The layout of the CPP providing flow maintenance is the similar to that shown above in Fig. 2.1 where the new software is used.

After pump running, the PLC makes periodic real-time readings on the demanded flowrate q^*, current flowrate q, and current pressure p in the pipe network. Once a difference between q^* and q is detected, the PLC performs the following actions:

1. First, the PLC estimates the friction factor C_S of the new system characteristic s by applying p and q readings in (1.1) where p replaces h. The new working point $[p^*q^*]$ is to be located on this system characteristic.

2. Appropriate pressure may be found from (1.6) as follows:

$$p^* = C_p q^2 \qquad\qquad (2.9)$$

3. In the intersection of the nominal pump characteristic and the system curve, nominal point coordinates $[p_N \; q_N]$ are derived using the affinity laws. Additionally, the nominal shaft power P_N is retrieved in this point from the power characteristic (1.11).

4. Now, the searched speed and the corresponding shaft power can be found with the help of (2.7) and (2.8).

5. Both the speed and the power have to be validated. If their values fit the permissible range, VSD losses (2.2) are acquired from the lookup table (Table 2.1) based on the speed n^* and torque T data from (1.14).

6. If the consumed power fits the permissible range (2.4), the PLC sends the demanded speed signal n^* to the VSD.

2.2.4 Resume

1. Based on the inline energy losses monitoring method and HSP procedure, the new solutions of the pressure maintenance and flow maintenance problems were proposed assuming their energy-efficiency issues.

2. The new pressure maintenance system promises some benefits in aerospace equipment, to compensate unintentional leakages and decrease variations in the liquid volume due to temperature changes in district heating applications, and hot water circulation networks.

3. The new flowrate maintenance approach is perspective for heating circulating systems the delivered heat power of which is related to the flowrate instead of pressure and for the systems where throttling is either not effective or potentially dangerous.

4. The system proposed acts successfully either for pressure or for flow adjustment but cannot solve both of the problems simultaneously.

2.3 Pumping with Mutual Throttling and Speed Regulation [XIV][XV]

2.3.1 Introducing the hybrid energy management methodology

The pressure and flow loops of pump and valve systems have complex character due to the presence of multi-variable, nonlinear, and time-varying parameters. For that reason, it appeared problematic to achieve satisfactory regulation using the traditional PID control. Conventional PID regulators are suitable mainly for linear systems, as they require an accurate model of the control object and knowledge of all its parameters for tuning. Due to the great inertia and fluctuations of the liquid supply system, such a regulation often leads to pressure and flow instability due to the difficulties with the sufficiently accurate system description [37].

Several methods have been offered to resolve this problem. The first method proposed in [28] represents a feedforward modal controller, which envisages PID parameters adjusting in real time along with the network layout and pressure loop changing.

A simplified energy management approach called a proportional pressure control was proposed in [38]. Where the pump pressure level was adjusted according to the flowrate through the pump. Lower flowrates resulted in a lower pressure reference for the pump. This method did not improve the pumping efficiency. However, it was directed to energy saving in some pumping applications where separate system processes might be optimized in this way.

Following the same way, in [11] the pressure control was intended to keep proportionality between the pump head and flowrate. This was done by changing the speed in relation to the current flowrate. Such a regulation was suitable for closed heating systems where the pressure level above the radiator valves is kept almost constant despite changes in heat consumption. The result was lower energy consumption by the pump and a lower risk of noise from the valves.

A similar solution of Grundfos provides minimization of the pump power requirement by changing pressure demand proportionally to the pump speed. Selection of the control curve is based here on hydraulic conductivity and its saturation. This method has affected pump pressure regulation that is always above the minimal demanded level. Unfortunately, hydraulic losses were not

completely minimized, thus minimal energy consumption was not reached yet [38].

In this chapter, a new energy management methodology is offered. This instrument is intended for carrying out both pressure and flowrate adjustments using mutual throttling and speed control.

The essence of the methodology is the CPP organization allowing pumping with MEC. Namely, this means minimization of the network resistance while all other system requirements are met. The core of this approach is represented by the new CPP layout with appropriate hardware and software in the frame of the energy management methodology providing the system monitoring and making optimal decisions.

To design the general CPP layout, the demanded head/flowrate operating region is provisionally assigned. At this, performance accuracy is assumed to be regularly alternating within a sufficiently broad range at high load instability [28]. As a consequence, the hybrid pump and valve combined system topology (Fig. 2.6) is created as an association of two channels – the pump control loop and the valve control loop – fed by an *energy management module* (EMM). Both the pump VSD and the valve drive receive control signals from this EMM, which searches a solution of the consumed power minimization problem. Individual drive feedbacks are introduced to eliminate offsets caused by the speed and valve position instability. An online parameter estimation module is integrated within the proposed framework in order to cope with changing operating conditions.
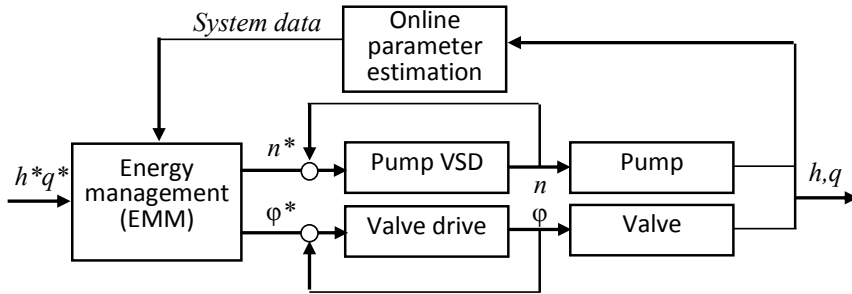
Figure 2.6 Layout of the offered system

The EMM resolves the following problem: within the prescribed head/flow operating region $[h*q*] \in \{[h_{min}, q_{min}],.. [h_i, q_i],.. [h_{max}, q_{max}]\}$, find an i-th working point $[h_i q_i]$, in which MEC is achieved, $P_{in\,i} \to$ min.

To provide the best utilisation of the available power depending on the process demands and load alternations, the EMM provides three important functions:

- performance analysis,
- system learning,
- hybrid management.

2.3.2 Performance analysis of a hybrid system

The performance analysis aims to prescribe one of the multiple types of control dependending on the size of the demanded head/flowrate operating region.

If a fixed static head or a fixed pressure level is demanded ($h^* = h_{min} = h_{max} \leq h_{NOP}$; $p^* = p_{min} = p_{max} \leq p_{NOP}$), then accurate head/pressure maintenance is needed as explained in Section 2.2.2. If a demanded static head or a demanded pressure level overcomes the nominal value ($h^* = h_{min} = h_{max} > h_{NOP}$; $p^* = p_{min} = p_{max} > p_{NOP}$), then throttling is produced as explained in Section 1.3.1.
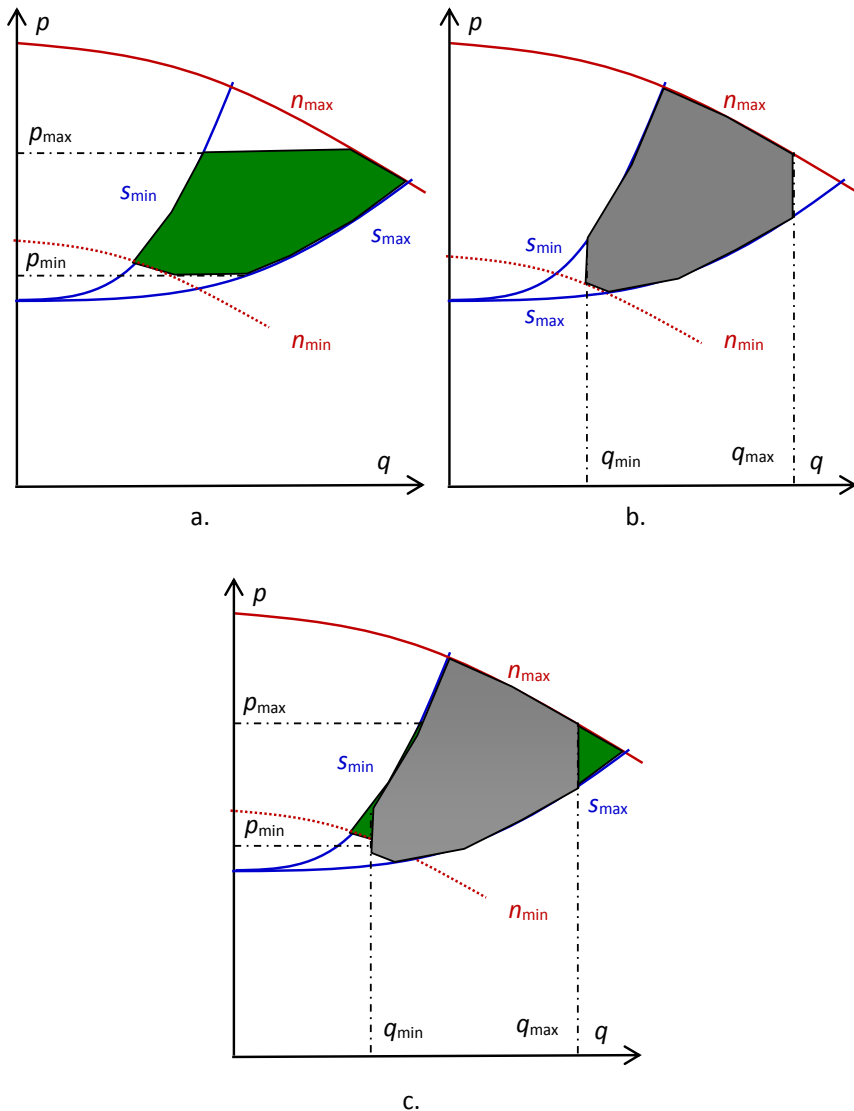
Figure 2.7 Achieving MEC at different demands

If the only targets of the application concern flow reduction in a CPP or the demanded flowrate is to be supported in a narrow margin ($q^* = q_{min} = q_{max} \leq q_{NOP}$), then accurate flow maintenance explained in Section 2.2.3 is the correct way to take. If a demanded flowrate overcomes the nominal value ($q^* = q_{min} = q_{max} > q_{NOP}$), then throttling is produced as explained in Section 1.3.1.

If the demanded head and flow margins are smart enough, mutual head and flow management may be introduced. In this case, much is dependent on the range and the rate of the demanded head/flow changes with time as well as the load instability on the one hand, and on the management criteria on the other hand.

To achieve MEC and to produce a demanded head h^* within the permissible head tolerance [h_{min} h_{max}], speed tolerance [n_{min} n_{max}], and throttle tolerance [φ_{min} φ_{max}], the control system has to search a MEC working point and to run the pump at the required pumping speed n^*. At this speed, an appropriate setting of the throttle valve φ^* is to be assigned (Fig. 2.7, a).

On the other hand, to achieve MEC and produce a demanded flowrate q^* within the given flow tolerance [q_{min} q_{max}], other pumping speed n^* and throttle valve angle φ^* are to be required (Fig. 2.7, b). In the common case, superposition of both regions will meet an absolute MEC condition (Fig. 2.7, c). In this way, a flexible management procedure is proposed, which combines both throttling and speed adjustments.

2.3.3 Learning of a hybrid management system

Once the pump is running first, the procedure of the EMM learning is starting to prepare the map of all the permissible CPP working conditions. Its algorithm is shown in Fig. 2.8.

1. First, an AOR {n_{min}, n_{max}, C_{min}, C_{max}} is assigned and both the speed n and the system friction factor C are initialized. The pump is running at the initial speed while the valve is set to the initial position.

2. At this stage, current pressure and power are acquired from appropriate sensors. The flowrate may be obtained from the flowmeter or with the help of the sensorless flow estimation procedure described in 4.1.2.

3. The corresponding system map row is generated.

4. By regulation of the valve position, the friction is increased, and the next map row is generated.

5. These steps are repeated until the maximal friction is reached.

6. The same operations are repeated at other speeds.

```
                    ( Start )
                        │
        ┌───────────────────────────────┐
        │ n_min, n_max, C_min, C_max     │
        │ n = n_min, C_s = C_min         │
        └───────────────────────────────┘
                        │
        ┌──────────────────────┐
   ──→  │      Read p, P_in     │
        └──────────────────────┘
                        │
        ┌──────────────────────┐
        │      Estimate q       │
        └──────────────────────┘
                        │
        ┌──────────────────────┐
        │    New table row      │
        │    n, C, p, q, P_in   │
        └──────────────────────┘
                        │
        ┌──────────────────────┐
        │      C + ΔC           │
        └──────────────────────┘
                        │
   No  ◇ C > C_max? ◇
   ←────
                   │ Yes
        ┌──────────────────────┐
        │      C = C_min        │
        │      n + Δn           │
        └──────────────────────┘
                        │
   No  ◇ n > n_max? ◇
   ←────
                   │ Yes
                ( Stop )
```

The flowchart contains, in order:

- Start
- n_{min}, n_{max}, C_{min}, C_{max}; $n = n_{min}$, $C_s = C_{min}$
- Read p, P_{in}
- Estimate q
- New table row n, C, p, q, P_{in}
- $C + \Delta C$
- $C > C_{max}$? — No (loop back), Yes
- $C = C_{min}$; $n + \Delta n$
- $n > n_{max}$? — No (loop back), Yes
- Stop
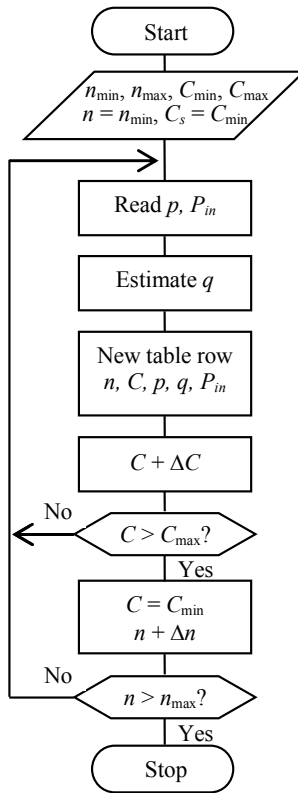
Figure 2.8 Learning procedure of the EMM

As it follows from this tabular example, the consumed power grows in step with the flowrate and speed increase. As the pump speed and power are restricted by their maximal and minimal values, the permissible consumed power is bordered as well. Therefore, at the first glance, it is advisable to choose the left most and top cells of this table to produce MEC operation.

Nevertheless, dependence of the consumed power on the head (pressure) and the flowrate is not linear. One may notice some couples of equal data in Table 2.2. For instance, 707 W appears at $n = 2200$, $C = 0.2$ and $n = 2500$, $C = 3.2$; 830 W – at $n = 2500$, $C = 0.8$ and $n = 2800$, $C = 12.8$. In means, that subsidiary criteria have to be applied for the control in addition to MEC, such as a flowrate restriction. In operation, the demanded head/flow tolerance [$h*q*$] covers only at small part of the system lookup table and the choice of the best control has many more constraints. In general, however, the approach overcomes both the throttling and the speed adjustment borders associated with the limited tolerance of the prescribed head levels beyond the pump BEP.

Table 2.2 System map of the experimental setup

Speed n, rpm	Friction C	Pressure p, bar	Flow q, m³/h	Power P_{in}, W	Speed n, rpm	Friction C	Pressure p, bar	Flow q, m³/h	Power P_{in}, W
1800	25.6	1.08	0.71	312	2800	25.6	2.60	1.10	802
	12.8	1.06	1.00	320		12.8	2.57	1.55	**830**
	6.4	1.04	1.40	332		6.4	2.52	2.18	880
	3.2	1.01	1.95	348		3.2	2.45	3.03	940
	1.6	0.97	2.69	368		1.6	2.34	4.19	1016
	0.8	0.90	3.67	392		0,8	2,17	5,70	1109
	0.4	0.79	4.88	419		0.4	1.92	7.59	1214
	0.2	0.65	6.26	446		0.2	1.58	9.73	1319
2200	25.6	1.61	0.87	460	2900	25.6	2.87	1.14	876
	12.8	1.59	1.22	476		12.8	2.84	1.61	913
	6.4	1.56	1.71	497		6.4	2.79	2.25	963
	3.2	1.51	2.38	526		3.2	2.71	3.14	1029
	1.6	1.44	3.29	562		1.6	2.58	4.34	1114
	0,8	1.34	4.48	607		0.8	2.33	5.91	1218
	0.4	1.18	5.96	657		0.4	2.06	7.86	1335
	0.2	0.97	7.65	**707**	3100	25.6	3.28	1.22	1040
2500	25.6	2.07	0.99	611		12.8	3.24	1.72	1085
	12.8	2.05	1.39	634		6.4	3.18	2.41	1146
	6.4	2.01	1.94	666		3.2	3.09	3.36	1227
	3,2	1,95	2.71	**707**		1.6	2.95	4.64	1332
	1.6	1.87	3.74	762	3300	25.6	3.72	1.30	1226
	0.8	1.73	5.09	**830**		12.8	3.67	1.83	1280
	0.4	1.53	6.77	902		6.4	3.61	2.56	1355
	0.2	1.26	8.69	976	3500	25.6	4.18	1.38	1436

2.3.4 Employment of a hybrid management system

The system shown in Fig. 2.6 includes a pump VSD, which motor fed by the *power electronic converter* (PEC) is supervised by the DTC system of the traditional topology [15]. The VSD estimates motor torque T and speed n by sensing stator currents and voltages. The valve servo system includes a servomotor fed by its own PEC under the control equipment. The EMM incorporates the lookup tables of the speed and consumed power.

During pump operation, the PLC conducts a periodic real-time detection on the demanded tolerance [$h*q*$] and the current pressure and the flowrate [$h\ q$] in

the pipe network. At any time, when their change is detected, the energy management algorithm shown in Fig. 2.9 is starting.
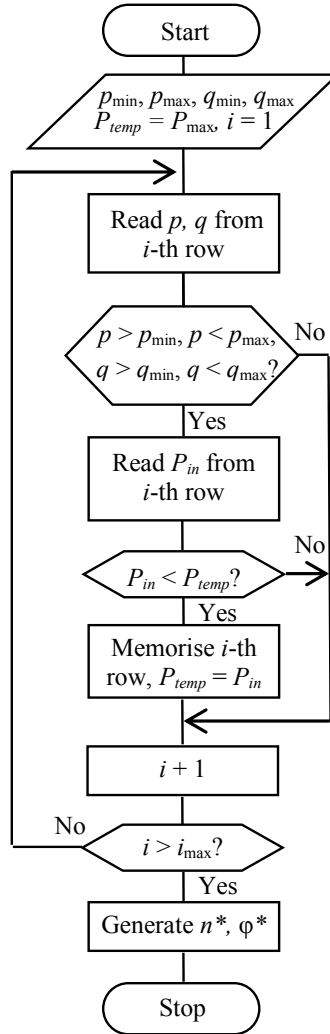
Figure 2.9 Energy management algorithm

1. First, the demanded tolerance $[p^*\ q^*] = \{p_{min},\ p_{max},\ q_{min},\ q_{max}\}$ is assigned and the initial power P_{temp} and the row counter i are initialized.

2. If the i-th row of the power lookup table fits the $[p^*\ q^*]$ tolerance and its consumed power P_{in} is less than P_{temp}, this line number will be stored in the PLC memory.

3. In the same way, all the rows of the lookup table are scanned to find the row providing pumping condition with the minimal power.

4. Once the last row is scanned, the row of the minimal power is selected from the speed lookup table for the generation the demanded speed $n*$ and valve position $\varphi*$ needed for MEC.

While the normal amount of liquid is detected, the CPP has a stable operation under this control. Once the requested pressure or the flowrate reach the level, where the pump cannot guarantee the stable pressure level in the network, an "underpressure" or "underflow" signal is detected by the control system. At this, the PLC needs to stop the pump. On the contrary, since liquid consumption reduces below a permissible level, the "overpressure" signal is detected, at which the PLC stops the pump as well.

2.3.5 Resume

1. The new energy management methodology is intended for both pressure and flowrate adjustments independently or simultaneously, using mutual throttling and speed control.

2. In contrast to the traditional variable-speed pumping at which demanded pressure or the demanded flowrate may not overcome their nominal levels, the developed hybrid system permits high-pressure or high-flow operation within a permitted pressure-flow area.

3. In contrast to the traditional pumping at which either the demanded flowrate or demanded pressure is fixed, the developed hybrid system opens the possibility for optimal energy management within a permitted pressure-flow area, including the modes when both the demanded flow and pressure are assigned simultaneously.

4. Unlike the well-known PID control, here the model-based predictive control is introduced, at which the minimal supply power is provided at changing network and demand situations.

2.4 Summary of Chapter 2

The following scientific results were obtained based on the above part of the research:

1. To navigate a working point to the low-loss pumping areas, a method for inline monitoring of energy losses has been proposed.

2. To raise the permissible pumping speed without increase of pumps number, a procedure of high-speed pumping has been designed.

3. Based on these keystones, an energy management methodology has been offered, which provides best energy utilization at fluctuating demands and loads associated with pumping.

4. As an outcome, a hybrid management system has been elaborated to carry out pressure and flowrate maintenance with mutual throttling and speed control.

CHAPTER 3. EXPERIMENTAL AND SIMULATION RESEARCH OF ENERGY MANAGEMENT

3.1 Research in Experimental Setup

3.1.1 Experimental setup layout and composition

To optimize pump performance, reduce the number of test runs of real machines, and provide their safety, specialized test benches have been developed by research institutions. Experimental setups developed by different pump manufacturers mostly relate to the management, optimal configuration, and proper layout of control equipment.
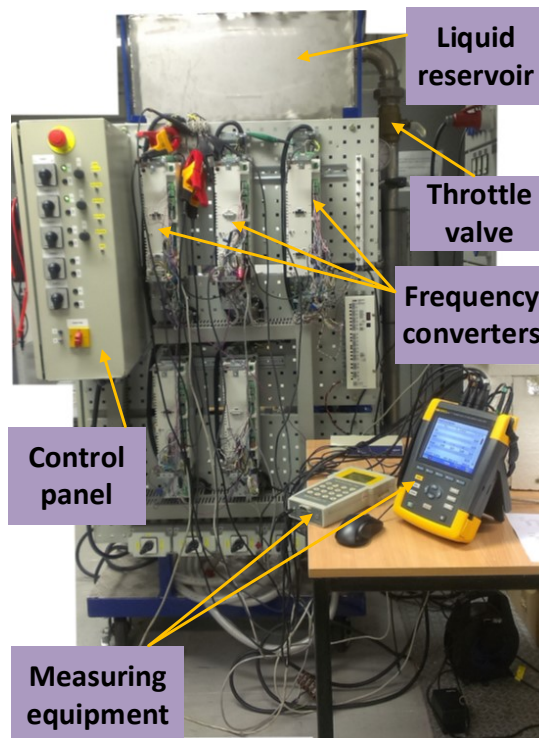

Figure 3.1 Experimental setup

To explore the CPP operation, an experimental setup (Fig. 3.1) with the following equipment was used in this research:

- centrifugal pump Ebara CDX 120/12, 0.9 kW, 2800 rpm, with impeller diameter of 157 mm;

- VSD ABB ACQ810-04-02A7-4, 1.1 kW, 3 A, 400 V, 2800 rpm equipped with the pump control DriveStudio firmware;

- ABB PLC AC500 PM 571 connected to the VSD via the Profibus with 1.6 µs cycle-per-instruction time when processing floating-point calculations;

- pressure transmitter MBS 3000 from DANFOSS, 4 – 22 mA;

- ultrasonic flowmeter PORTAFLOW SE from Micronics.

The main objectives of the developed setup are as follows:

- investigation, validation and demonstration of control techniques;
- assessment and verification of novel software;
- support for commercial consulting, research and testing for enterprises and students.

CPP performance is managed with the applied software. The characteristics of the pump and piping network can be changed during experimentation, and the experimental results enable observation of pumping processes in several adjustment methods. The setup ensures broad opportunities for pressure, flowrate, power, and energy use control and monitoring. Setup data are shown in Table 3.1.

Table 3.1 Experimental Setup Data

Parameter	Value	Parameter	Value
Tank total volume, m^3	0.12	Pipe material	Steel
Liquid volume, m^3	0.09	Pipe roughness, mm	0.15
Type of valve	Ball	Pipeline length, m	3.70
Pipe inner diameter, mm	58.00	Pipeline bend	90°
Wall thickness, mm	1.50	Pipeline elevation, m	1.60

Induction motors have the following data: power – 1.1 kW, voltage – 400 V, current – 4.5 A, speed – 2760 rpm. Every induction motor is supplied from an individual PEC with a DTC control board on the Texas Instruments 2812 processor. It includes a circuitry for digital and analogue input/output signals conditioning, RS-232 and RS-485 communication adapters, and flash memory. The main functions of the control board are as follows:

- control of the modulation process, running the speed control, and providing the correct reference to the power unit;

- adjustment of a pumping process, setting speed references, and keeping the process variables at the setpoint;

- tuning up and monitoring the process of pumping.

All these functions are accessible through the Fieldbus protocols that enable acquisition of all the parameters from the PEC continuously. The control board supports also embedded Modbus communication and such protocols as Profiubus, Device NET, and CanOpen.

The DTC unit of a PEC reads the motor currents and voltages from sensors and converts them to the dc orthogonal signals for the built-in model operation. In reply to the reference speed signal, the DTC unit identifies desired supply voltages for the VSD to run the pump.

The reference speed of the VSD comes from the output of the PLC, which estimates, restricts, and converts the difference of the requested and estimated data. Any time when the pipeline state changes under the disturbance, the PLC assigns the new pump speed to execute process adjustment, accuracy of which depends on the controller resolution, its algorithm, as well as the VSD parameters.

A PLC of AC500 series from ABB was assembled during current research and equipped as follows:

- communication module CM572 DP to connect PLC to a Profibus adapter FPBA-01;

- digital-analogue module DA501 for PLC operation without connection to a computer via a network;

- CPU module PM573;

- profibus DP adapter FPBA-01;

- toggle switches;

- measuring instruments.

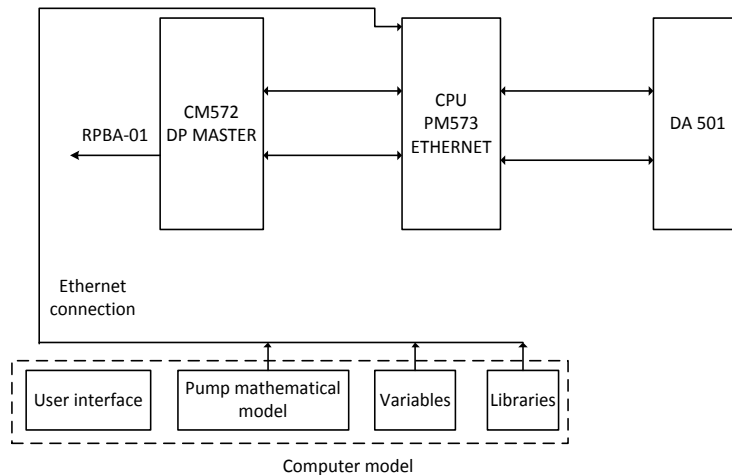The PLC functional circuit and appearance are shown in Figs. 3.2 and 3.3.

Figure 3.2 Functional circuit of PLC and computer software: CPU PM573 – Central processing unit to store and process the VSD and PC data, CM572 DP – Profibus communication module between CPU and Profibus DP-adapter RPBA-01 to exchange VSDs and PLC parameters, DA 501 – digital-to-analog input/output interface
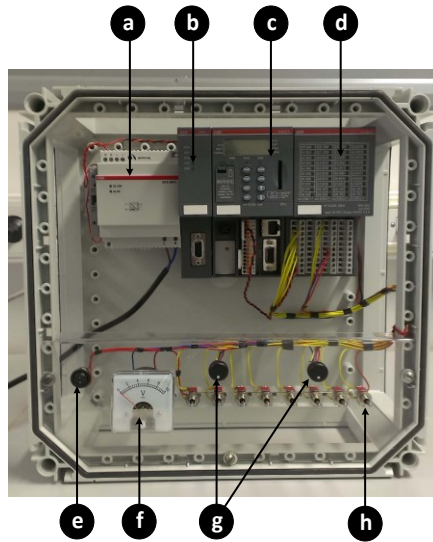
Figure 3.3 PLC AC500: (a) – Power supply, (b) – CM 572 DP MASTER, (c) – CPU PM573 ETHERNET, (d) – DA 501, (e) – ON/OFF switch, (f) – Voltmeter, (g) – Potentiometers, (h) – Digital inputs

As a tool suitable both for pump control and for PLC, an ABB DriveStudio toolkit was used. To obtain the required system information, ABB DriveSTudio applies the model-based flow monitoring method. For pressure and flow estimation and for plotting the pump and system curves in the experimental setup, the DriveStudio pressure/flow calculation functions are used that provide an accurate derivation of the flowrate without external flowmeter installation. The flow is calculated based on the database information, such as pump inlet and outlet diameters, pump characteristics, voltage and power measurements. The manufacturer's pump curve for power at the nominal speed is obtained from the database as the basis for the calculation.

To obtain the required quality of the setup responses on the step inputs and disturbances as well as on the non-step inputs, the VSD tuning was conducted. As a rule, permissible and approvable drive outputs have to meet such requirements as:

- approaching the desired pressure and speed;

- keeping the steady-state flux, torque, current, and voltage around the NOP CPU module PM573;

- providing the transient overpressure and overspeed within the restrictions or 150 to 200 % of the nominal values for 0.2 to 10 s.

PLC programming was conducted using the Structured Text language and Continuous Function Chart language from the *Controller Development System* (CodeSys). All control algorithms for the developed systems were programmed with the help of the *Standard Template Library* (STL) programming language

54

[39]. The CodeSys software was used for multiple purposes. The environment helps not only to build a program using STL but also to visualize the data received from the PEC. To represents the data in the graphical form, a user interface has been developed (Fig. 3.4) where

  a – switch on/Switch off toggle button,
  b – arrow pressure indicator,
  c – pressure reference bar,
  d – arrow pump speed indicator,
  e – emergency indicator ($p<p_{min} \parallel p>p_{max}$),
  f – digital indicators of the pressure reference value, reference speed, and
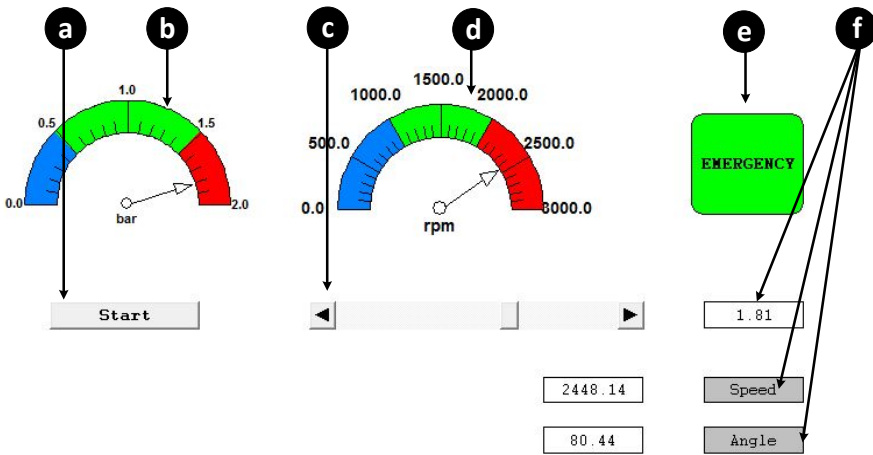 valve angle.

Figure 3.4 User interface of the experimental setup

The developed pressure/flow PID controller has a transfer function:

$$W_{r\omega}(s) = k + k_{int} + k_{diff} = k\left(1 + \frac{1}{\tau_{int}s} + \tau_{diff}s\right) \qquad (3.1)$$

including the proportional (k), integral (k_{int}) and differential (k_{dif}) coefficients. Here, s is a differential operator, τ_{int} is an integral time constant, and τ_{dif} is a differential time constant to be tuned. Tuning of the cascading control system is executed step by step, starting from the innermost loop. First, a proportional regulator is assigned and small inputs are applied to the system without its capturing.

In this way, the transients and steady processes are investigated along with the smooth rising of the k gain. As the gain increases, the response enhances but a too high value will make the system liable to vibrate. Next, to eliminate stationary deviations, an integral control component is introduced.

First, an integral time constant is assigned high enough and then decreased smoothly to improve the response. Once the system is liable to vibrate, the integral time constant change is completed. If the loop response remains slow, the differential component may be added. Initially, this time constant is set sufficiently small.

Then, it is stepped up gently and the overshoot and vibration are observed. Once their level becomes dangerous, the change of the differential time constant is completed. Thereby, the speed loop and thereafter the pressure loop are tuned. Once the linear system is properly tuned, the regulator limiters are assigned and the testing input signals are increased to examine the VSD responses of the constrained system.

3.1.2 General algorithm of throttling and speed control

The structure of the developed algorithm is shown in Fig. 3.5. In the beginning, the variables are initialized and connections among PLC, PEC and control console are validated. Once the initial data are uploaded from the database to the system memory, the rotational speed obtained from the PEC is checked. The system should achieve at least the minimum speed of 500 rpm while the throttle valve has to be open at least at sixty degrees.

The system boosts the speed and throttle valve angle until they achieve the required level. Then the next stage starts, at which the current speed n_{act} is compared with the reference signal n_{ref} and the PID controller regulates their difference using the ACQ810 converter.

During the control, the pump speed n is adjusted so that the pump performance curve is moved to the location, which was previously estimated by the model. In the same way, the valve angle is adjusted aiming to locate the pump performance curve at the calculated position corresponding to the estimated operation point.

Finally, the pressure at the pump discharge side is estimated with the help of the pressure sensor MBS3000 and compared with the permissible levels (0.5 – 3.5 bar). In the case of overpressure, the program shuts down the centrifugal pump.
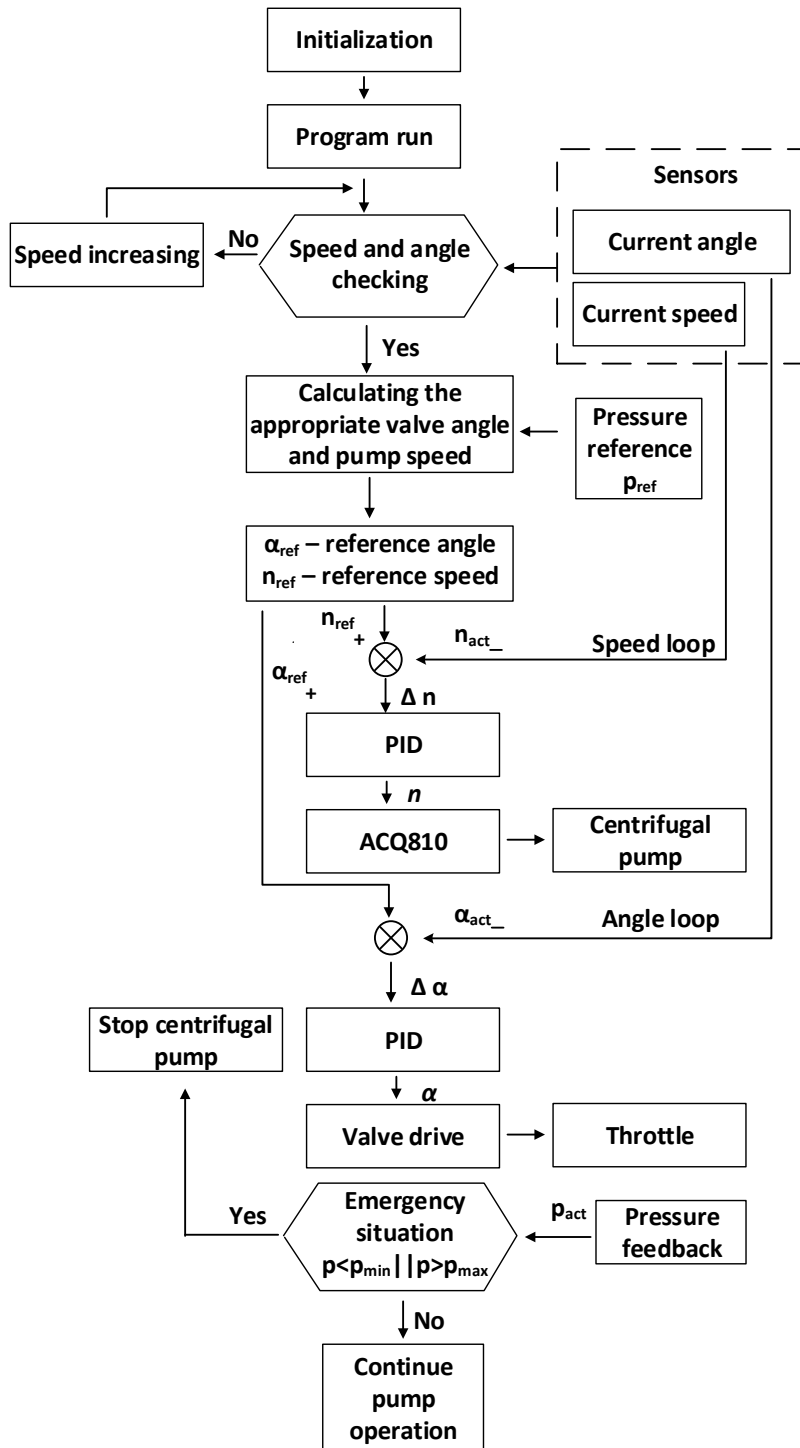
Figure 3.5 General control algorithm

3.1.3 Experimentation with ABB DriveStudio and AC500 PLC

In this section, three experiments demonstrate the use of the experimental setup.

The first experiment is aimed to stabilize pressure at the rate of 0.45 bar upon the variable piping conditions.

The PLC generated the reference VSD speed using the PID pressure regulator, which estimated, restricted, and converted the difference of the demanded and measured pressure levels. Any time when, under an influence of disturbances, the pressure changed, the PLC changed the pump speed, and the pressure PID control was executed. The control accuracy depends on the resolution of the PID regulator, its algorithm, as well as the VSD parameters.

To plot the pump and system curves, the DriveStudio flow calculation function was applied, which provided adequately accurate derivation of the flowrate without installation of a separate flowmeter. The flow was calculated using the database information, such as pump inlet and outlet diameters, pump characteristics, voltage and power measurements. The manufacturer's pump curve for power provided at the nominal speed was acquired from the database as the basis for the calculation.

To study the system performance at the pressure stabilization mode, the model was running with a PI regulator at the constant demanded pressure. After that, the cross-sectional area of the pipeline was changed sequentially between different valve angles. Consequently, the pumping speed followed the valve angle thus supporting the pressure at the demanded level. The torque, speed, and pressure traces recorded using the TREND tool from CoDeSys software are shown in Fig. 3.6.
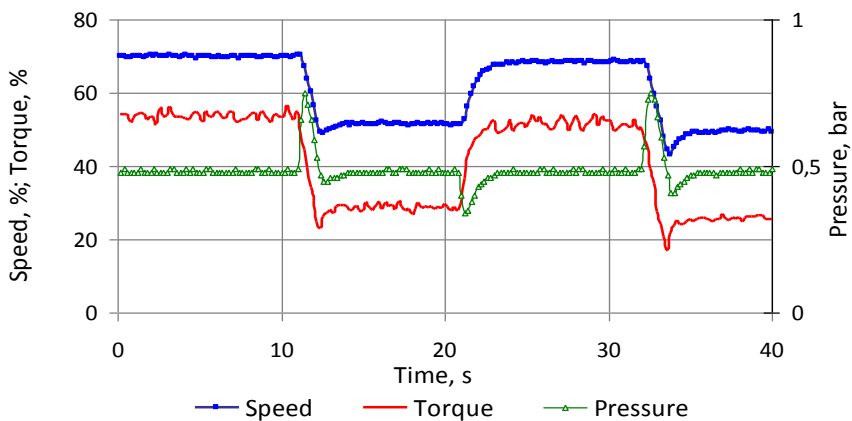

Figure 3.6 Speed, torque, and pressure responses of the experimental setup (pressure stabilization)

As it follows from the experiment, once the system curve rushes left, the working point moves up along the pump characteristic thus increasing the pressure. Since the pressure sensor feels the pressure growth, the PLC decreases the referred speed motivating the VSD to select the reduced voltage space vector of the PEC.

As a result, the motor speed drops thus stabilizing the pressure on the demanded level. In addition, vice versa, if the system curve rushes right, the working point moves down decreasing the pressure. Since the pressure sensor feels the pressure lowering, the PLC increases the referred speed motivating the VSD to select the enlarged voltage space vector of the PEC. As a consequence, the motor speed grows stabilizing the pressure on the demanded level.

The aim of the second experiment was to change the pressure in the range form 0.25 to 1.5 bars at a constant system state. Torque, speed, and pressure were traced using the ABB DriveStudio toolkit and recorded using the TREND tool from CoDeSys software. The system responses are shown in Fig. 3.7.
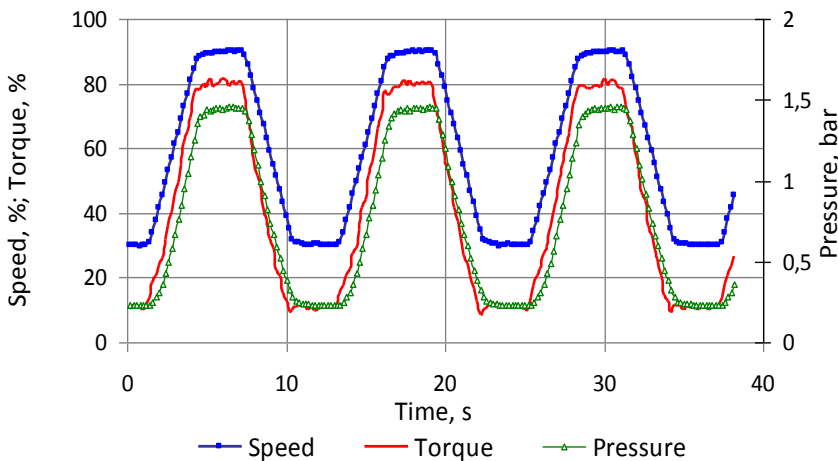
Figure 3.7 Speed, torque, and pressure responses of the experimental setup (pressure regulation)

The third experiment was aimed to stabilize the flowrate of 4 m^3/h. To alter the system state, a discharge valve was used. Torque, speed, and pressure were traced using the ABB DriveStudio toolkit and recorded using the TREND tool from CoDeSys software. The system responses are shown in Fig. 3.8.

Fig. 3.8, a, shows the position of a throttling valve during the flow regulation. The valve was used to create artificial disturbances in the pumping system imitating the real variation of a system curve for centrifugal pumps due to the change of demand and pipeline properties. At the same time, Fig. 3.8, b, shows the torque, speed and flowrate responses of a control system during the flowrate stabilization. The control system shows relatively high accuracy during both the static and the dynamic mode.

Figure 3.8 Valve angle (a), speed, torque, and flow responses (b) of the experimental setup (flowrate stabilization)

3.1.4 Benefits and drawbacks of the experimental setup

The results of experimentation affect both the choice of the control algorithms and the assessment of the particular methods. Exper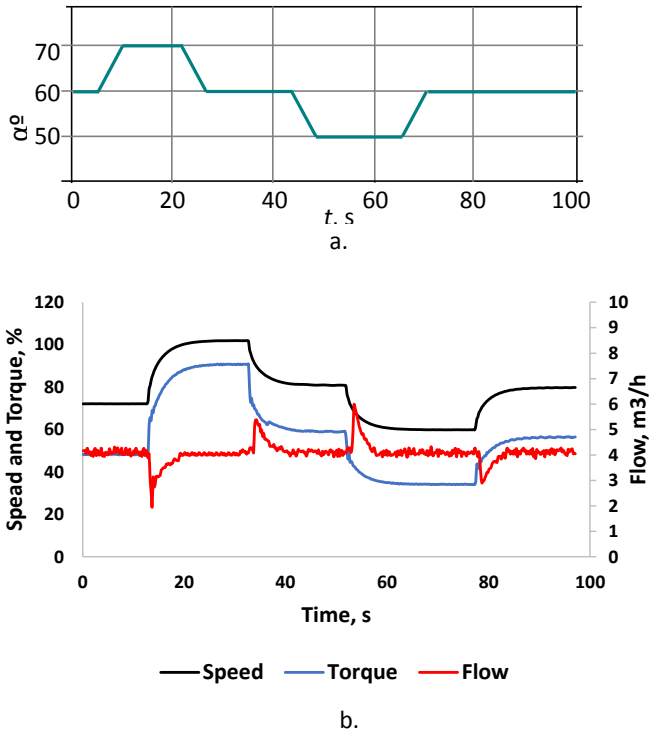imental hardware and software promote the comparison of the different models, thus helping selection of the best modules and parts. Above all, they support developers by reducing the design time and component expenses.

The experimental setup opens new possibilities for analysis and comparison of CPP equipment in terms of its power economy aspect. It serves for exploring different steady state and dynamic behaviours in multiple applications. Therefore, this category of experimental technique may be effectively applied in the studies of all the possible CPP modes.

The strong point of real pumping tests is a good concern. Nevertheless, this method often leads to expensive and rigid systems unsuitable for tuning and reorganization. Insofar as the CPP is a very complex system, verification and validation of the obtained experimental results should be proved by other methods, namely, the software system simulations and the study of physical imitators. The advantages of these two approaches are better flexibility, relatively lower cost, and a shorter study period.

3.2 Matlab Simulation of Energy Management [XIII]

3.2.1 Problem statement and related studies

Nowadays, Matlab/Simulink is the most popular tool for complex systems simulation and design. Multiple computer models were developed using that toolkit to observe and design the behaviour of pumps working in industrial, domestic, and medicine applications. These programs help determine the best total head, pressure, flux distribution, or flowrate, and obtain minimal energy losses or maximal efficiency.

One method demonstrated, for instance, in [18] concerns the CPP design based on transfer functions and operational equations of pumping components suitable for mathematical analyses, operational calculus, and Laplace transforms. An analogous toolbox was proposed in [40] for solving the mathematical equations that describe different pumping processes. The main drawbacks of this approach lie in its high laboriousness and low accuracy because of roughness in the representation of non-linear multidimensional processes with a limited number of mathematical functions.

Another methodology introduced in [41] provides model development using the replacement circuits in which pumps are simulated by current sources whereas the pipeline and valves are represented by voltage sources. This analogy provides a pump study in a software environment related to electrical circuitry applications. A similar model applied in [42] brings enough information about such pumping variables as total head, flowrate, power input, and energy consumption. At the same time, as [43] shows, the benefit of the given replacement does not lie in very accurate results but rather in the provision of means for a comparative study of different control methods and systems.

The third group of models concentrates on the pump modelling as a specific load for VSDs. Particularly in [44] an inverter with voltage-frequency control represents the single-phase induction VSD at the "capacitor-start" configuration. To simplify simulation, the constant-duty ratio modulation has been used at which the voltage amplitude and the power supply frequency were obtained by changing the duty of a pulse train. The pump and the hydraulic circuit were simulated there in the Simscape environment with the hydraulic inlet, a reservoir modelled as the well, and a tank that stores water at constant pressure. The model of [45] includes a three-phase PEC, PLC, a three-phase induction motor, centrifugal pump, consumption network, and sensor sub-models. To study the VSD, a replacement circuit was used whereas a PEC was represented by the simplified model, and a pump – by the Riccatti head-flow and torque-flow equations.

In [46], a mathematical model of a water pumping system with PLC, PEC, a three-phase induction motor, and a centrifugal pump was proposed. Using the appropriate Matlab library, this model can describe the DTC unit in detail.

Along with that, the equations and relations responsible for the pumping process itself concern here the well-known affinity laws only, thus omitting many pump technological peculiarities. In [47], a direct current motor and in [48] the brushless motor models were implemented with the help of SimPowerSystems toolbox. At the same time, electrical and mechanical parts of the machine were represented by a second-order state-space model capable of generating pressure and some other signals along with indirect derivation of the torque and power. To scale the load, some tests were previously carried out. Similarly, in [49] driving torque for a centrifugal pump was roughly generated, proportional to the square of the rotational speed. All above examples bring errors and mistakes in the representation of the pumping process because of their focus on the VSD instead of the pump itself.

In some papers, for example [50], Matlab was used as an auxiliary instrument to accompany and to support different experiments on the real pumps. In other studies, a centrifugal pump was modelled as a constant head.

These sections present a new simulation model of the CPP operation. The model was developed to be able to check quickly the power in the most painful points based on real values, each time more. This can make it possible to choose equipment and to select the operation modes that would provide the highest energy benefits. The model was prepared in a Matlab/Simulink environment. Thanks to its universality, it may be recommended for the CPPs of different sizes of pumping plants.

3.2.2 CPP model composition and specification

The general model layout merges the DriveSize part from ABB and the original Simulink part. The former part keeps the motor and the converter databases connected to the lookup table. The latter one involves the pressure control module, the brake power, the VSD loss, and the input power estimators. The power loss estimations are based on the signals containing information about rotational speed and load of the pump. The pressure control module allowing both the throttling and the speed adjustment is composed of a throttle valve model and an ideal angular velocity source. To estimate the brake power, an ideal torque sensor is coupled with the centrifugal pump model.

The model shown in Fig. 3.9 was developed in Simulink v. 8.1 (R2013a). It consists of several main blocks: a centrifugal pump, a liquid reservoir represented in the figure as a hydraulic reference block, a straight pipeline between the pump inlet and outlet sections, a ball-throttling valve as well as the hydraulic sensors like pressure and flowmeters. The following signals were processed:

- In1 – speed input;
- Conn2 – hydraulic pressure (Pa) measurement output;
- Conn4 – input of regulation valve;
- Out1 – flow measurement output;

- Out2 – torque measurement output;
- Out3 – pressure (bar) measurement output;
- Out4 – speed measurement output.

Figure 3.9 General structure of a Simulink CPP model

The angular velocity source block allows assigning the reference rotational speed. It generates the speed proportional to the input reference signal. Measuring equipment involves a special converter to transfer numerical values into physical ones.

The centrifugal pump in this figure is represented in the form of datasheet model. The parameters of a centrifugal pump should be taken from the manufacturer's datasheet. For instance, the values for this particular model are given in Table 3.2.

Table 3.2 Main parameters of the CPP model

Class of parameterization	p-q	Units
Flowrate/pressure	[0; 50; 80; 90; 110; 130; 160]/ [3.01; 2.45; 2.25; 2.15; 2.18; 1.55]	L/min; Bar
Brake power/flowrate	[500; 600; 800; 870; 920; 1000; 1060; 1100]/ [0; 40; 60; 80; 100; 120; 140; 160]	L/min; W
Nominal rotational speed	2760	rpm
Liquid density	1000	kg/m^3
Interpolation method	Cubical	-
Extrapolation method	From last two points	-

The values of the main parameters were copied into the model of a centrifugal pump directly from the datasheet of the pump EBARA CDX120/12 used in the experimental setup. This block has three pins:

- S – to connect the centrifugal pump to an ideal angular velocity source being a conserving port of a mechanical rotation;
- T – inlet of a centrifugal pump;
- P – outlet of a centrifugal pump.

Pin "S" is generally a digital number that corresponds to a rotational speed of a pump. Pin "T" and "P" represent the flow and pressure at suction and discharge side of a centrifugal. To trace the values of pressure and flow in the model the standard blocks – "Hydraulic pressure sensor" and "Hydraulic flow sensor" are used. The main points in the centrifugal pump block are describing the performance and power curve of the simulated centrifugal pump. These key points are stored in the form of two vectors. Each vector is one-dimensional and contains values from the pump datasheet given by a manufacturer.

Both hydraulic sensors are parts of Simulink hydraulic sensors library. The flowrate sensor is an ideal flowrate measuring device [51]. Its working principle is based on the conversion of a volumetric flow through a pipe into a numerical signal based on the calculated flow. It does not take into consideration such phenomena as pipeline friction, pressure losses, etc. In the pressure sensor model, the operation principle is almost the same. It converts the differential

value of the hydraulic pressure measured between two points into a numerical signal.

The model of the throttle valve represents a ball-type valve taken from the library of flow control valves. The working principle of a ball valve is based on the dependence between the flowrate through the valve, orifice diameter, and pressure drop across the device.

3.2.3 Simulation of pressure maintenance

The developed model of the pressure control system in Fig. 3.10 represents generally a pressure control loop.

The signal from pin "Out3", which is a pressure measurement output, comes to the PID regulator. The input signal of the PID regulator represents a difference between the reference signal and the feedback from pin "Out3". The PID regulator includes functional blocks of amplification, integration, derivation, and saturation. The last one restricts the setpoint pressure given by a reference signal to a predetermined maximal value. The saturation block restricts the set-point pressure given by a reference signal to a predetermined maximal value. The control output signal from the PID regulator is connected to the pump model speed input pin "In1". Parameters of the classical PID regulator are tuned during the simulation to obtain a better control output.

For the simulation study, a pumping system of the experimental setup was used as a simulation object.

First, three system curves were examined for different rotational speeds: 2760, 2500, 2200, 1800, 1000. Fig. 3.11 shows a family of simulated and real system curves, obtained during experiments and simulation at the same rotational speeds. The accuracy of the designed model varies from 0.4 % to 3.5 %, which shows a relatively high accuracy of the model.

To simulate the system performance at the pressure stabilization mode, the model was running at the constant reference pressure of 0.5 bar. After that, the cross-sectional area of the pipeline was suddenly changed using the valve component. Accordingly, the pumping speed was changed to maintain the pressure at the demanded level. In Fig. 3.12, the simulated pressure response is shown.

In accordance with obtained observations, the difference between the simulated (Fig. 3.12) and the experimental (Fig. 3.6) results in the steady-state mode ranges between 7 and 14 %. In dynamics, it looks higher.
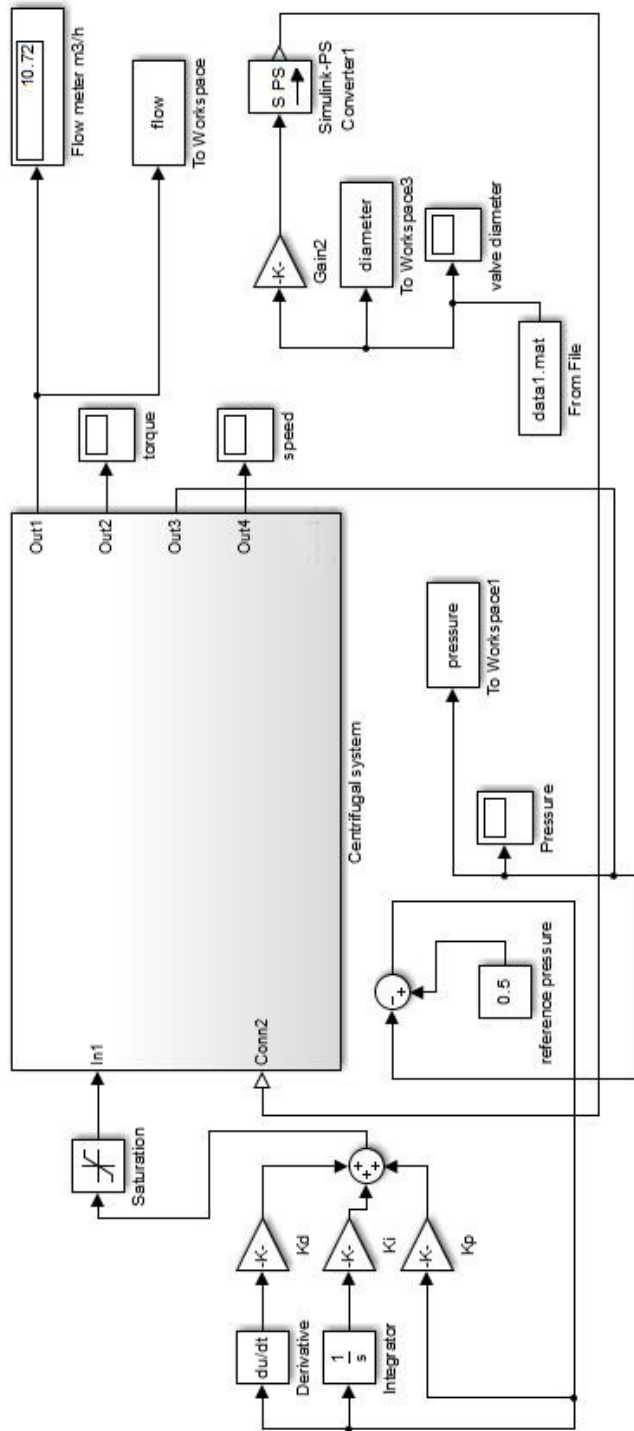
Figure 3.10 The model of the pressure control system developed
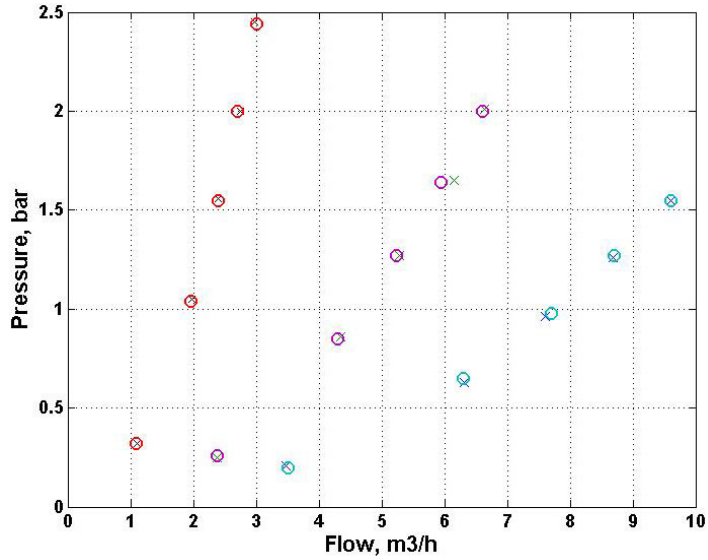
Figure 3.11 A family of system curves at – n=2760, 2500, 2200, 1800, 1000 rpm for pump model – 'o', and for the experimental setup – 'x'
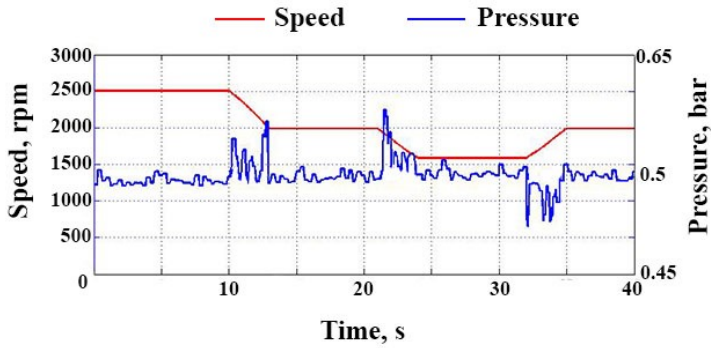
Figure 3.12 Simulated pressure stabilization at changing pipeline conditions

Another simulation was conducted, in which the system state was stable whereas the pressure was varied in the range from 0.25 to 1.5 bars periodically, according to a trapezoidal waveform. To simulate the trapezoidal signal, a standard *Triangle Generator*, from Simscape library and a *Saturation* block were used [52]. Fig. 3.13 shows the appropriate responses. Their comparison with experimental diagrams shown in Fig. 3.7 proves the adequacy and accuracy of the model.
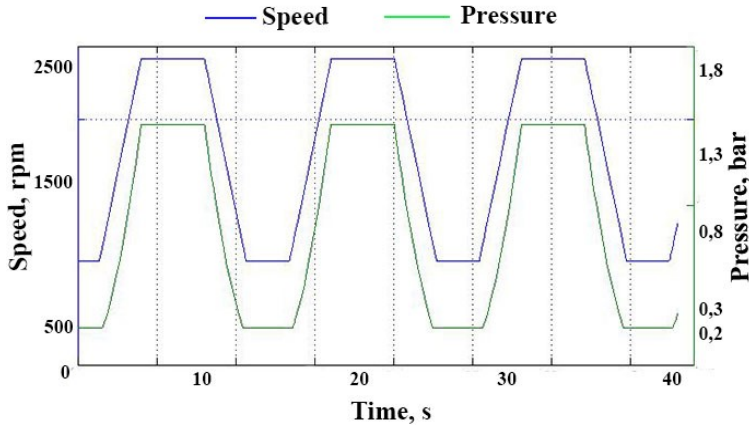
Figure 3.13 Speed and pressure responses of the Matlab model (pressure regulation)

Next, the flowrate stabilization process was simulated. Comparison of the stabilization quality in the model (Fig. 3.14) and in the experimental setup (Fig. 3.8) proves the model validity as well.
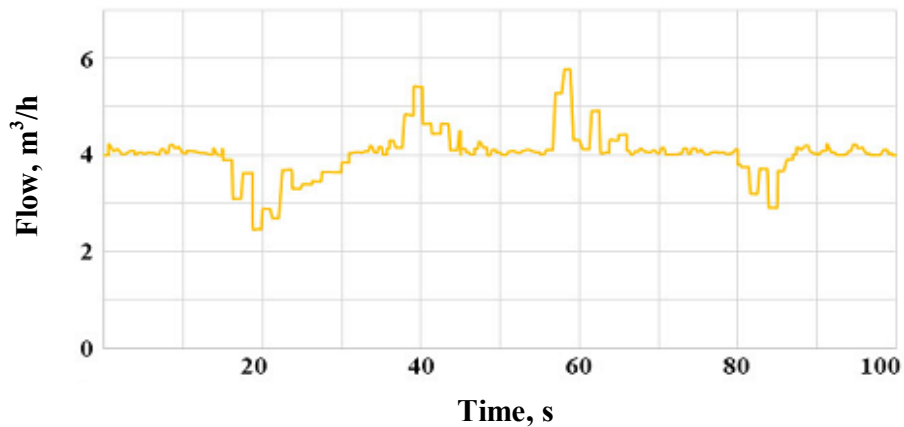
Figure 3.14 Flow response of the Matlab model

As the last step, an efficiency estimation problem was solved using the developed model. To assess the efficiency of the CPP at throttling, the rotational speed of the pump was preserved at the nominal level. On the opposite, to assess the efficiency at the speed control, the VSD was adjusted.

During experimentation, the working point was initially located close to the BEP as shown in Fig. 3.15.

After measuring the efficiency at the BEP, the demanded pressure was decreased from 1.55 to 0.55 bar. Both of the pressure control methods were applied – the throttling and the speed control – to adjust the demand. The comparative table (Table 3.3) and the diagram (Fig. 3.16) for the simulation and experimental results are given below.
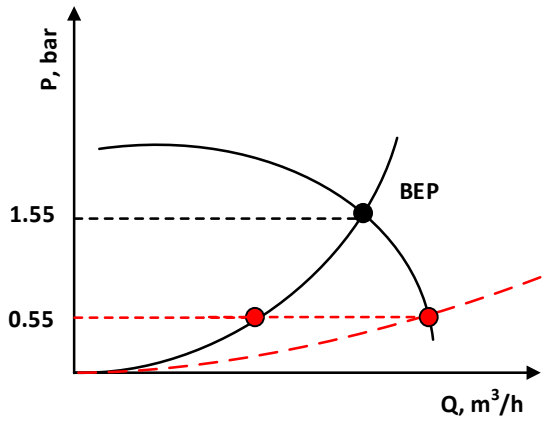
Figure 3.15 An efficiency estimation problem

Table 3.3 Efficiency estimation by simulation and experimentation

Pressure	Efficiency, %	
	Simulation	Experimantation
1.55 bar	37.5	34.0
0.55 bar (VSD)	36.2	32.6
0.55 (Throttling)	25.8	21.4

Figure 3.16 Efficiency estimated using simulation and experimentation at the nominal speed of 2760 rpm and the pressure levels of 1.55 and 0.55 bar

3.2.4 Modelling and simulation of throttling

The throttling system under study includes the following parts: a dc motor with a gearbox, a power supply, a motion sensor, and a control system.

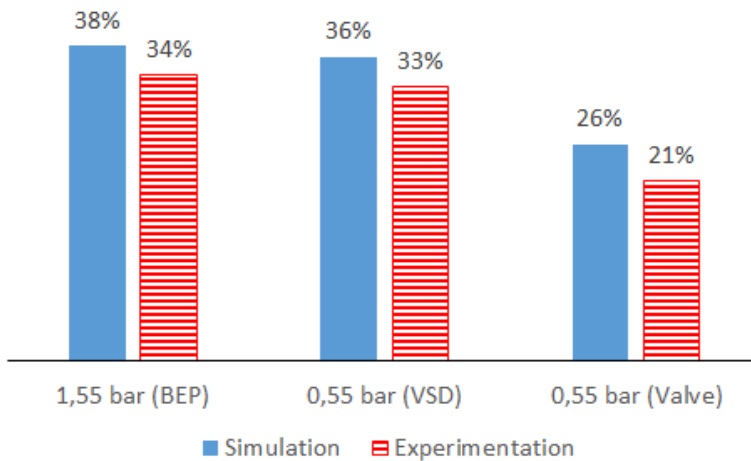The permanent magnet dc motor [53] is a connecter via the gear to the valve for direct regulation of the valve angle. Following the angle change, the location of the working point is varied as well. The motor has been chosen according to the technical requirement of the equipment for pumping units. Technical parameters of the simulated drive are given in Table. 3.4.

Table 3.4 Motor and gearbox specifications

DC motor		
Model number	Z42BLDP2425-30S	Units
Type	Permanent magnet	
Protect feature	IP68	
Nominal power	25	W
Nominal voltage	24	V
Rated speed	3000	rpm
Nominal current	1.8	A
Torque	0.0796	Nm
Shaft construction	Square head for gear connection	
Gearbox		
Model number	JGY370	
Protection class	IP54	
Noise	<45	dB
No-load speed	24	rpm
Torque	0.55	Nm

The developed model of an electrical drive of the throttle valve is shown in Fig. 3.17.

The model is composed of the following parts: dc voltage source, PWM voltage source, H-Bridge, dc motor, worm gear, relay, switching blocks and inertia blocks, control system, ideal rotational motion sensor, current sensor, Simulink to physical signal (S-PS) and physical signal to Simulink (PS-S) converters, and measuring equipment.

The dc voltage source feeds the controlled PWM voltage block – the source of the PWM voltage. The voltage on the output of the block was calculated according to the reference voltage across its input pins +ref and –ref. The REF and PWM outputs were directly connected to appropriate input pins of the H-bridge. The simulation mode for this block was set to Average instead of PWM in order to accelerate the simulation process. The impedance of the motor is minor at the PWM frequency of 4 kHz.
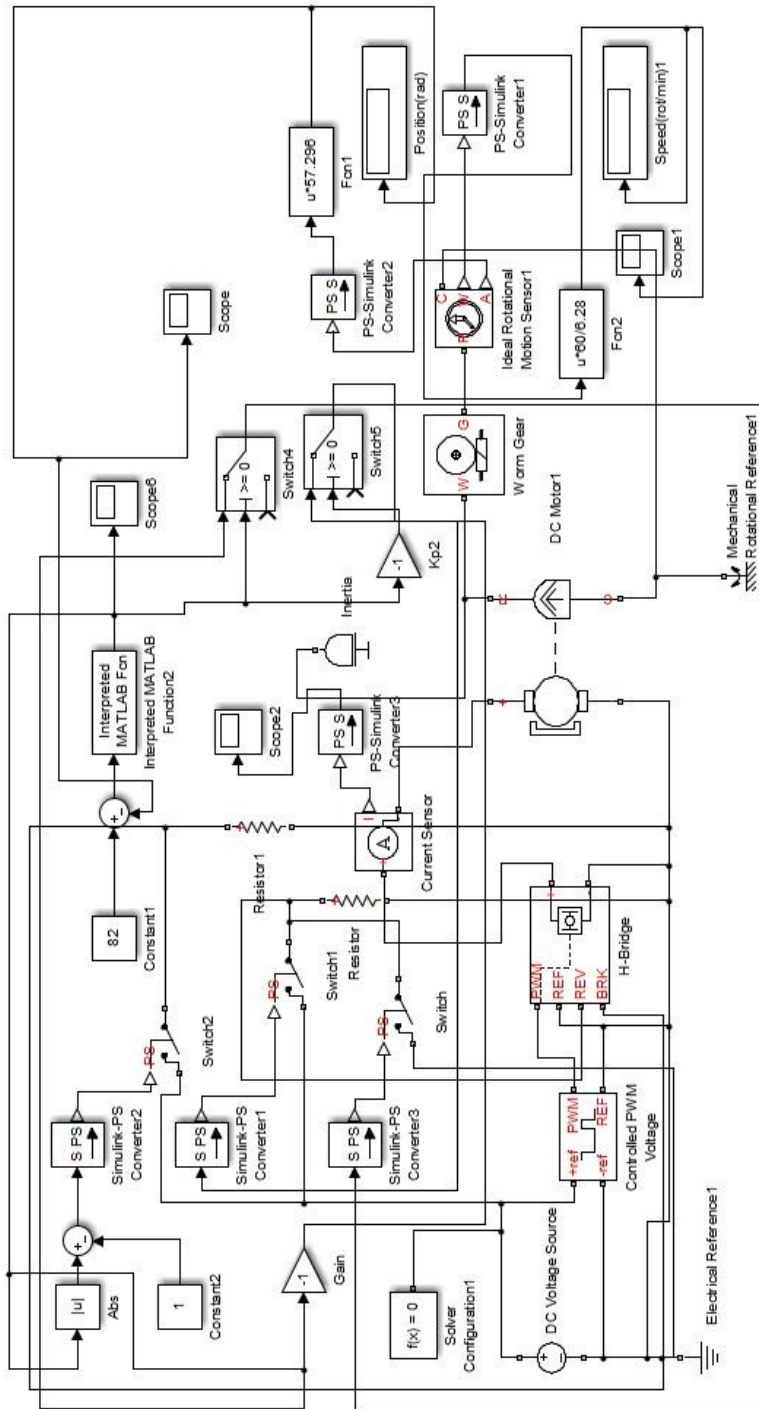
Figure 3.17 Model of electrical drive for a throttle valve

71

The H-bridge connected to the motor controls the direction of rotation and plays the role of the motor driver. Its output voltage is a function of the input signal at the PWM pin. The block can be connected to the motor using the options with one semiconductor breaker and one freewheeling diode. Thus, the bridge operates at a synchronous mode. The REV pin is used by the control signal to change the polarity of the output voltage to adjust the valve position when the reference angle is less than the current one. The BRK pin is used by the control system to stop the drive when the current angle equals the reference value.

The Inertia block from the library of mechanical rotational elements simulates inertia of a real throttling valve. The Worm gear block from Gears library reduces the rotational speed and increases the torque of the actuating mechanism. The Ideal rotational motion sensor from the library of mechanical sensors estimates the rotational speed and the angle displacement by converting the variables measured across to mechanical rotation nodes into a control signal.

Simulation shows that the model successfully imitates the desired angle position. Fig. 3.18 demonstrates an angle response obtained during the control process.
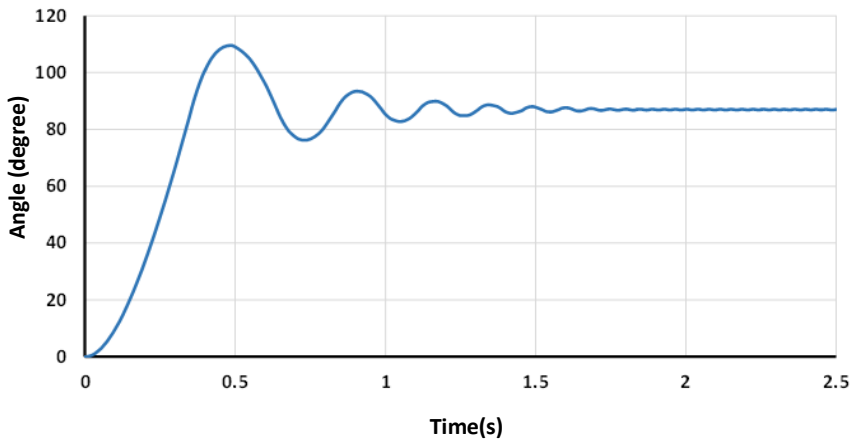
Figure 3.18 Simulated angle response at the reference of 85 degrees

3.2.5 Estimation of the consumed power by simulation

Fig. 3.19 provides information related to the distribution of input power in accordance with the pressure on the discharge side of a centrifugal pump and the position of the current operating point. To create the diagram, the output pressure was imitated in the range from 1.5 to 2.0 bar.

Regions colored with green have minimal energy consumption for the given pressure levels. When the operating point is located in the red area, the consumption reaches its maximum. When the working point is in the grey area,

the energy consumption is lowest but the level of flow is not sufficient to meet the minimal requirements.
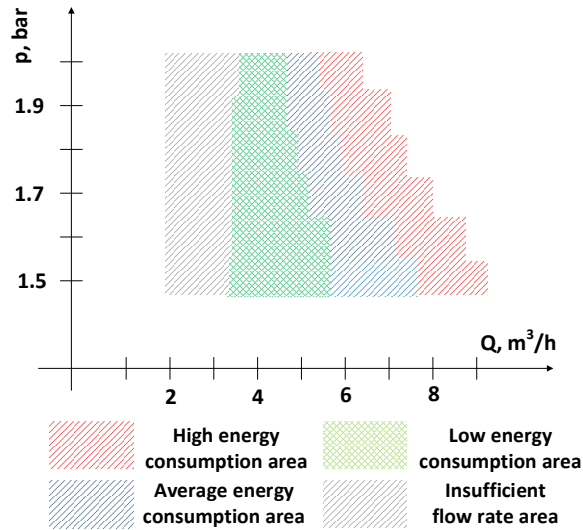
Figure 3.19 Power allocation (green area corresponds to the best working zone)

The comparative data received with the help of imitation and experimental tests are presented in Table 3.5. The obtained records illustrate a predictive potential of energy saving.

Table 3.5 Comparison of estimated power for 1.8 bar

Flow, m³/h	Input Power, W		Hydraulic Power, W
	Simulation	Experimentation	
7	1100	1060	353
6	1000	970	302
5	870	830	252
3.5	700	670	176
2.5	530	510	126

Energy rates in red and green regions were calculated for the pressure value of 1.8 bar. Fig. 3.20 shows the consumed energy for a one-hour period.

The energy cost was estimated as follows [54]:

$$Cost_e = \sum_e P \times UC \times t,$$ (3.2)

where

P – pump power, W,
UC – electricity unit cost,
t – time duration, s,
e – number of pumps in a system.

Energy of pumping for pressure 1.8 bar
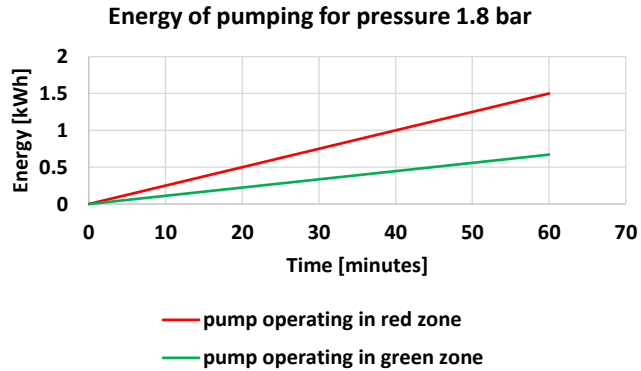
Figure 3.20 Energy estimates (green area corresponds to the best working zone)

Corresponding 24-hour rate price in Estonia was obtained from [55]; the cost of pumping in the red zone is 4.84 eurocents during an hour of operation, and in green zone – 3.21 eurocents.

To predict possible energy savings in an industrial scale, an example of a pumping plant was examined. For this purpose, an average-size centrifugal pump CRN-150-6 from Grundfos was chosen. These pumps are used for water supply in urban districts with multi-storey buildings. Technical data of the pump are shown in Table 3.6.

Table 3.6 Main technical data of a centrifugal pump CRN 150-6

Type	Vertical, multistage centrifugal type
Nominal speed (rpm)	2975
Nominal power (kW)	75
Flow at BEP (m^3/h)	180
Head at BEP (m)	120

Simulation was conducted for a pressure rate of 12.2 bar. Table 3.7 represents the data received.

Table 3.7 Simulation results for 12.2 bar

Flow (m^3/h)	Input power, kW	Hydraulic power, kW
160	77.99	54.22
140	69.08	47.44
120	60.03	40.67
100	52.14	33.89
80	45.79	27.11

Energy saving for a station with five CRN-150-6 centrifugal pumps operated for 6 hours per day is as follows:

$$\Delta E = 5 \times (77.99 - 45.79) \times 6 \times 365 \approx 352.5 (MWh) \qquad (3.3)$$

3.2.6 Challenges of Matlab simulation

Matlab simulation environment ensures versatile opportunities for monitoring of energy usage at variable CPP combinations. The operation of various pumps in multiple piping systems can be observed using this system. The characteristics of pumps and piping network can be inserted into software, and the results of simulations enable observation of pumping using various adjustment methods. Unfortunately, accurate VSD characteristics cannot be modeled and, being realized with the help of Matlab/Simulink, have many simplifications, limitations, and restrictions. The most significant of them are the following:

1. In the motor models, all stator coils are considered as identical and the rotor bars disposed in the similar way. The air gap between the stator and the rotor is assumed constant and independent of the rotor position. However, in pumping motors the variation of these parameters reaches 3 – 7 %.

2. Special emphasis is to be placed on the modelling of the major DTC modules, such as Clarke transformer, motor model, regulators, and voltage-switching unit. As a rule, every drive manufacturer has his unique hardware, algorithmic, and software tools for their implementation that cannot have right representation by the unauthorized instruments.

3. The ratio between the torque and the speed in the DTC model is valid at constant moment of inertia only. Its instability for centrifugal pumps approaches 3 – 7 %.

4. Taking into account temperature instability, some vendors provide their VSDs with the specific mode of the real resistance measuring and recalculation along with component heating. At simulation, this ability is not commonly used.

5. At simulation, PECs of the VSDs are considered as ideally fast and precision voltage source inverters. Ignorance of the direct current link voltage instability and asymmetric alternating current results in the simulated process distortion and control errors.

6. Voltage and current sensors are idealized as well. Often, their saturation and nonlinear phenomena are omitted appearing the invalid simulation responses for high-level references.

3.3 Hardware-in-the-Loop Imitation of Energy Management [I][II][X][XI]

3.3.1 Problem statement

To further increase the accuracy and productivity of complex real-time system simulation and design, the *hardware-in-the-loop* (HIL) methodology is introduced [56] – [59]. Such an approach assumes the study of the system using mathematical models, in which the components of real equipment are included.

In contrast to the traditional mathematical modelling, in the HIL model part of the application is merged with a mathematical model of the remaining system parts. The results obtained are further applied to the real system based on the theory of similarity.

This technique serves as an effective platform suitable for adding the complexity of the plant under the control to its mathematical representation called "plant simulation". Most of HIL imitators include electrical and electromechanical sensors and actuators that act as the interface between the plant simulation and the embedded system under test. Signals from electrically emulated sensors are controlled by the plant simulation being read by the embedded system under the test. Likewise, this embedded system implements all the control algorithms therefore the changes in the control signals result in the changes of variables in the plant simulation.

The world of pumps comprises a numerous variety of pump types and sizes. Multiple applications and requirements call for many constructional designs within a wide range of the flowrates, heads, powers, and efficiencies. Changes in the design result in differences in pump characteristics and give rise to a wide scope of hydraulic properties. It is often difficult to compare one type of a CPP with another. For that reason, the HIL methodology is an effective tool to resolve the complexity of the pumping simulation.

In contrast to architectural, shipbuilding, or airplane designs where this approach is widely used, in this research, the real control system is used whereas industrial pumps are replaced with the specially developed imitators. Along with the real apparatus, such models contain set-point and disturbance imitators as well as environment simulators whereas mathematical descriptions look unclear. Real-life equipment included into the simulation loop allows a decrease in a priori uncertainty and exploration of the processes without evident analytical characterization.

3.3.2 Composition and specification of the HIL imitator

The function of the HIL imitator (Fig. 3.21) is charged to the couple of interconnected induction drives of ACS800 series from ABB, namely the pump imitator and the pipeline imitator. The first HIL part represents both the hardware and the software of the reduced-power fully equipped pump drive with the arrangement the same as that of the real drive.

The second part of the HIL model representing the pipeline imitator is built on similar equipment. Both have the same composition consisting of induction motors, PECs, and remote consoles with housing, measuring, and cabling equipment. The motor data are given in Table 3.8.

The third part of the imitator is based on the PLC interacting with the above drives. The fourth part is the originally designed pump simulating toolbox with the speed reference and the torque reference sub-systems.
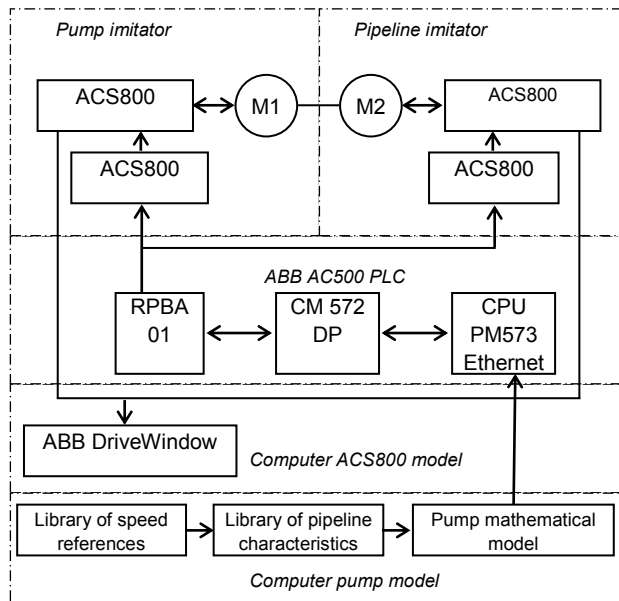
Figure 3.21 Pump HIL imitator

Table 3.8 Motors of the HIL Imitator

Quantity	Pump motor	Pipeline motor
Type	M2AA132S	M2AA160L
Power, kW	5.5	15
Voltage, V	400	400
Current, I	11	29
Torque, Nm	36	98
Speed, rpm	1450	1460

ABB ACS800 VSDs are the wall-mounted low-harmonic units with a broad spectre of control possibilities. They provide voltage variation from 0 to 415 V in the frequency range of 8 to 300 Hz and power up to 75 kW. The front-end active rectifier and the motor-side inverter connected via the dc link combine their power stages. Every cabinet contains the PEC, the control panel mounted on the front cover, the cooling system with the heat sink on the backside, and the connection box under the bottom cover. Both the front-end active rectifier and the motor-side inverter have six power transistor switching modules with freewheeling diodes. The switch gating is based on the space-vector modulation principle. The line filters suppress voltage and current harmonics. In the motoring mode, the rectifier converts the three-phase grid supply into the dc link voltage, which further feeds the motor-side inverter running the ac motor. In contrast, in the braking mode the motor-side inverter returns energy back from the motor to the supply grid through the dc link and the active front-end rectifier. To generate the switch gating signals and to perform the fault protection, line currents and dc link voltages are measured automatically using

built-in sensors. The PECs use measured voltage and current signals to estimate torque through the ACS800 built-in motor mathematical model. Herewith, PECs possess some predefined macros with factory settings suitable for flexible drive tuning by a customer.

Additionally, ACS800 is equipped with the ABB DriveWindow model-based control and measurement software, allowing the real-time parameter tracing and adjusting [60]. Its logical controllers fulfil the basic PEC operations. DriveWindow provides the remote control of the pump and pipeline imitators, their monitoring, graphical trending, tuning, and parameter registration. During the tests, the output data from the DriveWindow software related to the measuring parameters are recorded, displayed, and exported in graphical and numerical forms for the subsequent analyses. Two main control modes of the motor drives are supported, namely, the scalar speed control at the constant voltage-frequency ratio, and the DTC [61].

To adjust the pump drive imitator, the scalar mode is applied because the main function of the pump VSD is the speed control. To control the pipeline imitator, the DTC has been chosen because the main function of the imitator is the torque regulation.

The pump model is communicated with the pump and pipeline imitators via the AC500 PLC consisting of the communication module CM572 DP, Profibus-DP Master module PM573, and Profibus DP adapter RPBA-01.

To manage the HIL, a user interface shown in Fig. 3.22 was developed in the CoDeSys environment with the help of STL.
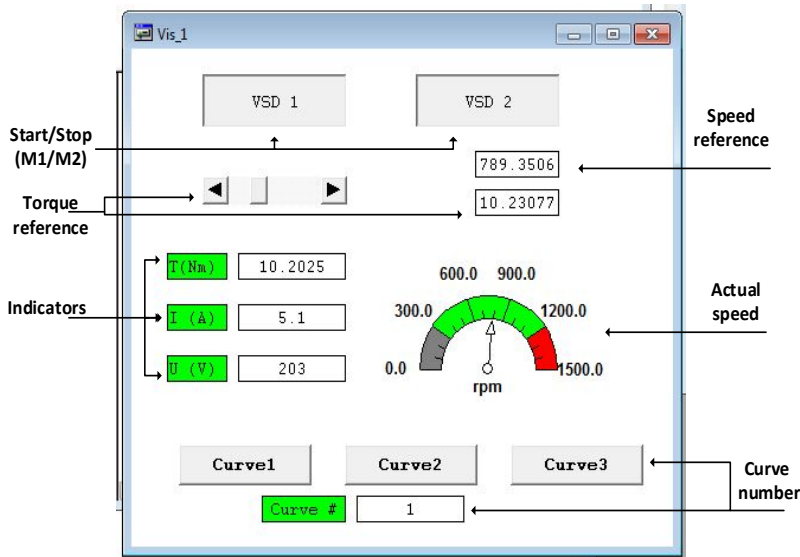

Figure 3.22 Graphical user interface of the HIL imitator

Graphical user interface includes the following elements [62]:

- Start/Stop toggle buttons for switching on/off both the pump (VSD 1) and the pipeline (VSD 2) imitators;
- torque reference bar;
- digital torque and speed indicators;
- digital current and voltage indicators;
- arrow speed indicator;
- system switches.

During operation, the pump imitator assigns the desired pumping speed. In turn, the pipeline imitator is responsible for following the torque reference from the pump model to supply the required torque on the shaft thus permitting the drive running under all kinds of working conditions. This system takes torque as a reference dependent on the demanded shaft speed. The ACS800 torque control system estimates the current torque using the measured voltage and the current signals and the built-in motor mathematical model. With the torque demanded and current values, the PEC manipulates the motor supply voltage, supporting adequately fast dynamic torque response.

In turn, the current torque value of the pipeline imitator can affect the speed reference of the pump imitator to change the speed at the load alternations. The appropriate controller is implemented in the frame of ACS500 PLC.

To achieve universality, non-dimensional characteristics were introduced in the HIL imitator. In order to determine the dimensional characteristics of a geometrically similar pump based on a known dimensional characteristic of another pump, physical characteristics were transformed into non-dimensional ones using normalization. To work out a non-dimensional characteristic, the NOP flowrate, head, power, and efficiency are used as the basis, considered as 100 % whereas the values deviating from the normal are expressed in percentages of the nominal data. Once the basis of the desired characteristics is known, other values required for curves plotting may be calculated. Such non-dimensional characteristics enable not only comparison of different quantities of the same type but also testing of pumps at varying operational conditions.

3.3.3 HIL imitation of flowrate and pressure maintenance

When the goal of the control is to maintain some demanded flowrate $q*$ at variable pipeline conditions, it is suitable to present the flowrate and torque data at the rated speed in the form of a lookup table stored in the memory of the control system. Table 3.9 exemplifies the data of the three system states of the experimental setup are displayed.

Table 3.9 Example of a lookup table

System state	I	II	III
Flowrate q_N, m³/h	9.60	6.64	2.98
Torque T_N, %	122	106	82

To imitate pumping, the system characteristic of the i-th state, $i \in \{$I, II, III$\}$ is to be chosen and the desired flowrate q^* is assigned. As a response, the control system reads the nominal flowrate q_N from the appropriate lookup table cell and calculates the required pumping speed n^* using (1.3) as follows:

$$n^* = n_N \frac{q^*}{q_N} \qquad (3.4)$$

Then, the control system assigns n^* as a demanded speed of the pump drive imitator. In addition, it calculates the required torque T^* using (1.16) as follows:

$$T^* = T_N \left(\frac{q^*}{q_N} \right)^2, \qquad (3.5)$$

and assigns T^* as the demanded torque of the pipeline imitator.

To imitate the flow stabilizing effect at a disturbance, the user selects another system characteristic. In reply, the control system recalculates the required pumping speed n^* using (3.4) and torque T^* using (3.5).

To imitate the flow control effect, the user sets another desired flowrate q^*. In reply, the control system recalculates the required pumping speed n^* using (3.4) and torque T^* using (3.5).

Case study. In the first experiment, the user has chosen System II (i = II) at the desired flowrate $q^* = 5.8$ m³/h. In reply, the control system derived the speed:

$$n^* = 2760\frac{5.8}{6.64} = 2410 \text{ rpm} \qquad (3.6)$$

of the Flow II curve (follow the solid black arrowed lines in Fig. 3.23). In addition, the control system has found the torque:

$$T^* = 106\left(\frac{5.8}{6.64} \right)^2 = 81 \ \% \qquad (3.7)$$

of the Torque II curve (other solid black arrowed lines).

To imitate the stabilizing effect of the flow at a disturbance, System I (i = I) was chosen at the same flowrate $q^* = 5.8$ m³/h. In reply, the control system derived the new speed:

$$n^* = 2760 \frac{5.8}{9.6} = 1667 \text{ rpm} \tag{3.8}$$

of the Flow I curve (follow the dotted black arrowed lines).
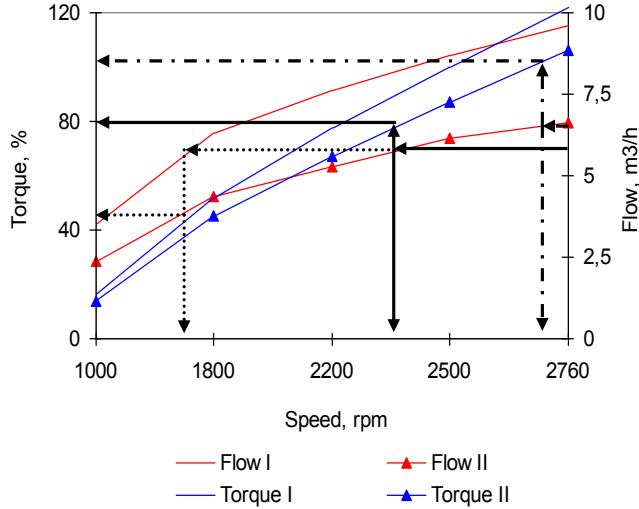
Figure 3.23 Case study of the flowrate maintenance

In addition, the control system has found the new torque:

$$T^* = 122 \left(\frac{5.8}{9.6} \right)^2 = 44 \text{ \%} \tag{3.9}$$

of the Torque I curve (other dotted black arrowed lines in Fig. 3.23).

To imitate the flow boosting effect, another flowrate $q^* = 6.6$ m³/h was assigned in System II. In reply, the control system derived the new speed:

$$n^* = 2760 \frac{6.6}{6.64} = 2743 \text{ rpm} \tag{3.10}$$

on the Flow II curve (follow the dashed black arrowed lines). In addition, the control system found the new torque:

$$T^* = 122 \left(\frac{6.6}{6.64} \right)^2 = 105 \text{ \%} \tag{3.11}$$

of the Torque II curve (other dashed black arrowed lines). To validate the model quality, the same characteristics were obtained from both the HIL imitator and the experimental setup.

An experiment conducted earlier on the experimental setup and illustrated in Fig. 3.8 was repeated in the HIL imitator. An example shown in Fig. 3.24 shows

the flow stabilization at the rate of 4 m^3/h. Torque and speed data were traced with ABB Drive Studio toolkit.
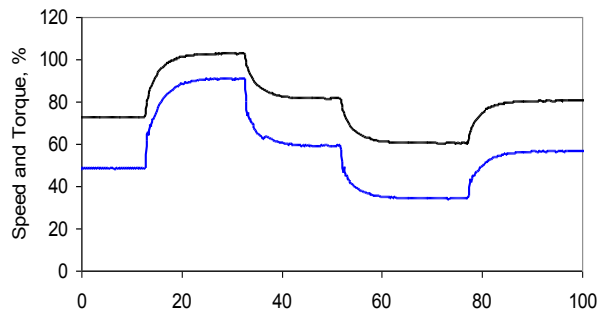
Figure 3.24 Speed and torque transients from the HIL imitator

In accordance with observations, maximal difference between the simulated and the experimental data in the steady-state flow control modes does not exceed 10 %.

When the goal of the control is to maintain some demanded pressure *p** at variable pipeline conditions, a similar imitation process is used. The speed and torque responses obtained from the experimental setup during the pressure stabilization at 0.5 bar upon the variable system state shown earlier in Fig. 3.6 were obtained also in the HIL imitator. Fig. 3.25 demonstrates, the appropriate responses.
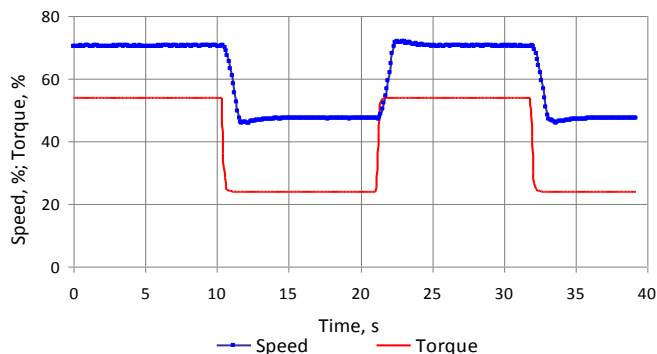
Figure 3.25 Speed and torque responses from the HIL imitator (pressure stabilization)

Responses obtained from the experimental setup during the pressure regulation in the range from 0.25 to 1.5 bar at constant system state were shown earlier in Fig. 3.7. Fig. 3.26, shows the corresponding speed and torque responses obtained from the HIL imitator. These diagrams prove the HIL simulation adequacy and accuracy.
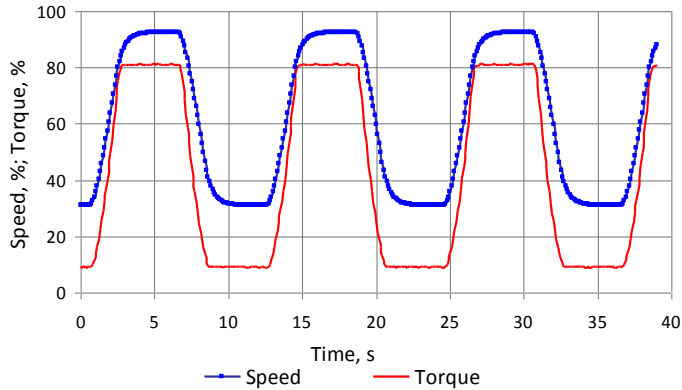
Figure 3.26 Speed and torque responses from the HIL simulator (pressure regulation)

3.3.4 Benefits and drawbacks of HIL imitation

The essential advantage of a HIL imitator could be easy presentation of complex nonlinear hardware and software blocks and components of the CPP without substantial amount of training data.

However, its limitation complicates the explanation of the physical phenomena and prediction in complex system modules and aggregates.

HIL simulation ensures new opportunities for energy use monitoring not in the whole pump-motor-VSD combination, but in many parts of the system. The motor and VSD characteristics are real in this simulation environment and the operation efficiency of the VSD can be estimated at several pump adjustment situations. The operation of the electromechanical pumping equipment can be explored accurately enough. The characteristics of the pumps and piping network can be approximated into the imitation software, and the results of simulations enable observation of the operation in various adjustment methods.

During transients, especially during speed changes, large deviations usually occur between the estimated and the real flowrates. Because of this, the HIL model does not cover liquid inertia since the dynamic estimation remains unaffected. However, liquid inertia needs to be considered for a controller synthesis.

However, the problem of maintaining equipment stability during and after transient disturbances cannot be so easily solved. Motor and mechanical equipment characteristics, transformers, and system impedances are among the many items contributing to stability. Unless correctly considered to assure proper design early enough, not all the proposed measures may be able to prevent instability.

When the liquid in a long full line is first accelerated by starting a pump or rapidly opening a valve, the inertia of the liquid for a variety of centrifugal

pumps cannot be shown conveniently by curves or tables. Therefore, accuracy in determining the pump is not usually high in HIL imitation.

Such benefits are based on adjustable models on the PLC basis that can be currently modified and corrected along with the test measurements on the system, motor, and PEC those characteristics are known. In addition, adjustable models describing the pumping process may be added to the control scheme of the PEC, and hence, no additional measurements would be required for the control. The speed control loop of the HIL could even be replaced by the PLC control loop to simplify the control scheme of a particular application and to improve the adjustment quantity of the process.

Unfortunately, the applicability of the HIL method is limited by systems, in which the process characteristics remain relatively constant or their change can be reliably detected. This approach is unsuitable for CPP applications with regularly changing process parameters. Another limiting factor can be the estimation accuracy of the HIL, resulting from the adjustment of the motor rotational speed and torque.

3.4 Summary of Chapter 3

1. The developed experimental setup involves both conventional industrial equipment and the original software that mutually help test the new methodology, understand its shortcomings, tune components, and correct errors. However, physical experimentation requires expensive but rigid systems unsuitable for tuning and reorganization. As the CPP is a very complex system, to verify and validate obtained experimental results, additional methods were used.

2. System simulations provide better flexibility, relatively lower cost, and a shorter study period. Thanks to successful representation of various pumping modes and piping disturbances, the models developed in this research within the Matlab/Simulink environment, supported the methodological findings and software enhancement.

3. In the HIL model, a part of the real system is merged with a mathematical model of the remaining system parts. To study pumping applications, the real control system was used in this thesis research whereas industrial pumps were replaced with the specially developed imitators. Such an approach makes it easy to present complex nonlinear hardware and software blocks and components of the PPC without a large amount of training data. Nevertheless, this approach is unsuitable for the exploration of fast-changing process parameters. Another limiting factor concerns inaccuracy due to rather coarse adjustment of the VSD speed and torque.

CHAPTER 4. ENHANCEMENT OF ADJACENT PROCESSES AND FUTURE RESEARCH

4.1 Sensorless Control

4.1.1 Introducing the sensorless control

Choices regarding management of pumping processes made in this thesis research will affect numerous future designs in the field. These concern the CPPs the pressure and flowrate maintenance of which is more complicated than that of positive displacement pumps that can provide the required flow independent of the system they are installed in.

Accuracy of process variables measurement is an important criterion used to compare one pumping system with another or to select a proper pump for a plant [36]. For this reason, the pressure, flow, and throttling maintenance systems displayed in Figs. 1.5, 1.6, and 2.1 were equipped with both the pressure gauges and the flowmeters.

However, in many installations, the metering structure and signal processing face various barriers. Sensors are not always popular among practitioners and are often not considered an option since their installation and tuning need additional efforts resulting in an increased cost and decreased reliability. Their accuracy is unsatisfying because of liquid density variation [63]. In some industrial applications, they have poor anti-noise disturbance ability to pipe vibrations and fluid turbulence, which increases the measurement errors dramatically.

Today, researchers pay attention to a sensorless model-based assessment (known also as soft-sensing or virtual sensing) of a priori unknown or difficult to measure natural (mechanical, hydraulic, electrical) process variables using readily available online electrical measurements [64] – [66]. These computing techniques can either replace existing hardware sensors or be used in parallel to provide redundancy and to verify whether the sensors produce correct data. Thanks to fewer numbers of electromechanical components, a CPP becomes more reliable, particularly in harsh environment typical for wastewater and compressible liquid pump stations.

This has several advantages such as [67]:

- cost savings as there is no need for sensors;
- increased reliability, as there are no additional components (transducer, cable, connections) that can cause malfunction;
- no maintenance and exchange of pressure or flow transmitters;
- better dynamics, with a response time of 1 – 2 sec;
- increased energy savings.

A criterion for the sensorless operation is that there must be an evident one-to-one relation between the pressure and the flowrate and the power and the flowrate, as this forms the basis for the computation. Commonly, it may be used with centrifugal pumps that have radial impeller. It was shown in [68] that the speed estimation accuracy of the model-based approach used in DTC rarely exceeds 3 %, torque assessment accuracy is below 4 %, and power calculation accuracy does not approach 5 – 7 %.

However, based on the results obtained in the above sections, the area of the sensorless control may be enlarged to the systems with high-pressure, high-flow, and high-speed operations outside the NOP.

4.1.2 Flow metering problems and their resolving

Different types of flowmeters exist depending on the fluid, technology, application, environment, cost; each type with respective characteristics, strengths and weaknesses. There are numerous established flow sensing devices including direct rate counting of a propeller immersed in the fluid and various indirect approaches. Propellers represent the least expensive alternative but they are subjected to fouling, corrosion, or wearing that could slow or stop their rotation. Among the indirect approaches, an ultrasonic Doppler effect is applied [69] or a flow can be frequently estimated as the velocity of fluid over a known area [70], [71]. Several methods [72] rely on forces produced by the flowing stream while it overcomes a known constriction. The weight transducer flowmeters involve weighing the liquid, thereby measuring its volume and calculation of the flowrate by differentiation with respect to time. In the power-to-flow converters, the speed of the rotating disc is kept constant by a servomotor in spite of changes in the flowrate whereas the differing power proportional to the flowrate is measured. Positive-displacement flowmeters accumulate a fixed volume of fluid and then count the number of times the volume is filled to measure the flow. In [50], fluid flowrates in pipes are measured by the estimation of vibrations with the help of laser vibrometers. In [73], a capacitive electromagnetic flowmeter working in a voltage-sensing mode has been developed. In addition, Vortex meters are used as indirect tools that evaluate the flow by the shedding frequency with thermo-resistive, capacitive, or piezoelectric sensors.

Many efforts on the meter structure and signal processing have been made to improve their quality; however, the results still are not so satisfactory. In medicine, sensors for the flowrate measuring meet such problems as thrombus formation, insufficient durability, and need for calibration [64]. In wastewater applications and other compressible liquid equipment, density variations [63] decrease metering accuracy. In some industrial applications, they cannot be installed.

Because the pressure measurement is less expensive than the flow metering, measurement of either discharge pressure or pump differential pressure is substituted for pump flow measurement. The success of this approach depends

on the nature of the pump curves. It only works if pressures change significantly with a pump flow.

For that reason, the sensorless flow metering may be introduced to many CPP applications. To this aim, a model expressed by the flowrate characteristics is to be used and an accuracy and cost have to be assessed in the scope of predictive model-based flowrate control. Using this functionality, a flow control is performed, which enables flow calculation without a separate flowmeter in CPPs where flow data are not required for invoicing purposes.

An experimental setup shown in Fig. 3.1 suits well for the sensorless control.

Fig. 4.1, shows a user interface of the flowrate control.
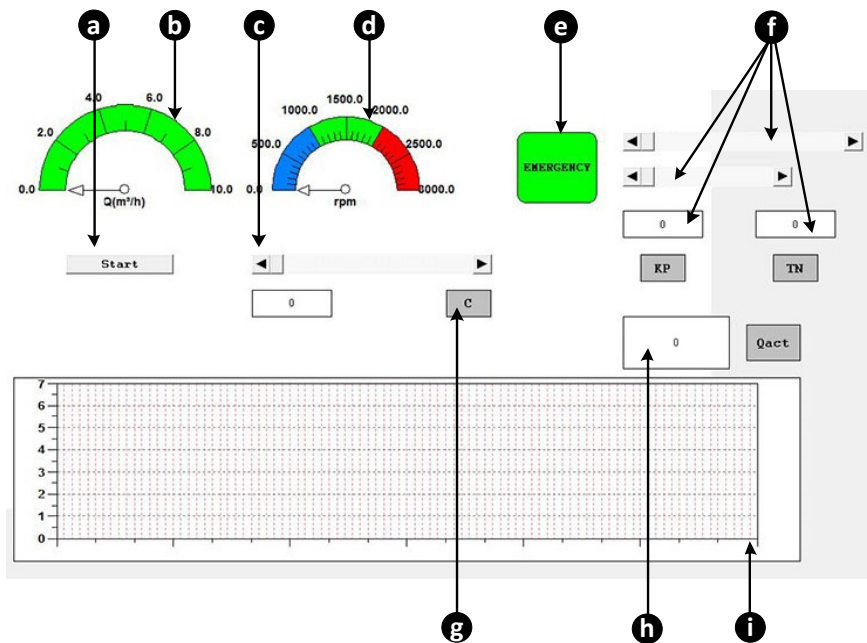
Figure 4.1 User interface for the flowrate control

It contains the following components for process parameters control, graphical, and numerical indicators:

    a – Start/Stop toggle button,
    b – flowrate arrow indicator,
    c – flowrate reference bar,
    d – arrow speed indicator,
    e – emergency situation indicator ($q < q_{min} \| q > q_{max}$),
    f – buttons for PID controller adjustment,
    g – digital flowrate indicator,
    h – calculated flowrate indicator,

i – flowrate chart.

An algorithm of the sensorless flowrate control is shown in Fig. 4.2.
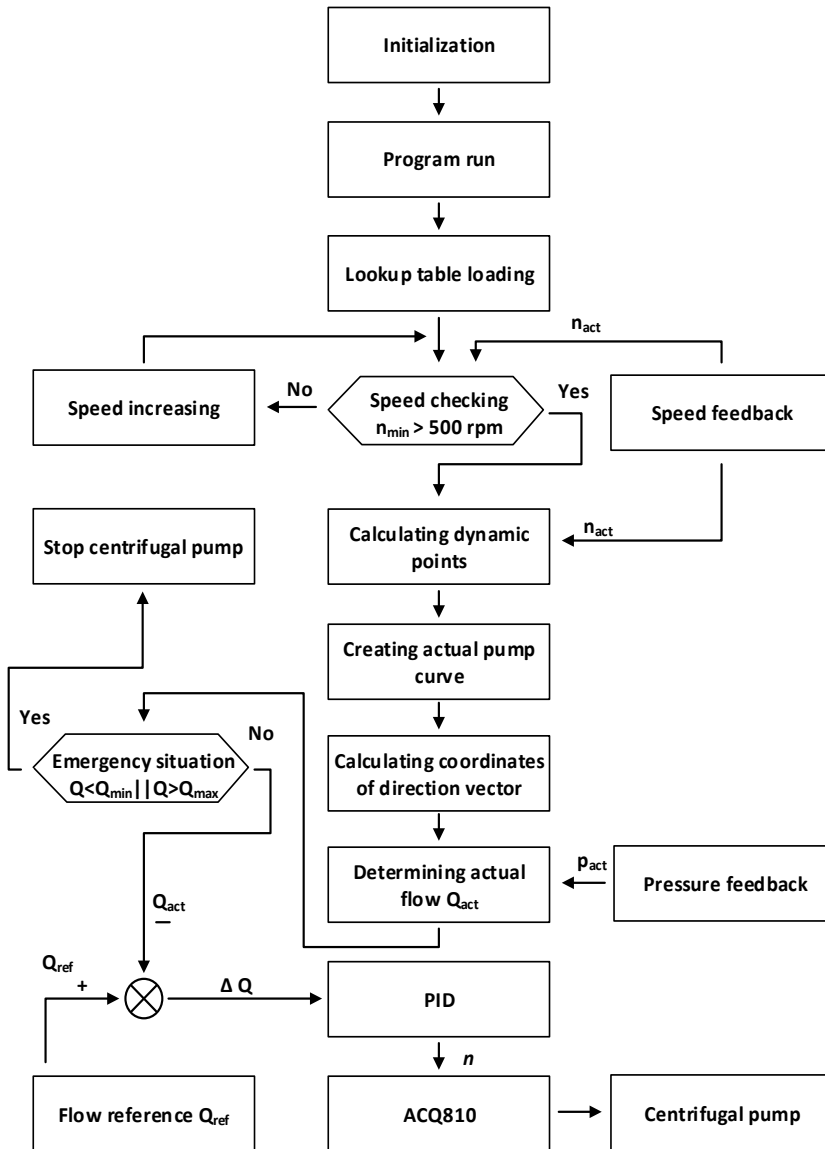
Figure 4.2 Algorithm of the sensorless flowrate control

The algorithm of the developed program works in the following manner.

At the initial step, the program loads some basic data like the global variables, local variables, checks connection between PLC modules and the frequency converter ACQ810, etc. After the program launching with the help of the start toggle button (a), the operator can choose the required level of flow q_{ref}

with the help of the flow reference bar (c). For more convenience, the reference value is also indicated with the help of the indicator (g) and later this value can be corrected to meet industrial needs. Simultaneously, the program uploads initial data from the lookup table. These data include the nominal values of pressure p and flowrate q that correspond to the nominal rotational speed $n \approx 2800$ rpm. At the next stage, the program checks the current speed n_{act} of the centrifugal pump. The PLC receives the speed information from the PEC and, while it is below 500 rpm, the system increases the demand. When the speed equals or is higher than the minimal value, the next step of the algorithm starts. At the current stage, the program calculates several pairs of values p_{var} and q_{var} that are located on the performance curve corresponding to the speed n. While the speed n lies in the boundaries – 500 rpm $< n <$ 2800 rpm, p_{var} and q_{var} are estimated as follows:

$$p_{\mathrm{var}} = p_{initial}\left(\frac{n_{act}}{n_{initial}}\right)^2, \qquad (4.1)$$

$$q_{\mathrm{var}} = q_{initial}\left(\frac{n_{act}}{n_{initial}}\right), \qquad (4.2)$$

where n_{act} corresponds to the current speed value at the moment of observation.

Thus, with the help of n_{act} and values $p_{initial}$, $q_{initial}$ from Table 4.1, the program calculates new values for the p_{var} and q_{var} corresponding to the initial values from Table 4.1. The program calculates these values dynamically and the new lookup table with dynamical values is shown in Table 4.2. Later the data from Table 4.2. were used for the calculations to find the value of the curent flowrate q_{act}.

Table 4.1 Initial values

$q_{initial}$	9.60	7.80	6.6	5.4	4.8	3.0
$p_{initial}$	1.55	1.8	2.0	2.15	2.25	2.45

Table 4.2 Dynamic values

q_{var}	q_1^*	q_2^*	q_3^*	q_4^*	q_5^*	q_6^*
p_{var}	p_1^*	p_2^*	p_3^*	p_4^*	p_5^*	p_6^*

In this way, with the help of n_{act} and values $p_{initial}$, $q_{initial}$ from Table 4.1, the PLC calculates new values for p_{var} and q_{var} that correspond to the initial values from Table 4.1. The program calculates these values dynamically, and the new lookup table with dynamical values is shown in Table 4. 2. Later, the data from Table 4.2 are used for the calculation of the flowrate q_{act}.

In the new lookup table, $q_1^*..q_6^*$ and $p_1^*..p_6^*$ are dynamic values, calculated according to (4.1) and (4.2). With the help of Table 4.2, the new

performance curve of a centrifugal pump may be created for the speed n_{act} based on several main points $q_1^*..q_6^*$ and $p_1^*..p_6^*$ as Fig. 4.3 shows.
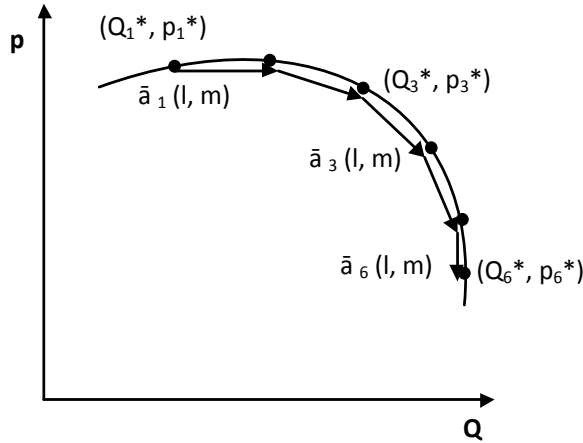
Figure 4.3 Calculated performance curve

During the further step, the program calculates the flow in the system, q_{act}. To this aim, an Euler's first order approximation method is used [74]: the actual performance curve is divided into several parts and is substituted by the polyline, which describes the performance curve with high accuracy because of the small step intervals [75]. Later, in accordance with actual pressure value p_{act}, which PLC receives from the pressure sensor installed on the discharge pipeline, the program calculates the actual flowrate value q_{act}:

$$\begin{cases} p_{act} = m \cdot t + p_n^* \\ q_{act} = l \cdot t + q_n^* \end{cases}, \tag{4.3}$$

$$q_{act} = l \cdot \left(p_{act} - p_n^*\right)/m + q_n^*, \tag{4.4}$$

where $n - 1,…,6$ and (m, l) are the coordinates of a directional vector $\bar{a}$ in Fig. 4.3, and t is the scale coefficient.

Thus, equation (4.4) connects the current value of the flow q_{act} and the current pressure p_{act} with previously calculated values of q_n^*, p_n^*. To perform these calculations, the standard mathematical functions from CoDeSys library were used.

At the next stage, the program compares the calculated value q_{act} with critical values. During the tests critical values were $q_{min} = 2$ m^3/h, and $q_{max} = 8$ m^3/h. If the flowrate value exceeds these boundaries, an emergency indicator (e) displays the alarm, and the experimental setup switches off. Once the flow is within the boundaries, the new step starts and the program compares q_{act} with the reference value q_{ref}. PI controller regulates an output signal of the speed with

the help of PEC, which changes the speed while the pumping system changes its performance curve to an appropriate one. As a result, the system automatically maintains the desired flowrate in the system.

4.1.3 Pressure measurement problems and their resolving

Pressure is a key process variable in almost every boosting pumping applications where the close-loop system tends to keep the pressure at the required level. Commonly, the pump speed reference is generated by the speed controller as a function of pressure [68].

Pipeline pressure can be estimated by the pressure difference of sensors since the liquid characteristics, rotational speed of the pump, and flow losses between the corresponding pump flanges can be obtained. These direct measurements represent the most common approach to the pump control.

Any pressure transducer provides an interface between the pumping process and the control system. To follow linearly applied pressure, the pressure gauge output signal should be independent of other system variables the most significant of which is the temperature. The liquid applies the force to the transducer equipped with the sensing diaphragm. Mechanical reversible deformation is then converted to an electrical output signal, voltage, or current, proportional to the pressure when connected to the power source. The major typical transduction techniques are based on the differential transformer or the capacitive sensors. In this study, the transducers with voltage and current outputs were explored. Voltage pressure transducers operate at 5 to 10 VDC supply; their outputs are generally of 0 to 20 mV. Current pressure transducers called transmitters produce 4 to 22 mA output signals at widely varying voltage.

However, especially in small CPPs, the cost of pressure gauges with an appropriate metering system is comparable with the total cost of the pump [60].

Moreover, there exist a variety of reasons for the direct pressure feedback destruction. Among them, sustained overpressure, cavitation in liquid flow, pressure surges/spikes, mechanical blow, corrosion, vibration at the diaphragm resonant frequency, expansion due to changing media, such as fluid freezing in the pipeline, and other reasons may be listed.

Because of destruction, three types of the transducer failures can affect the pumping process:

- Total failure when the signals stop coming from the transducer.

- Transducer malfunction when a transducer suffers from the mechanical or electrical breakdown but continues generating the output signals. Obviously, as the signals are faulty, they do not reflect the real process values.

- In addition, the measurement errors (due to incorrect selection of the transducer or mistreatment) can lead to serious deviations of readings.

All these types of failures result in abnormal functioning of the pumping system, which can become a reason of serious damage and lead to dangerous consequences. Totally failed transducer can cause the system overload, excess pumping, overpressure, intensive working outside the normal range (far from the best efficiency point), and immediate damage of the piping system and the pump. The transducer with faulty signals containing errors and deviations (e.g. nonlinearity, dynamic error, or hysteresis) can cause the non-immediate damage and the long-term misuse of the pumping system and the piping. Long-lasting functioning under inaccurate pressure readings results in decreased equipment lifecycle, losses in efficiency, and hence in excess operation and service costs.

As a result, researchers' efforts concentrated on the development of sensorless pumping systems without pressure sensors [76]. Modern PEC-fed VSDs that can regulate and define the operational state of the driven units (i.e., speed, torque, power consumption, and efficiency) without excess sensors serve as the core components of such techniques. This model-based approach enables defining the operational state of the pumping system by utilizing the internal measurements and estimates of a PEC.

Unfortunately, the broadly used scalar-controlled PECs have many problems with power and speed estimations. In the traditional DTC practice, the real characteristic curves may differ noticeably from those published by the manufacturer in the datasheets of the pump thus decreasing the estimation accuracy of this method.

Threat, up to now, the model-based approach was not recommended for applications with regularly changing process parameters. Neither was it advised to perform the sensorless control far from the NOP.

Fortunately, the CPP shown in Fig. 2.1 opens novel possibilities for the sensorless control. Here, a PLC may implement the pressure control not only without pressure gauges but even without speed sensors and flowmeters because the tabulated data stored in the system memory in the form of lookup tables inline with the DTC module represent a fully upgradable database. The DTC system estimates the actual torque T and the speed using the sensed motor currents I and voltages U. Based on the power-torque relation (1.14), the current pressure may be estimated from these tables and adjusted as explained in Section 2.2.2. As a consequence, the DTC system runs the VSD with the requested speed to provide the demanded pressure.

4.1.4 Resume

Focus in this section was on a sensorless model-based control of a priori unknown or difficult to measure process variables either for replacement of existing hardware sensors or for use in parallel to provide redundancy and to verify whether the sensors produce correct data.

1. The sensorless flow metering and pressure estimation can be introduced to many CPP applications. They have higher reliability and energy efficiency, being least expensive than their competitors.

2. As the sensorless systems are not very accurate in view of the speed estimation, torque assessment, and power calculation, they were recommended mainly for the closed circulating systems, such as the heat circulation CPPs, within their operation near the NOP and around the BEP.

3. However, based on the results obtained in this thesis research, the area of the sensorless control may now be enlarged to the systems with high-pressure, high-flow, and high-speed operations outside the NOP.

4.2 Improvement of Education in the Field of Pumping Management

4.2.1 Learning goals and problems

Today, many institutions seek better ways to enhance their education which, according to the UNESCO documents, should provide organisational arrangements for creation, application, and defining teaching and learning processes and resources that motivate students to learn not only the skills directly related to their speciality, but also the neighbour knowledge domains valuable in the professional environment.

Analysis of multiple electrical engineering curricula revealed that a very small number of possibilities are available for future electrical, mechanical, and hydraulic specialists to study pumping. This situation created a reason for the development of a new laboratory stand and an appropriate teaching methodology.

Laboratory experimentation on the pumping stand aims to provide the learners with knowledge and skills in the CPP and pumping VSD composition and action, their abilities to operate the imitator, and their understanding of system loading, power, and pump characteristics. Additionally, it helps to answer such practical questions, as:

- What are the benefits and drawbacks of centrifugal pumps?
- Why is the pumping speed control required?
- Why do the pump manufactures provide only the rated speed characteristics?
- Why does the imitator incorporate two drives whereas the real pump has only one?
- Why do the testing and the loading VSDs operate in different modes?
- Why the CPP is a nonlinear system?
- How will the flowrate change at the constant motor speed if the head or the pressure increases?

- How will pressure change at the constant motor speed if the flowrate increases?
- How will the head change at constant motor speed if the flowrate increases?
- What are the functions of ACS 800 and AC500?
- Why do different pumps have different characteristics?
- Why do different pumping VSDs have different load characteristics?

4.2.2 Laboratory stand

To study pumping processes, the HIL imitator (Fig. 3.21) was applied as an educational instrument.

The laboratory stand (Fig. 4.4) incorporates two ABB ACS 800 VSDs, namely, the loading drive VSD 1 imitating the pump and the testing drive VSD 2 imitating the pump drive. Every VSD includes a squirrel-cage induction motor and a PEC. The loading motor is of 5.5 kW/400 V/11 A and the testing motor is of 15 kW/400 V/29 A. The motor shafts are mechanically coupled through a clutch to provide their joint rotation.

Both PECs are 3-phase systems with an input voltage of 380…500 V, output voltage of 0…415 V, input frequency of 48…63 Hz, output frequency of 8…300 Hz, maximal current of 62 A, and maximal output power of 22 kW. The testing drive operates in the scalar control mode to follow the demanded speed at constant voltage-frequency ratio with boosting.

The loading drive performs in the DTC mode to follow torque demands for studying loads. Electrical equipment is installed within cabling cabinets, with front panels (Fig. 4.5) equipped with control buttons and sockets.
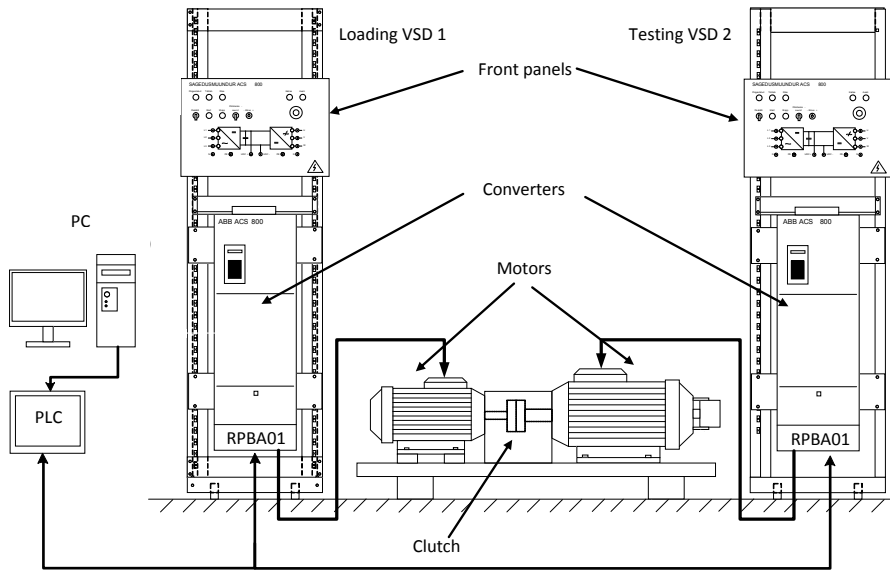
Figure 4.4 Layout of the laboratory stand

Figure 4.5 Control panel of ACS 800. An arrow shows the main switch

To control the imitator, a computer and the PLC ABB AC500 are used. The PLC functional circuit and appearance were shown in Figs. 3.2 and 3.3. User interfaces of the PLC CoDeSys and the pump imitator are shown in Figs. 4.6 and 4.7.

Figure 4.6 ABB Configurator interface: (a) – Run, (b) – Stop, (c) – PLC login, (d) – PLC logout

Figure 4.7 User interface of the imitator. (a) – PUMP TYPE selector, (b) – REFERENCE selector, (c) – REFERENCE VALUE slider, (d) – RUN button, (e) – PIPE SIZE selector, (f) – STOP button, (g) – PROCESS DATA

4.2.3 Experimentation methodology

The proposed laboratory experimentation cycle includes the following operations:

96

- Inspect the connections between the computer and PLC. Ensure that the PLC power cable is plugged and the bulb of the PLC power supply lights up.
- Power ON VSD 1 and VSD 2 (main switches in Fig. 4.5).
- Power ON the computer and PLC (e, Fig. 3.3).
- Launch the *ABB Configurator* and open the project Centrifugal Pump (Fig. 4.6).
- In the project *Centrifugal Pump*, open the user interface AC500.
- In the user interface *AC500* (Fig. 4.6), login to PLC (c, or Online/Login/Download the new program) and run the program (a, or Online/Run). If the bulb "Rikke" lights up, press Reset on both VSD control panels.
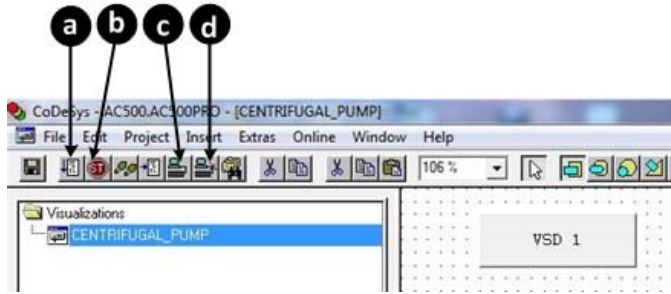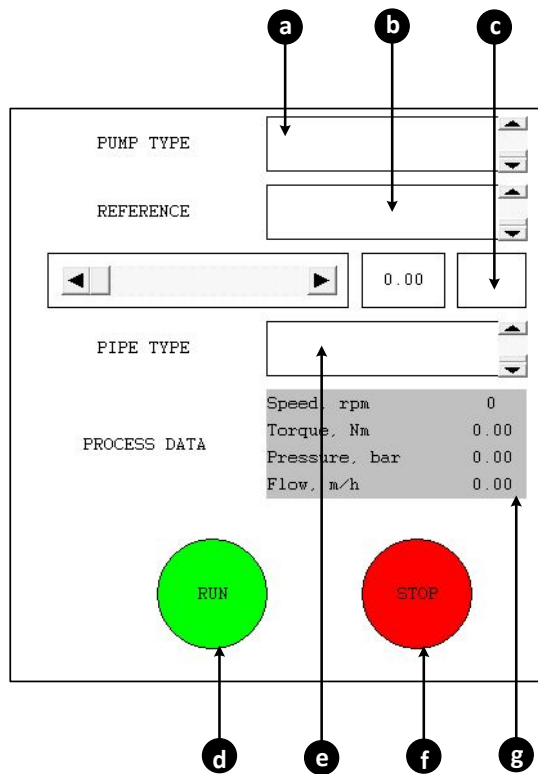- In the user interface of the imitator (Fig. 4.7), assign given PUMP SIZE (a), REFERENCE: SPEED CONTROL (b), initial speed about 200 rpm (c), and given PIPE SIZE (e), whereupon RUN the simulator (d).
- To record the loading characteristic $T(n)$, increase gradually the speed with the slider (c) up to the nominal level of 2760 rpm. Upon speeding, read 10…15 speed/torque values (g), and fill them in the protocol.
- To record the pump characteristics $h(q)$ and $p(q)$, assign the rated speed (c) and increase gradually the pipe diameter (e). Read 10…15 pressure/head/flow values (g) and fill them in the protocol.
- Using obtained $T(n)$ data, calculate power $P(n)$ and plot the loading, break power, efficiency, and pump characteristics required for a given variant: $T(n)$, $\eta(n)$, $h(q)$, $P(q)$, $p(q)$, $P(n)$, or $\eta(q)$.
- After the work completion, STOP the imitator and the program (b, Fig. 4.7 or Online/Stop) and log out (d, Fig. 4.6 or Online/Logout). Close the project and *ABB Configurator*.
- Switch OFF the PLC (e, Fig. 3.3) and PC, then power OFF VSD 1 and VSD 2 (main switch in Fig. 4.5).

4.2.4 Resume

1. To offer a course of pumping for students of electrical engineering, mechanical engineering, and hydraulics, a new laboratory stand and an appropriate teaching methodology were designed.

2. Laboratory experimentation on the pumping stand aims to provide the learners with knowledge in CPP and VSD composition and action, their abilities to operate the imitator, and their understanding of system loading, power, and pump characteristics. Additionally, it helps answer many practical questions.

3. The new educational tool became a resource, which motivates students to learn not only the skills directly related to their speciality, but also the neighbour knowledge domains valuable in the professional environment.

During the tests, students can choose between two centrifugal pump types - CDX 120/12 and CDX 120/20. In addition, three main control modes are available – speed, flow and pressure control. The functionality of the test bench allows investigation of the performance, system characteristics and calculation of mechanical and hydraulic power of the pumps.

4.3 Future Research [VI]

4.3.1 Applying the HIL approach to design vessel electric propulsion

Contemporary vessels include many on-board electric and electronic devices. The common trend is moving towards complete vessel electrification with the electrical feeding of both the propulsion and the auxiliary modules. In contrast to the vessels in which the prime mover is a steam turbine, gas turbine, or diesel engine, more and more boats, yachts, and cruise ships obtain electric propulsion that benefits substantially from motor drives thanks to advances in the fields of power electronics, electrical motors, fast microcontrollers, and digital technology.

One of the main considerations to be addressed by a marine designer concerns the development, dimensioning, and assessment of a vessel electric propulsion drive. Taking into account simulation complexity, most of the propulsion research centres employ specific test benches to verify their designs. In a typical trial stand, the machine under the test is a propulsion motor imitator coupled to another electrical machine generating the counter-torque to emulate the propeller. In [77] such a setup was designed based on an electromechanical dynamometer capable of imitating a changeable load suited for propulsion testing. This stand was built by coupling a 15 kW dc machine to a 15 kW ac synchronous motor with the common shaft. The use of the dc machine is an evident drawback of such a solution because of its limited dynamics possibilities. In [78], a doubly fed induction loading system was presented to imitate a 20 MW DTC-fed marine propeller. Problems that are overcome in this testing equipment are related to restricted speed range, extra forced commutation at synchronous speed, and low-quality PECs.

The functional circuit of the vessel propulsion HIL imitator is the same as is shown in Fig. 3.21 where the computer pump model is replaced with the vessel propulsion model. The setup incorporates two electrical drives, namely the propulsion drive imitator and the propeller imitator. To adjust the propulsion drive imitator, the scalar mode is applied and to control the propeller imitator, the DTC was used. DriveWindow provides the remote control of the propulsion and the propeller imitator VSDs, their monitoring, graphical trending, tuning, and parameter registration. The computer model of a vessel incorporates a library of speed references, a library of vessel characteristics, and an appropriate mathematical model communicating with the vessel propulsion imitator via the PLC.

To determine real engine power and torque, the low-power model parameters were scaled in percentage relative to the nominal values. In this vessel model, the static hull resistance and total thrust force depend on the referred vessel velocity and laws generated with the help of the library of the speed references. The brake power and total propulsive efficiency, the complex functions of velocity, were obtained from the manufacturer's diagrams. To use them, an interpolation was applied, which needs multiple data to store hence the lookup tables occupy significant memory space.

The following exploratory problems can be solved with the help of the platform developed:

- comparative analysis, identification, and testing propulsion parts;
- experimentation on the steady-state and dynamic operation modes using the developed physical prototypes;
- application of multiple motor drive models that support commissioning and identification procedures;
- combination of both the marketable simulation toolboxes and the author's original software;
- speed-dependency and load-dependency study of the drives to find the optimal equipment configurations;
- assessment of the most economical performance modes to choose the best propulsion operation.

4.3.2 Applying the hybrid system to improve aircraft pumping

The hybrid pumping system proposed in this research seems highly prospective for the improvement of aircraft pumping control systems.

With the development of aviation towards a growth of manoeuvrability, velocity, and power, the performance indexes of actuation systems have to grow, especially in view of stability, reliability, and efficiency. In this connection, *electro-hydraulic actuators* (EHAs) are focused in the research field of actuation systems thanks to their small volume and high survivability [28]. As the volume control mode of EHAs lacks the loss of throttling, it has high efficiency, but its response cannot satisfy contemporary fast-acting requirements. Pump and valve hybrid EHA as the combination of servo valve system and pump control system might serve as a solution in this issue. Introduction of the mutual control can increase both the efficiency and the response by adjusting pump and valve operation according to the flight fluctuating load properties.

At this, maximal working pressure can be obtained at different flight stages, such as aircraft take-off, cruising, landing, etc. At every stage of flight, the aircraft may request an action at any time. Herewith, the changes of oil pressure will affect the performance of the position loop, thus the stability of the pressure loop is the key factor to satisfy the working request of the position loop.

The system layout may be based on Fig. 2.6. Here, the oil pressure loop serves as a position loop; therefore, any pressure fluctuation lags to the movement of the position network. Because the bandwidth of the servo valve is higher than the bandwidth of the motor, the response of the pressure loop is increased by a position loop signal. As a result, the motor may run ahead the change of pressure.

The benefits of the pressure loop involving both the pump and the valve in the hybrid EHA have the complex character of a multi-variable, nonlinear, and time-varying system. Its model-based management algorithm promises to replace traditional PID controllers used in today's aviation.

4.3.3 Resume

1. Scientific results and practical outcomes of this thesis research may positively affect some neighbour research areas, in which challenges similar to those of centrifugal pumping management occur.

2. The developed HIL setup with improved software is suitable for exploring vessel electric propulsion systems in the scope of design, dimensioning, and assessment of vessel electric propulsion drives.

3. The principles, algorithms, and methods used in the developed hybrid system may essentially improve pumping complexes of aircrafts.

4.4 Summary of Chapter 4

This Chapter is devoted to the enhancement of adjacent processes and future research problems.

1. Primary attention is paid to a sensorless model-based control of unknown or difficult to measure process variables either for replacement of existing hardware sensors or for their use in parallel to provide redundancy and to verify whether the sensors produce correct data. As a result, some flow and pressure measurement problems were resolved.

2. Improvement of education in the field of pumping management is another important result of the thesis research. The developed HIL methodology, hardware, and software have found their place in laboratory experimentation with pumping.

3. Scientific results and practical outcomes of this work may positively effect some neighbour research areas, in which challenges similar to those in centrifugal pumping management are encountered. Among those systems are, vessel electric propulsion systems and aircraft pumping plants.

REFERENCES

[1]   The Kyoto protocol, [Online]. Available: http://unfccc.int/kyoto_protocol/items/2830.php

[2]   Tracking Industrial Energy Efficiency and CO2 Emissions, OECD/IEA, 2007, 324 p.

[3]   P. Skworcow, D. Paluszczyszyn and B. Ulanicki, Pump schedules optimisation with pressure aspects in complex large-scale water distribution systems, *Drinking Water Engineering Sciences*, 7, 2014, pp. 53 – 62.

[4]   Pump Systems Optimization : Energy Efficiency and Bottom-Line Savings. [Online]. Available: http://pumpsystemsmatter.org.

[5]   Energy Efficiency Best Practice Guide, State Government Victoria, [Online]. Available: www.sustainability.vic.gov.au

[6]   Global water withdrawal, Sectoral competition for water withdrawals for human uses. [Online]. Available: http://www.waterpolitics.com

[7]   P. G. Kini, R. C. Bansal and R. S. Aithal, Performance analysis of centrifugal pumps subjected to voltage variation and unbalance, *IEEE Transactions on Industrial Electronics*, 55 (2), 2008, pp. 562 – 569.

[8]   H. Anderson, Centrifugal pumps, Elsevier, 2014.

[9]   K. Fernandes, B. Pyzdrowski, D. W. Schiller and M. B. Smith, Understand the basics of centrifugal pump operation, CEP magazine, May 2002, pp. 52 – 56.

[10]   J. R. Pottebaum, "Optimal Characteristics of a Variable-Frequency Centrifugal Pump Motor Drive," *IEEE Transactions on Industry Applications*, vol. IA-20, no. 1, 1984.

[11]   Grundfos Industry Pump Handbook, 2010, 160 p.

[12]   H. A. Wiegand and L. B. Eddy, Characteristics of centrifugal pumps and compressors which affect the motor driver under transient conditions, *Transactions of the American Institute of Electrical Engineers*, Part II: *Applications and Industry*, 79 (3), Jul. 1960, pp. 150 – 156.

[13]   R. Carlson, "The correct method of calculating energy savings to justify adjustable-frequency drives on pumps," *IEEE Transactions on Industry Applications*, vol. 36, no. 6, pp. 1725-1733, Nov/Dec 2000.

[14]   J. Viholainen, J. Kortelainen, T. Ahonen, N. Aranto and E. Vakkilainen, Energy efficiency in variable speed drive (VSD) controlled parallel pumping, *6th International Conference on Energy Efficiency in Motor Driven Systems (EEMODS 2009)*, Nantes, France, vol. 2, pp. 519 – 530.

[15]   V. Vodovozov, Electrical Drive: Performance, Design and Control, Lambert Academic Publishing, Saarbrücken, 2014, 320 p.

[16]   S. Shiels, When trimming a centrifugal pump impeller can save energy and increase flow rate, *World Pumps*, Nov. 1999, Elsevier, pp. 37 – 40.

[17]   Centrifugal Pump Handbook, Sulzer Pumps, 2010, 302p.

[18]   D. Popescu, A. Mihaela, and D. Denisa, The control of variable speed pumps in series operation, *Advances in Environment Technologies, Agriculture, Food and Animal Science*, 2013, pp. 212–216.

[19]   American National Standard for Centrifugal and Vertical Pumps for Allowable Operating Region, ANSI/HI Pump Standards Library, Hydraulic Institute, 1997, 4 p.

[20]   Variable Speed Pumping – a Guide to Successful Applications, Hydraulic Institute, 2004, 22 p.

[21]   D. A. T. Trana, Y. Chena, M. Q. Chauc and B. Ning, A robust online fault detection and diagnosis strategy of centrifugal chiller systems for building energy efficiency, *Energy and Buildings*, Elsevier, 2015, pp. 441 – 453.

[22]   M. Koor, A. Vassiljev and T. Koppel, Optimization of pump efficiencies with different pumps characteristics working in parallel mode, *Advances in Engineering Software*, Nov. 2015, pp. 1 – 8.

[23]   Z. Yang and H. Børsting, Energy efficient control of a boosting system with multiple Beijing variable-speed pumps in parallel, *49th IEEE Conference on Decision and Control*, Atlanta, GA, USA, 2010, pp. 2198 – 2203.

[24]   ABB   Oy   Efficiency   Estimation   Guide,   [Online].   Available   at: https://library.e.abb.com/public/ab22cf21c367d260c12573e9004d88a4/efficiency_calc_guide.pdf?fi lename=efficiency_calc_guide.pdf

[25]   DriveSize, Available at: http://new.abb.com/drives/software-tools/drivesize.

[26]   B. Nesbitt, Handbook of Pumps and Pumping, Elsevier, 2006, 424 p.

[27]   H.-Z. Tan and N. Sepehri, On condition monitoring of pump pressure in a hydraulic servo-drive system, *The American Control Conference*, Arlington, VA, USA, 2001, pp. 4478 – 4483.

[28]   Y. Ji, S. Peng, L. Geng, Z. Wang and L. Qiu, Pressure loop control of pump and valve combined EHA based on FFIM, *9th International Conference on Electronic Measurement and Instruments (ICEMI 2009)*, Beijing, China, pp. 3-578 – 3-582.

[29]   J. Tamminen, T. Ahonen, A. Kosonen, J. Ahola and J. Tolvanen, Variable speed drive-based pressure optimization of a pumping system comprising individual branch flow control elements, *16th European Conference on Power Electronics and Applications (EPE 2014-ECCE Europe)*, Lappeenranta, Finland, pp. 1 – 11.

[30]   G. Gao and D. Cao, "Design of constant pressure water supply system for a residential district based on PLC," *2016 IEEE International Conference of Online Analysis and Computing Science (ICOACS)*, Chongqing, 2016, pp. 33-35.

[31]   C. Wei, X. Meixiang and F. Kangling, A PLC-based fuzzy PID controller for pressure control in coke-oven, *31st Chinese Control Conference*, Hefei, China, 2012, pp. 4754 – 4758.

[32]   A. Sniders and T. Komass, Invariant method of load independent pressure control in steam boiler, *Electrical, Control and Communication Engineering*, 1, 2012, pp. 5 – 10.

[33]   T. Ahonen, J. Tamminen, J. Ahola and J. Kestilä, Frequency-converter-based hybrid estimation method for the centrifugal pump operational state, *IEEE Transactions on Industrial Electronics*, 59 (12), 2012, pp. 4803 – 4809.

[34]   L. Szychta and R. Figura, Analysis of efficiency characteristics of squirrel-cage induction motor for pump applications, *20th International Conference on Electrical Machines (ICEM 2012)*, Marseille, France, pp. 73 – 78.

[35]   Control Strategies for Centrifugal Pumps with Variable Flow Rate Requirements, DOE Pumping Systems Tip Sheet, 12, 2007, 4 p.

[36]   F. J. T. E. Ferreira, J. A. C. Fong and de A. T. Almeida, Ecoanalysis of variable-speed-drives for flow regulation in pumping systems, *IEEE Transactions on Industrial Electronics*, 58 (6), 2011, pp. 2117 – 2125.

[37]   Peng Xiaohong, Xiao Laisheng, Mo Zhi and Liu Guodong, The variable frequency and speed regulation constant pressure water supply system based on PLC and fuzzy control, *International Conference on Measuring Technology and Mechatronics Automation (ICMTMA 2009)*, Zhangjiajie, China, 2009, pp. 910 – 913.

[38]   Y. Gao and N. Ding, "Electro-hydraulic proportional pressure control system of hydraulic machine," *IEEE 10th International Conference on Industrial Informatics*, Beijing, 2012, pp. 370-373.

[39]   H. Berger, Automating with STEP 7 in STL and SCL, John Wiley & Sons, 2014, 553 p.

[40]   Lan He and Lepeng Song, The pump house constant pressure fuzzy self-tuning PID control system simulation, *International Conference on Electric Information and Control Engineering*, Wuhan, China, 2011, pp. 5525 – 5527.

[41]   T. Brezina, J. Kovar and T. Hejc, Modeling and control of system with pump and pipeline by pole placement method, *14th International Symposium on Mechatronics*, Trencianske Teplice, Slovakia, 2011, pp. 6 – 9.

[42]   J. Viholainen, E. Vakkilainen and J. Tolvanen, VSD control in simulated systems, *World Pumps*, 2009 (512), pp. 40 – 44.

[43]   N. Aranto, T. Ahonen and J. Viholainen, Energy audits: University approach with ABB, *6th International Conference on Energy Efficiency in Motor Driven Systems (EEMODS 2009)*, Nantes, France, vol. 2, pp. 499 – 508.

[44]   A. Boussaibo, M. Kamta, J. Kayem, D. Toader, S. Haragus and A. Maghet, Characterization of photovoltaic pumping system model without battery storage by Matlab/Simulink, *9th International Symposium on Advanced Topics in Electrical Engineering*, Bucharest, Romania, 2015, pp. 774 – 780.

[45]   J. Ghafouri and H. Khayatzadeh, Dynamic modeling of variable speed centrifugal pump utilizing Matlab/Simulink, *International Journal of Science and Engineering Investigations*, 1 (5), 2012, pp. 1 – 7.

[46]   A. Ali, M. Al Soud, E. Abdallah and S. Addallah, Water pumping system with PLC and frequency control, *Jordan Journal of Mechanical and Industrial Engineering*, 3 (3), 2009, pp. 216 – 221.

[47]   P. B. Narayana, B. R. S. Reddy, P. Motepalli and S. Dubey, Design and simulation of solar DC pump in Simulink, *International Conference on Energy Efficient Technologies for Sustainability (ICEETS 2013)*, Nagercoil, India, pp. 429 – 431.

[48]   T. Leão, J. Fonseca, E. Bock, R. Sá, B. Utiyama, E. Drigo, J. Leme and A. Andrade, Speed control of the implantable centrifugal blood pump to avoid aortic valve stenosis: Simulation and

implementation, *5th IEEE RAS & EMBS International Conference on Biomedical Robotics and Biomechatronics (BIOROB 2014)*, São Paulo, Brazil, pp. 82 – 86..

[49] F. A. O. Aashoor and F. V. P. Robinson, Maximum power point tracking of photovoltaic water pumping system using fuzzy logic controller, *48th International Universities' Power Engineering Conference (UPEC 2013)*, Dublin, Ireland, pp. 1 – 5.

[50] G. Dinardo, L. Fabbiano and G. Vacca, Fluid flow rate estimation using acceleration sensors, *7th International Conference on Sensing Technology*, Wellington, New Zealand, 2013, pp. 221 – 225.

[51] K. Mariem, K. M. Arbi, B. f. Mouldi and R. Habib, Modeling and simulation of photovoltaic water pumping system, *International Conference on Electrical Sciences and Technologies in Maghreb (SISTEM 2014)*, Tunis, Tunisia, 2014, pp. 1 – 4.

[52] SimScape 3, [Online], Available: https://www.scribd.com/document/203875789/MATLAB-SIMSCAPE-manual.

[53] T. Kenjo, S. Nagamori, Permanent-magnet and brushless dc motors, Clarendon Press, 1985.

[54] D. Kaya, E. A. Yagmur, K. S. Yigit, F. C. Kilic, A. S. Eren and C. Celik, Energy efficiency in pumps, *Energy Conversion and Management*, 49, 2008, pp. 1662 – 1673.

[55] Eesti Energia, [Online]. Available at: https://www.energia.ee/en/elekter/elektriturg.

[56] M. Bacic, On hardware-in-the-loop simulation, *44th European Conference on Decision and Control CDC-ECC*, Seville, Spain, 2005 pp. 3194 – 3198.

[57] A. Cebi, L. Guvenc, M. Demirci, C. Karadeniz, K. Kanar and E. Guraslan, A low cost, portable engine electronic control unit hardware-in-the-loop test system, *IEEE International Symposium on Industrial Electronics (ISIE 2005)*, Dubrovnik, Croatia, pp. 293 – 298.

[58] C. Koehler, A. Mayer and A. Herkersdorf, Determining the fidelity of hardware-in-the-loop simulation coupling systems, *IEEE International Behavioral Modeling and Simulation Workshop (BMAS 2008)*, San Jose, California, pp. 13 – 18.

[59] K. Marouani, H. Guendouz, B. Tabbache, F. Khoucha and A. Kheloui, Experimental investigation of an emulator "Hardware In the Loop" for electric naval propulsion system, *21st Mediterranean Conference on Control & Automation (MED 2013)*, Platanias-Chania, Crete, Greece, pp. 125 – 130.

[60] ABB Product Notes: Flow Calculation in ABB Industrial Drives, ABB, Helsinki, Finland, 2006, 200 p.

[61] ABB, Technical Guide No. 1: Direct Torque Control, ABB Inc: Helsinki, Finland, 2002.

[62] I. T. Avery, Codesys. Cel Publishing, 2012, 96 p.

[63] Y. Huang, H. Zhang and Z. Sun, Measurement of mass flow rate using a vortex flowmeter, *Proceedings of IEEE on Sensors*, 2003, pp. 344 – 347.

[64] D. Ogawa, M. Yoshizawa, A. Tanaka, K. Abe, P. Olegario, T. Motomura, H. Okubo, T. Oda, T. Okahisa and Y. Nos, Evaluation of flow rate estimation method for rotary blood pump with chronic animal experiment, *27th IEEE Annual Conference Engineering in Medicine and Biology, Shanghai, China*, 2005, pp. 7616 – 7619.

[65]   H. Y. Yang, S. H. Lee and M. G. Na, Monitoring and uncertainty analysis of feedwater flow rate using data-based modeling methods, *IEEE Transactions on Nuclear Science*, 56 (4), 2009, pp. 2426 − 2433.

[66]   V. Vodovozov and I. Bakman, Sensorless pressure calculation for parallel redundancy in pumping systems, *16th Conference on Power Electronics and Applications (EPE 2014-ECCE Europe)*, Lappeenranta, Finland, pp. P.1 −P.9.

[67]   Sensorless Pump Control for VLT 6000 HVAC / FCM 300, Danfoss, 2002, 22 p.

[68]   Z. Raud, V. Vodovozov, T. Lehtla and E. Pettai, Simulation Tools to Study Power Electronics, *13th European Conference on Power Electronics and Applications (EPE 2009)*, Barcelona, Spain, paper 0013.

[69]   J. Igarashi, K. Mizutani and N. Wakatsuki, Flow rate measurement using an ultrasonic beam, *IEEE International Ultrasonics Symposium*, Orlando, FL, USA, 2011, pp. 1525 − 1528.

[70]   R. A. Furness, Fluid Flow Measurement, Harlow: Longman in association with the Institute of Measurement and Control, 1989, 139 p.

[71]   F. Arregui, E. Cabrera and R. Cobacho, Integrated Water Meter Management, IWA Publishing, 2006, 272 p.

[72]   A. Suryawanshi and A. Joshi, Urine flow rate measurement based on volumetric pressure measurement principle, *1st International Symposium on Physics and Technology of Sensors (ISPTS 2012)*, Pune, India, pp. 334 − 337.

[73]   B. Wang, Y. Fu, Z. Huang and H. Li, Volumetric flow rate measurement with capacitive electromagnetic flowmeter in oil-water two-phase flow, *Instrumentation and Measurement Technology Conference (IMTC 2010)*, Austin, TX, USA, pp. 775 − 778.

[74]   J. Stewart, Single Variable Calculus, Cengage Learning, 2015, 960 p.

[75]   I. Vaisman, Analytical Geometry, World Scientific, 1997, 296 p.

[76]   V. Vodovozov and I. Bakman, Sensorless Pressure Control of Centrifugal Pumps, *8th International Conference-Workshop on Compatibility and Power Electronics (CPE 2013)*, Ljubljana, Slovenia, pp. 304 − 309.

[77]   R. Ahmadi, H. Behjati and M. Ferdowsi, Dynamic modelling and stability analysis of an experimental test bench for electric-ship propulsion, *Electric Ship Technologies Symposium (ESTS 2013)*, Arlington, VA, USA, pp. 110 − 115.

[78]   J. Shen, Y. Wei and X. Zhang, Applications of doubly-fed machine in simulating load of marine electric propulsion, *8th International Conference on Electrical Machines and Systems (ICEMS 2005)*, Nanjing, China, pp. 1377 − 1380.

ABSTRACT

Simulation and Experimental Study on Energy Management of Circulating Centrifugal Pumping Plants with Variable Speed Drives.

This thesis research addresses pumping management and variable speed drive designs and how they may affect human lives through energy optimization.

Taking into account prospective needs in the minimization of energy cost and alternation in pumping plant demands and loads, urgency of the study is reasoned. It was found that a primary reason of pumping energy constraints lies in the ignorance of specific power losses and disregard of high control possibilities of the contemporary variable speed drives. Neglect of these factors leads to pump oversizing and efficiency reductions. The second problem concerns unreasonable restrictions of high-pressure, high-flow, and high-speed pumping areas that often result in the use of a multi-pump system instead of a single-pump version.

This research opens novel possibilities for low energy consumption by enlarging the acceptable region for pumping and specifying the best efficiency area. In order to overcome the obstacles above, a method of inline energy losses monitoring and a procedure of high-speed pumping are offered in the frame of a common energy management methodology and a new energy management system. The proposed approach combines the benefits of throttling and speed control and brings together both the pressure and the flowrate adjustment possibilities. As a result, minimization of energy consumption and reduction of maintenance costs have been obtained as outcomes of the thesis research.

KOKKUVÕTE

Muudetava kiirusega ajamitega tsentrifugaalpumpadega varustatud tsirkulatsioonpumbajaamade energiahaldussüsteemide simuleerimine ja eksperimentaalne uurimine

Käesolev doktoritöö keskendub sellele kuidas pumpade seire- ja muudetava kiirusega ajamisüsteemid võivad vähendada energiakulu.

Käesoleva töö teeb aktuaalseks suundumus energia maksumuse vähendamisele pumbajaamades ühelt poolt, ja teiselt poolt pumbajaamade koormuse sage muutumine. Käesolevas töös on leitud, et pumpamisele kuluva energia ebaefektiivse kasutamise peamised põhjused on energiakadude ignoreerimine ja muudetava kiirusega ajamite poolt pakutavate võimaluste mittekasutamine, mis omakorda põhjustavad pumpade üledimensioneerimist ja energiaefektiivsuse langemist. Lisaks põhjustab pumpade kasutamine nende ebaratsionaalses tööpiirkonnas vajaduse kasutada mitmepumbalisi süsteeme kohtades, kus piisaks ühest pumbast.

Käesolev doktoritöö näitab ära võimalused energiakulu vähendamiseks suurendades pumpade karakteristikutel pumpade tööpiirkondi ja määrates nendes tööpiirkondades parima efektiivsusega piirkonnad. Saamaks üle töös näidatud takistustest, on käesolevas töös esitatud meetod süsteemis olevate energiakulude seiramiseks ja meetod pumpamiseks suurtel pumba pöörlemiskiirustel, mis on käesolevas töös väljapakutud metoodika ja energiahaldussüsteemi koosseisus. Käesolevas töös väljapakutud metoodika kombineerib ventiilreguleerimise ja kiiruse juhtimise häid omadusi. Käesoleva töö doktoritöö valmimise käigus on saavutatud pumbasüsteemide energiatarbe ja hoolduskulude vähenemine.

ELULOOKIRJELDUS

Isikuandmed

    Ees- ja perekonnanimi: Levon Gevorkov

    Sünniaeg ja -koht: 07.06.1980, Tbilisi

    Kodakondsus: Gruusia

Kontaktandmed

    Aadress: Akadeemia tee 5, 417A, Tallinn 12611, Eesti.

    Telefon: +37256903135

    E-posti aadress: levon.gevorkov@ttu.ee

Hariduskäik

Õppeasutus (nimetus lõpetamise ajal)	Lõpetamise aeg	Haridus (eriala/kraad)
Ivane Javakhishvili State University of Tbilisi.	2003	Raadio füüsika ja elektroonika/ Füüsikateaduse magister

1. Keelteoskus (alg-, kesk- või kõrgtase)

Keel	Tase
Gruusia	Kõrgtase
Vene	Kõrgtase
Inglise	Kõrgtase

Teenistuskäik

Töötamise aeg	Tööandja nimetus	Ametikoht
2014 - ...	Tallinna Tehnikaülikool, Inseneriteaduskond, Elektroenergeetika ja mehhatroonika instituut	Nooremteadur
2006 - 2013	Georgian Water and Power (www.gwp.ge)	Peaspetsialist
1998 - 2005	Georgian National Institute of Informatics and Telecommunications	Elektroonikainsener

Kaitstud lõputööd

"Korrelatsiooniteguri mõõteriist", Magistritöö, Ivane Javakhishvili State University of Tbilisi, 2003.

CURRICULUM VITAE

1. Personal data

   Name: Levon Gevorkov

   Date and place of birth: 07.06.1980, Tbilisi

2. Contact information

   Address: Akadeemia tee 5, 417A, Tallinn 12611, Estonia.

   Phone: +37256903135

   E-mail: levon.gevorkov@ttu.ee

3. Education

Educational institution	Graduation year	Education (field of study/degree)
Tbilisi State University	2001	Radio-physics and electronics Bachelor of Science
Tbilisi State University	2003	Radio-physics and electronics Master of Science

4. Language competence/skills (fluent; average, basic skills)

Language	Level
Armenian	Fluent
Georgian	Fluent
Russian	Fluent
English	Fluent

5. Professional Employment

Period	Organisation	Position
2014 -…	Tallinn University of Technology, Tallinn, Estonia	Junior researcher
2006-2013	Georgian Water and Power (GWP), Tbilisi, Georgia	Senior Electrical Engineer
1998-2005	Georgian National Institute of Information and Telecommunication	Engineer

Defended theses

Master of science thesis: Measuring Instrument of Factor of Correlation, 2003, Supervisor: Prof. Kartlos Khomasuridze (Tbilisi State University).

DISSERTATIONS DEFENDED AT
TALLINN UNIVERSITY OF TECHNOLOGY ON
POWER ENGINEERING, ELECTRICAL ENGINEERING, MINING ENGINEERING

1. **Jaan Tehver**. Boiling on Porous Surface. 1992.
2. Salastatud.
3. **Endel Risthein.** Electricity Supply of Industrial Plants. 1993.
4. **Tõnu Trump**. Some New Aspects of Digital Filtering. 1993.
5. **Vello Sarv.** Synthesis and Design of Power Converters with Reduced Distortions Using Optimal Energy Exchange Control. 1994.
6. **Ivan Klevtsov**. Strained Condition Diagnosis and Fatigue Life Prediction for Metals under Cyclic Temperature Oscillations. 1994.
7. **Ants Meister**. Some Phase-Sensitive and Spectral Methods in Biomedical Engineering. 1994.
8. **Mati Meldorf**. Steady-State Monitoring of Power System. 1995.
9. **Jüri-Rivaldo Pastarus**. Large Cavern Stability in the Maardu Granite Deposit. 1996.
10. **Enn Velmre**. Modeling and Simulation of Bipolar Semiconductor Devices. 1996.
11. **Kalju Meigas**. Coherent Photodetection with a Laser. 1997.
12. **Andres Udal**. Development of Numerical Semiconductor Device Models and Their Application in Device Theory and Design. 1998.
13. **Kuno Janson**. Paralleel- ja järjestikresonantsi parameetrilise vaheldumisega võrgusageduslik resonantsmuundur ja tema rakendamine. 2001.
14. **Jüri Joller**. Research and Development of Energy Saving Traction Drives for Trams. 2001.
15. **Ingo Valgma**. Geographical Information System for Oil Shale Mining – MGIS. 2002.
16. **Raik Jansikene**. Research, Design and Application of Magnetohydrodynamical (MHD) Devices for Automation of Casting Industry. 2003.
17. **Oleg Nikitin**. Optimization of the Room-and-Pillar Mining Technology for Oil-Shale Mines. 2003.
18. **Viktor Bolgov**. Load Current Stabilization and Suppression of Flicker in AC Arc Furnace Power Supply by Series-Connected Saturable Reactor. 2004.
19. **Raine Pajo**. Power System Stability Monitoring – an Approach of Electrical Load Modelling. 2004.
20. **Jelena Shuvalova**. Optimal Approximation of Input-Output Characteristics of Power Units and Plants. 2004.
21. **Nikolai Dorovatovski**. Thermographic Diagnostics of Electrical Equipment of Eesti Energia Ltd. 2004.
22. **Katrin Erg**. Groundwater Sulphate Content Changes in Estonian Underground Oil Shale Mines. 2005.

23. **Argo Rosin**. Control, Supervision and Operation Diagnostics of Light Rail Electric Transport. 2005.

24. **Dmitri Vinnikov**. Research, Design and Implementation of Auxiliary Power Supplies for the Light Rail Vehicles. 2005.

25. **Madis Lehtla**. Microprocessor Control Systems of Light Rail Vehicle Traction Drives. 2006.

26. **Jevgeni Šklovski**. LC Circuit with Parallel and Series Resonance Alternation in Switch-Mode Converters. 2007.

27. **Sten Suuroja**. Comparative Morphological Analysis of the Early Paleozoic Marine Impact Structures Kärdla and Neugrund, Estonia. 2007.

28. **Sergei Sabanov**. Risk Assessment Methods in Estonian Oil Shale Mining Industry. 2008.

29. **Vitali Boiko**. Development and Research of the Traction Asynchronous Multimotor Drive. 2008.

30. **Tauno Tammeoja**. Economic Model of Oil Shale Flows and Cost. 2008.

31. **Jelena Armas**. Quality Criterion of road Lighting Measurement and Exploring. 2008.

32. **Olavi Tammemäe**. Basics for Geotechnical Engineering Explorations Considering Needed Legal Changes. 2008.

33. **Mart Landsberg**. Long-Term Capacity Planning and Feasibility of Nuclear Power in Estonia under Certain Conditions. 2008.

34. **Hardi Torn**. Engineering-Geological Modelling of the Sillamäe Radioactive Tailings Pond Area. 2008.

35. **Aleksander Kilk**. Paljupooluseline püsimagnetitega sünkroongeneraator tuuleagregaatidele. 2008.

36. **Olga Ruban**. Analysis and Development of the PLC Control System with the Distributed I/Os. 2008.

37. **Jako Kilter**. Monitoring of Electrical Distribution Network Operation. 2009.

38. **Ivo Palu**. Impact of Wind Parks on Power System Containing Thermal Power Plants. 2009.

39. **Hannes Agabus**. Large-Scale Integration of Wind Energy into the Power System Considering the Uncertainty Information. 2009.

40. **Kalle Kilk**. Variations of Power Demand and Wind Power Generation and Their Influence to the Operation of Power Systems. 2009.

41. **Indrek Roasto**. Research and Development of Digital Control Systems and Algorithms for High Power, High Voltage Isolated DC/DC Converters. 2009.

42. **Hardi Hõimoja**. Energiatõhususe hindamise ja energiasalvestite arvutuse metoodika linna elektertranspordile. 2009.

43. **Tanel Jalakas**. Research and Development of High-Power High-Voltage DC/DC Converters. 2010.

44. **Helena Lind**. Groundwater Flow Model of the Western Part of the Estonian Oil Shale Deposit. 2010.

45. **Arvi Hamburg**. Analysis of Energy Development Perspectives. 2010.

46. **Mall Orru**. Dependence of Estonian Peat Deposit Properties on Landscape Types and Feeding Conditions. 2010.

47. **Erik Väli**. Best Available Technology for the Environmentally Friendly Mining with Surface Miner. 2011.

48. **Tarmo Tohver**. Utilization of Waste Rock from Oil Shale Mining. 2011.

49. **Mikhail Egorov**. Research and Development of Control Methods for Low-Loss IGBT Inverter-Fed Induction Motor Drives. 2011.

50. **Toomas Vinnal**. Eesti ettevõtete elektritarbimise uurimine ja soovituste väljatöötamine tarbimise optimeerimiseks. 2011.

51. **Veiko Karu**. Potential Usage of Underground Mined Areas in Estonian Oil Shale Deposit. 2012.

52. **Zoja Raud**. Research and Development of an Active Learning Technology for University-Level Education in the Field of Electronics and Power Electronics. 2012.

53. **Andrei Blinov**. Research of Switching Properties and Performance Improvement Methods of High-Voltage IGBT based DC/DC Converters. 2012.

54. **Paul Taklaja**. 110 kV õhuliinide isolatsiooni töökindluse analüüs ja töökindluse tõstmise meetodid. 2012.

55. **Lauri Kütt**. Analysis and Development of Inductive Current Sensor for Power Line On-Line Measurements of Fast Transients. 2012.

56. **Heigo Mõlder**. Vedelmetalli juhitava segamisvõimaluse uurimine alalisvoolu kaarleekahjus. 2012.

57. **Reeli Kuhi-Thalfeldt**. Distributed Electricity Generation and its Possibilities for Meeting the Targets of Energy and Climate Policies. 2012.

58. **Irena Milaševski**. Research and Development of Electronic Ballasts for Smart Lighting Systems with Light Emitting Diodes. 2012.

59. **Anna Andrijanovitš**. New Converter Topologies for Integration of Hydrogen Based Long-Term Energy Storages to Renewable Energy Systems. 2013.

60. **Viktor Beldjajev**. Research and Development of the New Topologies for the Isolation Stage of the Power Electronic Transformer. 2013.

61. **Eduard Brindfeldt**. Visually Structured Methods and Tools for Industry Automation. 2013.

62. **Marek Mägi**. Development and Control of Energy Exchange Processes between Electric Vehicle and Utility Network. 2013.

63. **Ants Kallaste**. Low Speed Permanent Magnet Slotless Generator Development and Implementation for Windmills. 2013.

64. **Igor Mets**. Measurement and Data Communication Technology for the Implementation in Estonian Transmission Network. 2013.

65. **Julija Šommet**. Analysis of Sustainability Assessment in Carbonate Rock Quarries. 2014.

66. **Tanel Kivipõld**. Real-Time Electricity Tariff System for Retail Market. 2014.

67. **Priit Uuemaa**. Industrial CHP Optimal Management Model in the Energy

Market under Incomplete Information. 2014.

68. **Anton Rassõlkin**. Research and Development of Trial Instrumentation for Electric Propulsion Motor Drives. 2014.

69. **Toomas Vaimann**. Diagnostics of Induction Machine Rotor Faults Using Analysis of Stator Signals. 2014.

70. **Aivar Auväärt**. Development of Energy Reserve Optimization Methodology for Households with Renewable Power Systems. 2014.

71. **Raivo Attikas**. Modelling of Control Systems and Optimal Operation of Power Units in Thermal Power Plants. 2014.

72. **Liisa Liivik**. Semiconductor Power Loss Reduction and Efficiency Improvement Techniques for the Galvanically Isolated Quasi-Z-Source DC-DC Converters. 2015.

73. **Victor Astapov**. Technical-Economic Analysis of Distributed Generation Units in Power Systems. 2015.

74. **Tiit Hõbejõgi**. Possibilities to Optimize Low Voltage Network Investments in Rural Areas. 2016.

75. **Märt Ots**. Practical Implementation of Price Regulation in Energy Sector. 2016.

76. **Ilja Bakman**. High-Efficiency Predictive Control of Centrifugal Multi-Pump Stations with Variable-Speed Drives. 2016.

77. **René Nukki**. Research and Development of Exterior-Rotor Permanent Magnet Synchronous Machines for Light Aerial Vehicles. 2016.

78. **Imre Drovtar**. Demand Side Management Possibilities and Viability for Voltage Support Services in Estonia. 2016.

79. **Andrii Chub**. Research, Design and Implementation of Galvanically Isolated Impedance-Source DC-DC Converters. 2016.

80. **Jaan Niitsoo**. Residential Grids Power Quality Analyses Concerning Nonlinear Consumer Loads and PV Panels. 2016.

81. **Einari Kisel**. Indicators for Assessing the Quality of an Energy Policy. 2017.

82. **Denis Lebedev**. Research and Development of Storage Based Energy Management System for Households. 2017.